STRUCTURAL GEOLOGY OF THE NORTHERN GALICE FORMATION,

WESTERN KLAMATH MOUNTAINS,

OREGON AND CALIFORNIA

A thesis presented to the Faculty

of the State University of New York

at Albany

in partial fulfillment of the requirements

for the degree of Master of Science

College of Science and Mathematics

Department of Geological Sciences

F. Ross Jones

1988

STRUCTURAL GEOLOGY OF THE NORTHERN GALICE FORMATION,

WESTERN KLAMATH MOUNTAINS,

OREGON AND CALIFORNIA

Abstract of

a thesis presented to the Faculty

of the State University of New York

at Albany

in partial fulfillment of the requirements

for the degree of Master of Science

College of Science and Mathematics

Department of Geological Sciences

F. Ross Jones

1988

ABSTRACT

The Galice Formation is a thick, turbiditic flysch
sequence that depositionally overlies the Josephine
ophiolite in the western Klamath Mountains of northwestern
California and southwestern Oregon. The Josephine ophiolite
and Galice have been interpreted as the basement and
sedimentary cover of a Late Jurassic back-arc basin that
opened proximal to the continental margin. During the
Nevadan orogeny (ca. 151-147 Ma), the ophiolite and
overlying Galice sediments were thrust eastward beneath the
continental margin along the regional Orleans fault. Two
distinct Nevadan deformational phases are recognized in the
Galice--an initial D_1 or "main-phase" deformation and a
later brittle deformation dominated by thrusting.

D_1 involved development of tight to isoclinal
northwest-vergent F_1 folds which possess an axial-planar S_1
cleavage. S_1 ranges from a weak pressure-solution cleavage
in the northernmost Galice, to a strong slaty cleavage or
schistosity in the southern Galice. S_1 is ubiquitously
parallel to bedding in the absence of recognizable F_1 fold
closures. Bedding is commonly transposed into parallelism
with cleavage in southern exposures of the Galice.

Syntectonic fibers in pressure shadows of pyrite grains
reflect a north-south gradient in Nevadan penetrative
strain. The fibers are straight and parallel to the trace
of slaty cleavage, suggesting that cleavage formed during a

stage of pure flattening. Percent shortening normal to S_1 determined from fibers in the northern Galice (SW Oregon) is approximately 33%. However, fibers from slates in northern California record an average of 70% shortening normal to S_1. A large increase in the intensity of S_1 towards the south also suggests a gradient in finite strain.

Main-phase Nevadan deformation was followed by an episode of brittle shearing. Nevadan thrusts reveal top-to-northwest sense to displacement, similar to vergence observed from F_1 folds. A second generation of folds, F_2, appear to be genetically related to the thrusts. Nevadan thrusts clearly overprint main-phase structures (F_1, S_1). In the northernmost Galice, angular F_1 folds are thrusted-out parallel to bedding in one of the fold limbs. Further to the south, F_1 folds are more typically truncated by thrusts that are parallel to S_1 cleavage planes. Small-scale thrust systems in thinly-bedded rocks have produced peculiar bedding truncations or "pseudocross-bedding". These small thrusts locally truncate the S_1 cleavage.

Fundamental conclusions obtained in this study are:
1) The Galice Formation is tightly folded on both outcrop and regional scales.
2) There is a north-to-south increase in Nevadan regional metamorphic grade and penetrative strain. This gradient may reflect a small southward component of underthrusting along the Orleans fault.

3) Nevadan vergence from folds and thrusts in the Galice is dominantly <u>northwestward</u>.

4) Most Nevadan thrusting in the Galice took place <u>after</u> the main-phase penetrative deformation and peak metamorphism. This ductile-to-brittle transition may have resulted from continued underthrusting during regional uplift.

ACKNOWLEDGEMENTS

TABLE OF CONTENTS

LIST OF FIGURES

Chapter 1: INTRODUCTION

1.1 Regional Perspective

The Klamath Mountains province is an excellent example of multiple accretion of diverse oceanic terranes at a long-lived convergent plate margin. The lithotectonic framework of the Klamath Mountains was first described by Irwin (1960) who recognized four, broadly arcuate belts in the Klamaths (fig. 1.1). The belts are bounded by eastward-dipping thrust faults and become successively younger to the west. Irwin (1966) named the belts (from structurally highest to lowest): the eastern Klamath belt, the central metamorphic belt, the western Paleozoic and Triassic belt and the western Jurassic belt. More recently, the Klamaths have been interpreted as an "amalgamation" of several allochthonous oceanic terranes which have accreted to the western margin of North America from the early Paleozoic to the middle Mesozoic (Hamilton, 1969; Irwin, 1981,1985). Terranes of the Klamath Mountains largely consist of ultramafic and ophiolitic thrust sheets, oceanic sedimentary and island arc sequences, diverse melanges and calc-alkaline plutons, primarily of Mesozoic age (Hotz, 1971a). The Klamaths are unconformably overlain by lower Cretaceous sedimentary rocks correlated with the Great Valley sequence in northern and central California (Irwin, 1981).
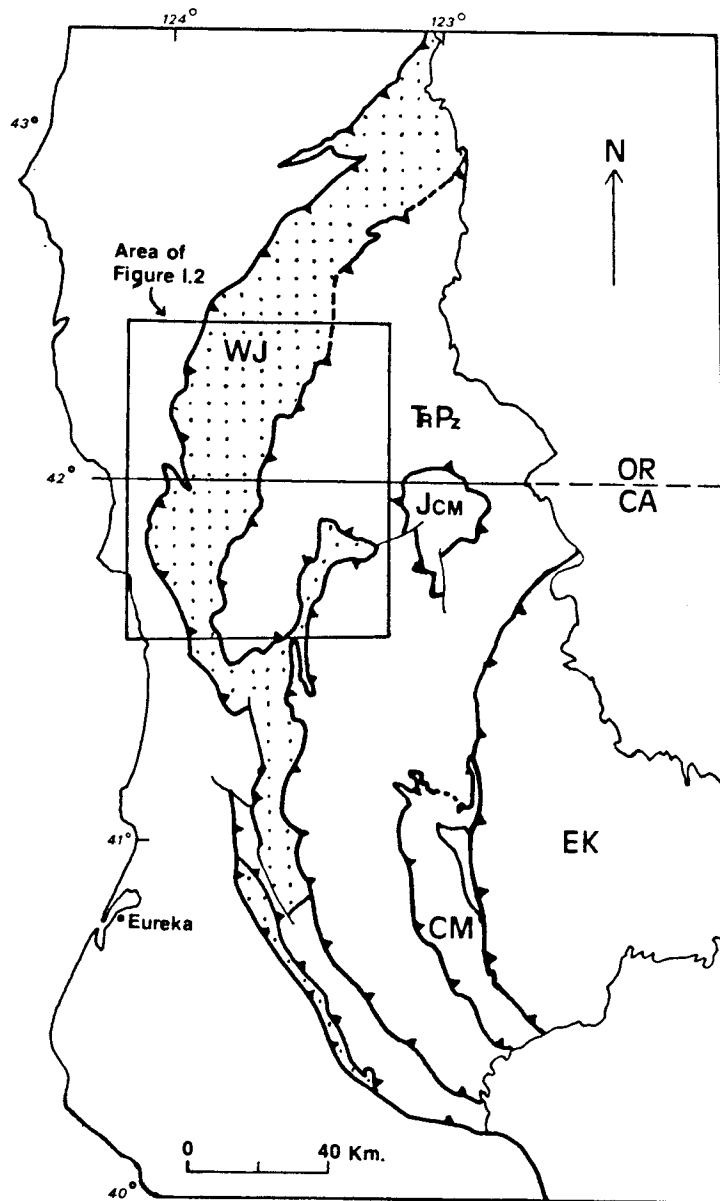
Figure 1.1 Map of the Klamath Mountains province showing
the configuration of four major thrust-bounded terranes:
EK= eastern Klamath belt, CM= central metamorphic belt,
TrPz= western Triassic and Paleozoic belt and WJ= western
Jurassic belt. Jcm is the Jurassic Condrey Mountain schist.
Plutons were omitted for clarity. From Jachens and others,
1986, fig.1 (modified from Irwin, 1981; Hotz, 1971).

1.2 The Galice Formation

The Galice Formation is exposed in the western Jurassic belt of the Klamath Mountains (fig. 1.2). It was first named by Diller (1907) for a locally-exposed sequence of slate, graywacke and rare pebble conglomerate at the "town" of Galice and along Galice Creek, approximately 25 kilometers northwest of Grants Pass, Oregon. Volcaniclastic units which are interstratified with shales and graywackes in exposures along the Rogue River were subsequently included in the "type" Galice Formation by Wells and Walker (1953). A geological map of the Galice Quadrangle (Wells and Walker, 1953) shows a conformable contact between the Galice Formation and underlying volcanics; however, some authors have interpreted this lithologic boundary as a fault (Park-Jones, 1988). This contact may have been depositional, but is evidently obscured by faulting. Wells and others (1949) estimated the stratigraphic thickness of the Galice to be 8 to 9 kilometers, but this figure is almost certainly too high, considering that it is isoclinally folded.

Specimens of the bivalve Buchia concentrica (Sowerby) were collected from several localities in the type Galice (Diller, 1907; Diller and Kay, 1924). This Late Jurassic index fossil has a known age-range of late Middle Oxfordian to Middle Kimmeridgian, or approximately 159-155 Ma (Imlay,
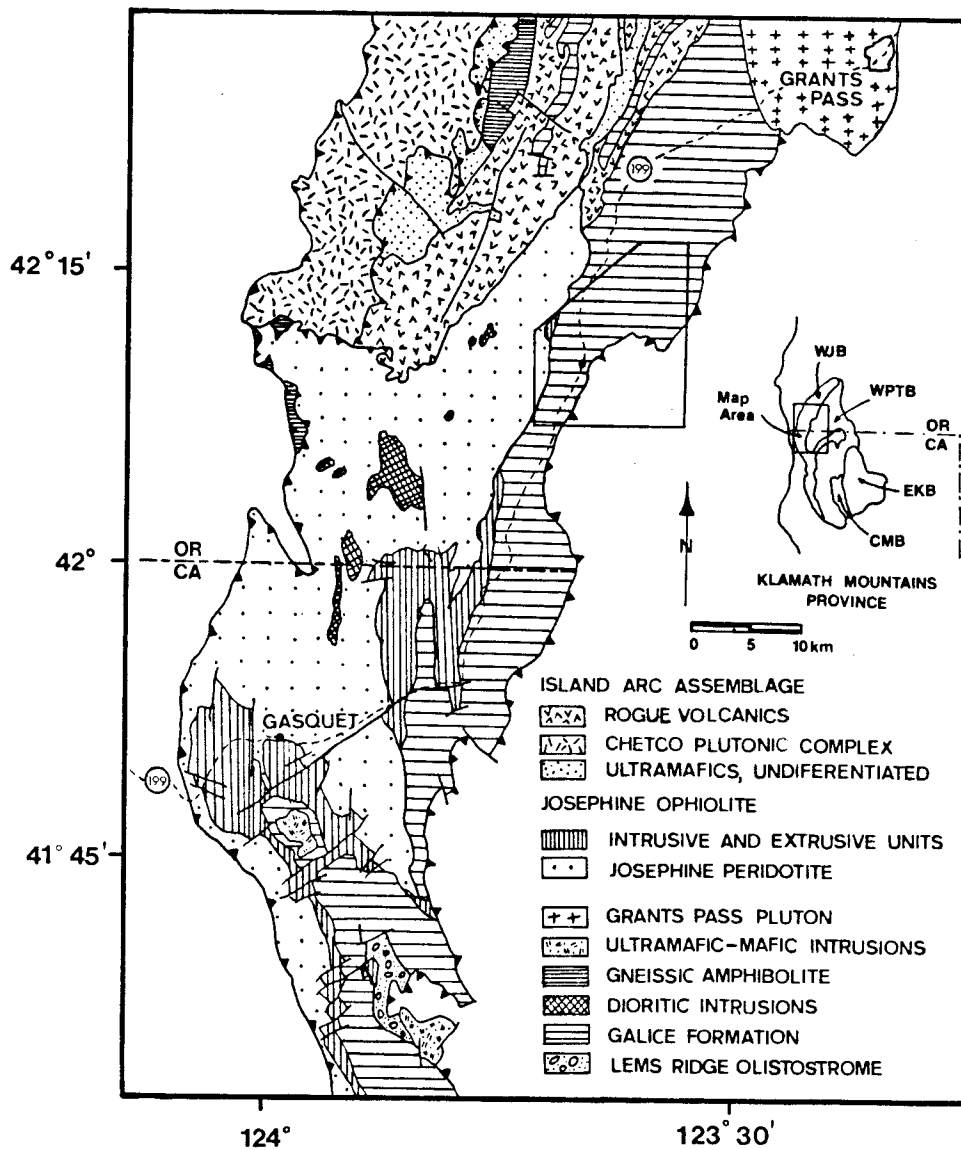
Figure 1.2 Geological map of the western Jurassic belt (modified from Harding, 1986). The area in the smaller, five-sided box is the northern field area of this study, shown in more detail in figure 1.6.

1980; Harland et al., 1982). A second younger age-constraint is provided by outliers of Cretaceous shallow marine and subaerial sedimentary rocks which overlie the Galice in angular unconformity. Cretaceous outliers overlie the Galice near O'Brien, Oregon, in Douglas County, Oregon, and along Grave and Days Creeks north of Grants Pass (see map by Hotz, 1971b). The Riddle Formation (Diller and Kay, 1924) unconformably overlies the Rogue Formation north of Grants Pass, and has been correlated with the Middle to Late Tithonian (ca. 148-144 Ma) Knoxville Formation in California (Imlay et al., 1959). Massive conglomerates and coarse-grained sandstones unconformably overlie the Galice at Indian Hill near O'Brien, Oregon (fig. 1.3). These rocks are believed to be the northern equivalents of the lower Cretaceous Horsetown Formation, a member of the Great Valley sequence in California (Wells et al., 1949). Fossils from this outlier are Late Hauterivian to Barremian, or about 126-119 Ma (Imlay et al., 1959). Interestingly, the stratigraphy of this sequence strongly resembles that of the older Knoxville Formation described by Diller and Kay (1924, p.3) as "gray sandstone and some shale with massive conglomerate at the base".

Graywacke and slate are exposed in a north-south trending belt which extends along the entire length of the western Klamath Mountains (Hershey, 1911; Irwin, 1960). Cater and Wells (1953) first correlated these rocks with the type Galice exposed along the Rogue River and Grave Creek.
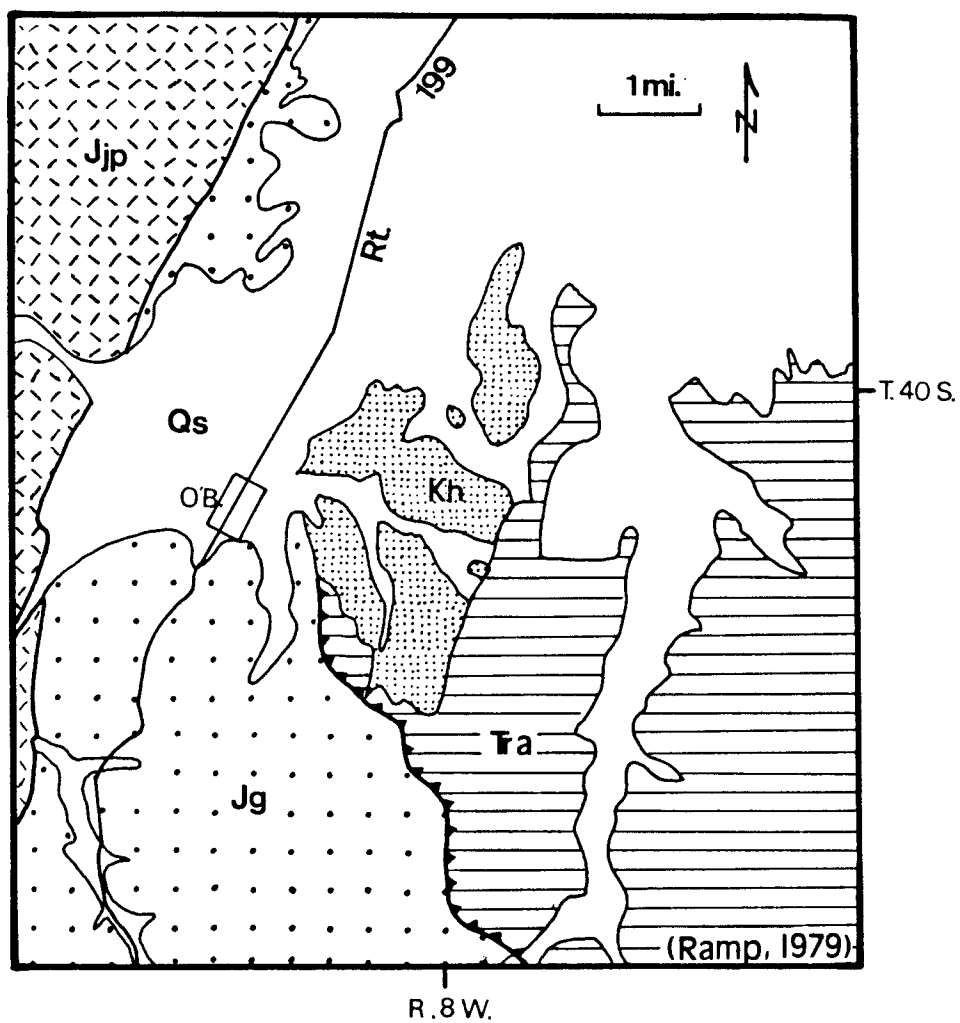
Figure 1.3 Geological map of the area near O'Brien, Oregon
(after Ramp, 1979).   Tra= Applegate Group, Jjp= Josephine
peridotite, Jg= Galice Formation, Kh= Horsetown Formation
and Qs= Quaternary sediments.

This correlation was based on the occurrence of <u>Buchia</u> <u>concentrica</u> at localities in northernmost California, and on lithostratigraphic similarities. Similarities in sedimentary petrography further support the conclusion that the two formations are correlative (Harper, 1980a,1983).

The type Galice Formation has been interpreted as conformably overlying volcanics of the Rogue Formation (Wells and Walker, 1953; Garcia, 1979; Harper and Wright, 1984). The contact is exposed along the Rogue River at Almeda Mine, and along Galice and Grave Creeks, but, as noted above, it may be faulted.

In contrast, a clear depositional contact between the Galice and the Josephine ophiolite is observable at several locations in northwestern California (Vail, 1977; Harper, 1983). Figure 1.4 shows two schematic stratigraphic columns for comparison. The Galice is exposed in two different thrust sheets (Harper and Wright, 1984); the "Galice" overlying the Josephine ophiolite is structurally higher than the type Galice Formation.

1.3 Lithology and Stratigraphy

The northernmost Galice Formation mainly consists of interbedded black shale and lithic wacke (fig. 1.5) which become strongly foliated slates and metagraywackes to the south. Thick sections of shale (0.5 km or more) with very
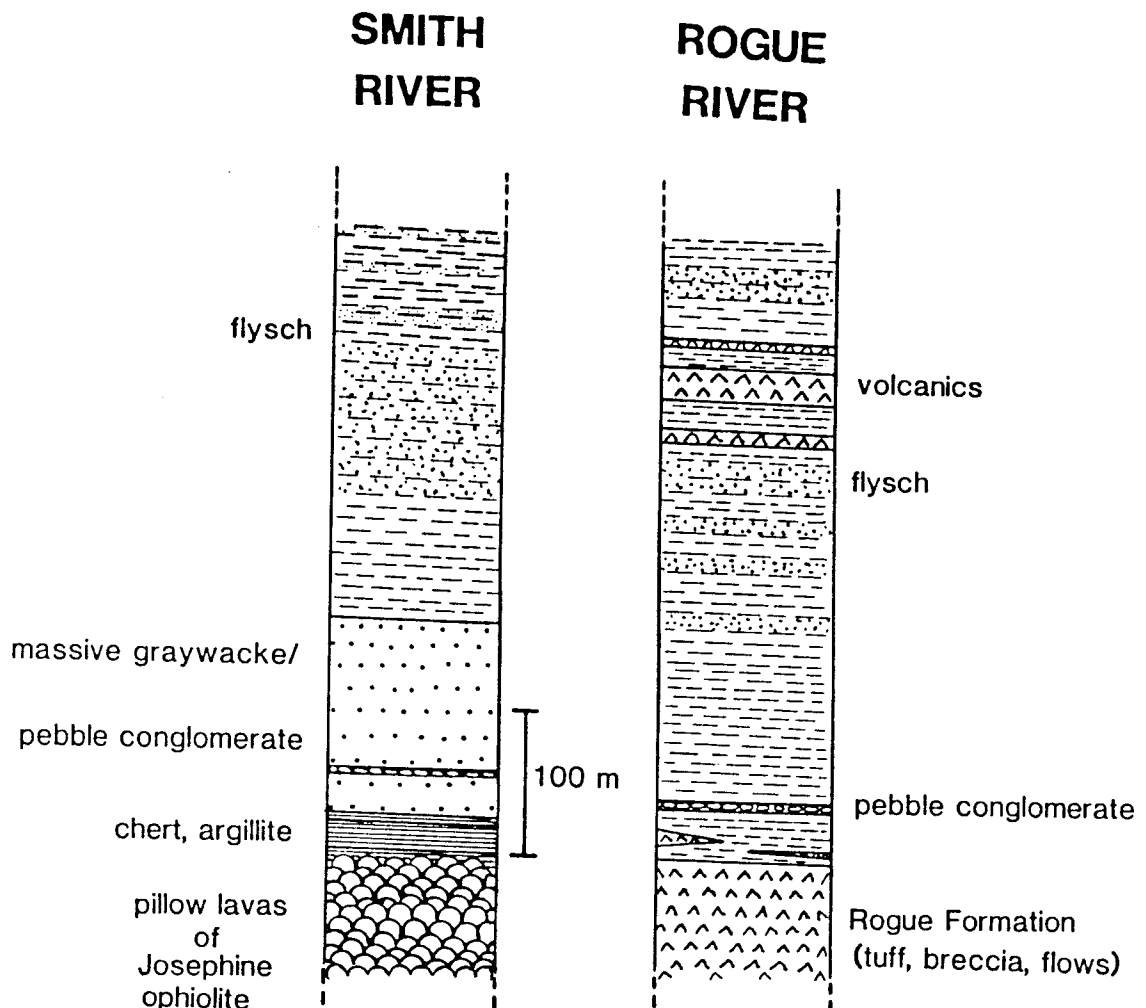
Figure 1.4 Simplified comparative stratigaphic columns showing the lower portion of the Galice Formation exposed at the type-locality along the Rogue River and Galice Creek, Oregon, and overlying the Josephine ophiolite along the Middle Fork Smith River in northern California.

Figure 1.5 Slightly dismembered beds of alternating shale and graywacke in the Galice Formation along the Illinois River near Cave Junction, Oregon. Beds are nearly vertical and strike approximately north-south.

few graywacke beds are found in some places. Similarly, there are intervals of massive graywacke (1-3 meter thick beds) containing no shale. Thin siltstone beds are commonly found interlaminated with shale. Siltstone is also a component of some graded beds, and is gradational between coarse-grained graywacke and shale. Volcanic rocks were not found in the Galice during field work for this thesis; however, volcaniclastic intervals were mapped by Snoke (1977) near the Preston Peak thrust in northern California.

Diller (1907) noted the occurrence of pebble conglomerate along Galice Creek at the type-locality. This rare conglomerate unit (units?) contains .5 to 4 cm subrounded clasts of chert, shale, volcanics, sandstone and quartzite in a fine sandy matrix (Diller, 1907; Wells et al., 1949). Massive conglomerate beds are more frequently exposed in the lower portion of the Galice, near the depositional contact with the Josephine ophiolite in northern California. Brown and black chert grains, up to 6 mm in diameter, are the dominant constituents of graywacke at the base of most graded beds. In addition to chert, other important components of wackes are detrital quartz, micas, feldspar, chlorite, pyrite, and lithic clasts such as tuffs, quartzite, argillite and serpentinite. Graywackes normally weather to a light tan or brown color.

Shales are gray to black on fresh surfaces and appear brown or reddish-brown in weathered exposures. Galice shales contain abundant opaque carbonaceous material and

pyrite. Most pyrite occurs in aggregates of microcrystalline spherules called "framboids" which will be discussed further in chapter 5. Sinuous dark trails on bedding surfaces are probably the trace fossil <u>Helminthoida</u> (R. Park-Jones, pers. comm.). Pyritized fossil trails were useful in finite strain analysis described in chapter 5.

Shales in the northern Galice near Cave Junction, Oregon are best termed "slaty shales"; however, pelitic rocks become true slates, and locally phyllites, to the south in northern California. Cleavage is usually subparallel to bedding, giving shales a strong bedding-parallel fissility. Foliation in graywackes is weak or absent in the northern Galice, whereas, to the south, wackes have a strong foliation and have been termed "semischists" (Harper, 1980a).

The absence of distinct marker beds or lithologies, combined with structural complexity and limited exposure, makes present stratigraphic correlation within the Galice impossible. Detailed geochronologic work using pollen from Galice shales may prove useful in future studies (G.D. Harper, pers. comm.).

A 21 to 31 meter-thick hemipelagic sequence consisting of metalliferous red and black chert interlayered with argillite is frequently found near the contact of the Galice with pillow lavas of the underlying Josephine ophiolite (Pinto-Auso and Harper, 1985). About 100 meters of massive graywacke and pebble conglomerate commonly overlie the

hemipelagic sequence where continuous, unfaulted sections are observed. Repeated massive graywacke intervals in the Galice might be fault-transported equivalents of this coarse basal unit. Thick sequences of black shale and some volcaniclastic intervals have been interpreted as occurring in the structurally highest strata of the type Galice Formation (Wells et al., 1949).

1.4 Tectonic Setting

Reconnaissance mapping by Irwin (1960) has shown that the Galice is the structurally highest unit of the Klamath province and occurs in a distinct belt which he termed the "western Jurassic belt" (WJB). The WJB is bounded to the east by the east-dipping Orleans fault (Hershey, 1911; Jachens et al., 1986), also named the "Preston Peak thrust" by Snoke (1977). At its western margin, the WJB is thrust over Cretaceous and Tertiary rocks of the Franciscan assemblage along the northern extension of the Coast Range thrust. The WJB contains two, east-dipping thrust sheets or "subterranes" (fig. 1.2): (1) A higher thrust sheet consisting of the Josephine Peridotite (Dick, 1976), the Josephine ophiolite (Harper, 1980b) and "Galice" Formation, and (2) A lower thrust sheet, exposed exclusively in southwestern Oregon, containing the Chetco plutonic complex (Hotz, 1971a), mafic gneisses of the Briggs Creek

amphibolite, the Rogue Formation and the type Galice Formation.

The Josephine ophiolite and overlying Galice flysch have been interpreted as the basement and sedimentary cover of a Late Jurassic back-arc basin (Harper, 1980b, Harper and Wright, 1984). The following evidence supports this conclusion:

1) Sedimentary Petrography. Graywackes in the Galice show a mixed continental margin/ volcanic arc source (Harper, 1980a). Volcanic rock fragments and isolated phenocrysts in coarse wackes and conglomerates suggest that the depositional basin was near an island arc, active in the Late Jurassic. Moreover, the metasedimentary rocks of the type Galice contain intercalated volcanic layers which strongly resemble volcanics of the Rogue Formation (Wells and Walker, 1953; Garcia, 1979). Diverse rock and mineral fragments in the Galice such as detrital glaucophane, chert, chromian spinel, quartzite and mica schist suggest that the Galice was also derived from erosion of sedimentary, metamorphic and ultramafic rocks of older Klamath terranes to the east.

Recent mapping and structural data from the type-Galice strongly suggest that interlayered volcanic units, averaging 15 meters in thickness, are thrust slivers of Rogue volcanics (R. Park-Jones, pers. comm.). Repetition of the volcanic units by tight folding is also possible, based on

large flattening strains evident from Galice slates and tuffaceous rocks at the type-locality.

2) <u>Regional Relationships</u>. Since the Galice overlies both the Josephine ophiolite and a coeval Late Jurassic island arc (Garcia, 1979), there is presumed to be a close spatial and temporal arc-ophiolite association (Harper and Wright, 1984). The predominantly mafic Chetco intrusive complex has been interpreted as the plutonic core of the Late Jurassic island arc (Dick, 1976; Garcia, 1982).

3) <u>Geochronology</u>. The age of the Josephine ophiolite is 162 +/-1 Ma, determined from U/Pb zircon dating of ophiolitic plagiogranites (Saleeby et al., 1986). Previous ages of 157 +/-2 Ma for the Josephine ophiolite (Saleeby et al., 1982) are slightly discordant. Zircons from a silicic tuff from the Rogue Formation have yielded a U/Pb age of 157+/-2 Ma (Saleeby, 1984).

This evidence suggests that the Galice was deposited on the Josephine ophiolite in a Late Jurassic back-arc basin between a coeval island arc and the continental margin (Harper and Wright, 1984) represented by the western Paleozoic and Triassic belt. Harper and Wright (1984) further suggested that opening of the Josephine basin resulted from the splitting of a Middle Jurassic arc. Recent geochronologic data from the Devils Elbow ophiolite, the southern equivalent of the Josephine ophiolite, suggest that rifting began at about 164 Ma (Wyld, 1985; Wyld and Wright, 1988), 5 m.y. before cessation of the Middle

Jurassic arc (ca. 159 Ma). Magmatism in the Middle Jurassic arc is constrained to the interval 177-159 Ma (Harper and Wright, 1984). The extrusive rocks of the Middle Jurassic arc are probably the volcanics of the western Hayfork terrane in the WPTB. This arc-splitting event produced an active arc/ back-arc basin/ extinct(?) remnant arc geometry proximal to the continental margin in the Late Jurassic (Harper and Wright, 1984).

The Galice contains partial and complete Bouma sedimentation cycles which are indicative of deposition by turbidity currents at medium to abyssal depths. It lithologically resembles Taconian flysch deposits such as the Martinsburg and Austin Glen formations in the central and northern Appalachian orogen. Taconian flysch was deposited in submarine fan systems in deep water during the Middle to Late Ordovician (Rowley and Kidd, 1981; Lash and Drake, 1984).

The Galice turbidites were apparently deposited in greater than 2,000 meters of water. Basal pelagic sediments are siliceous, rather than calcareous, suggesting deposition below the carbonate compensation depth (CCD). The CCD was approximately 2,500 meters below sea level in the Late Jurassic (Bosellini and Winterer, 1975). However, there may not have been a source of calcareous pelagic sediments at this time (W.S.F. Kidd, pers. comm.). Furthermore, calcareous lenses are present locally within the basal pelagic sequence of the Galice.

Nonetheless, depths of modern back-arc basins are
generally greater than 2,200 meters (Harper, 1982, and
references therein). Pelagic sediments in the basal section
of the Galice Formation probably accumulated on a
bathymetric "high", coincident with the spreading axis
(Pinto-auso and Harper, 1985). The depth of the axial high
in modern back-arc basins is normally in excess of 2,000
meters (Harper, 1982).

In addition to rhythmic Bouma sequences, sedimentary
structures such as shale rip-up clasts, flute casts and tool
marks are evidence for deposition by gravity-driven
turbidity currents. Sediment transport was to the west
(Harper, 1980a), oceanward from the Late Jurassic
continental margin, implying erosion of older rocks of the
Klamath Mountains.

Cessation and collapse of the Late Jurassic arc was
followed by imbrication of the present western Jurassic belt
into two east-dipping thrust sheets. The Josephine
ophiolite and overlying Galice were simultaneously
underthrust beneath the continental margin and thrust over
the Late Jurassic island arc (Rogue-Chetco terrane) during
the Nevadan orogeny (Harper and Wright, 1984).

1.5 Study Areas

Field work in the Galice overlying the Josephine
ophiolite focused on two areas along approximately 40

kilometers of its exposure. The northern study area is located in Josephine County, Oregon, near the towns of Cave Junction and Kerby (fig. 1.6). It covers much of the NE and NW quadrants of the USGS 15' Cave Junction quadrangle (1953). Figure 1.6 shows the geography of this area for reference to localities cited in this thesis. It also shows the major fault boundaries between the Galice and the Applegate Group (Wells et al., 1949) and Josephine Peridotote (Dick, 1976). The Illinois Valley has good road access, the major arterial being the Redwood Highway (US 199) which extends from Grants Pass, Oregon to the Pacific coast at Crescent City, California. The combined population of the northern Illinois Valley (Cave Junction and vicinity) is about 2,000.

A majority of the exposures of the Galice Formation are found along recent, yet presently inactive, logging road-cuts in the lower hills of the Siskiyou Range east of Kerby. The Siskiyou Range is underlain by the more resistent lithologies of the Applegate Group, and attain a maximum elevation in Oregon of 1,800 meters at Kerby Butte. The Galice is best exposed in steep logging road-cuts where stone has been quarried for road paving material. Semi-continuous fresh exposures of the Galice are interspersed with river gravels along the east and west forks of the Illinois River system near Cave Junction (fig. 1.7). Outcrops of the Galice in this area are, nevertheless, entirely restricted to road-cuts and some stream beds.
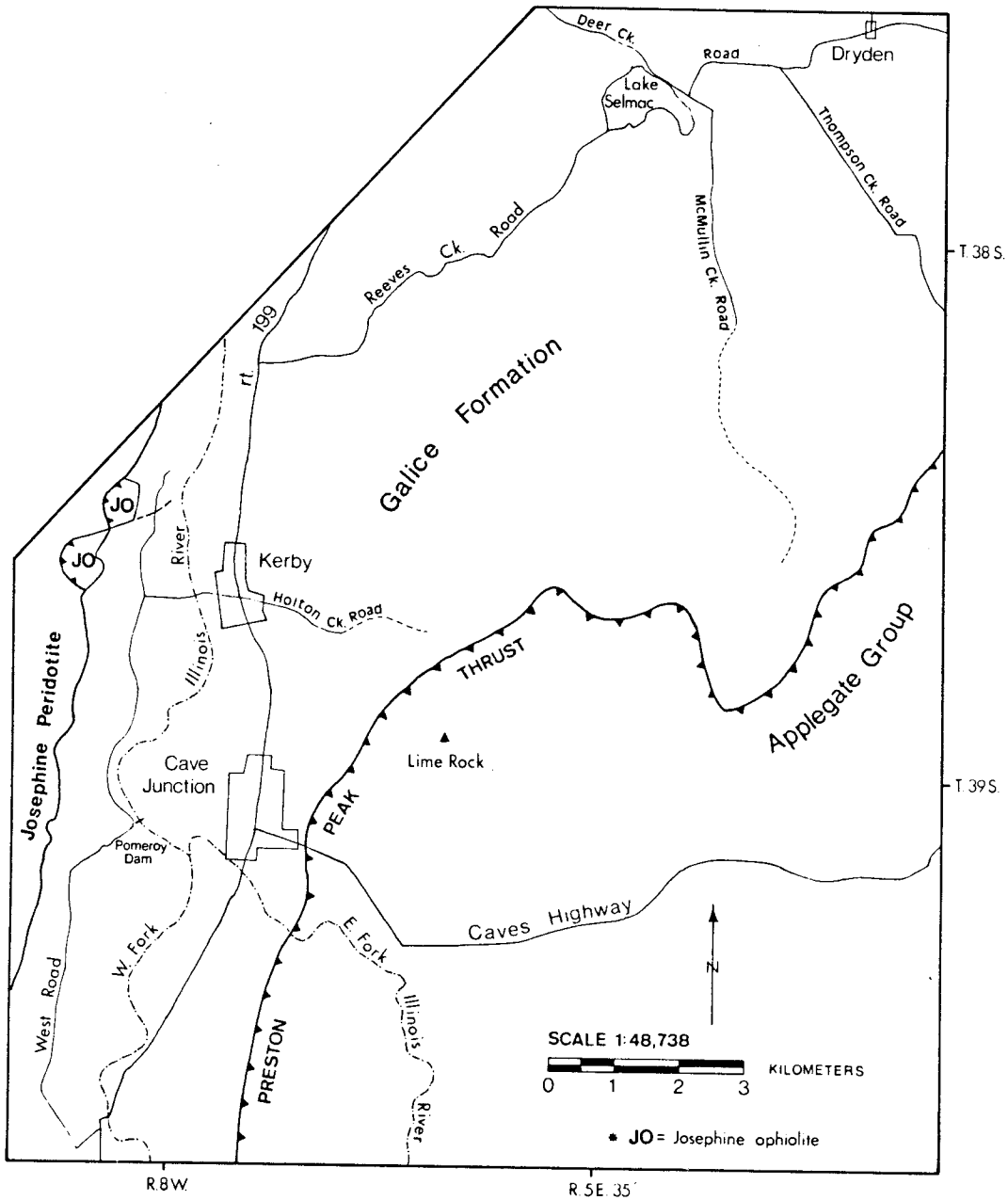
Figure 1.6 Reference map for the northern study area near
Kerby and Cave Junction, Oregon. Map shows the exposed
width of the Galice, as well as the major fault boundaries
with the Josephine peridotite and the Applegate Group.
"JO" refers to pillow lava and breccia of the upper portion
of the Josephine ophiolite.

Figure 1.7 Nearly vertical graywacke beds exposed along the west fork of the Illinois River near Cave Junction, Oregon. View is to the south-southwest.

Figure 1.8 Well-aligned load casts along the base of an overturned graywacke bed. Road-cut along West Road near Pomeroy Dam (see fig. 1.6).

Smaller stream exposures are covered with alluvium from landslides and debris from recent "clear-cutting" logging operations.

The structural geology of the northern Galice in southwestern Oregon (fig. 1.6) has not been studied in much detail by previous workers. Geological maps including this area have been compiled by Wells and others (1949), Ramp (1979, 1986) and Page and others (1981). A few comments concerning the structure of the Galice were made by Diller and Kay (1924).

A distinct advantage of studying the northern Galice is the preservation of sedimentary structures which indicate the direction of stratigraphic younging. Among the most common younging indicators are graded beds, flute and groove casts and peculiar well-aligned load casts (fig. 1.8). Original sedimentary textures and structures have not been obscured by metamorphic overprinting or intense foliation development. The widespread occurrence of younging indicators in graywacke beds facilitates recognition of large-scale overturned folds.

A second area where structural data was collected is in Del Norte County, California, near the Oregon border (fig. 1.9). Continuous, across-strike exposures occur along stream-cuts in steep valleys of the Smith River drainage system. Traverses across the Galice were made along Oregon Mountain Road, the Siskiyou and Middle forks of the Smith River and Knopti Creek (fig. 1.9).
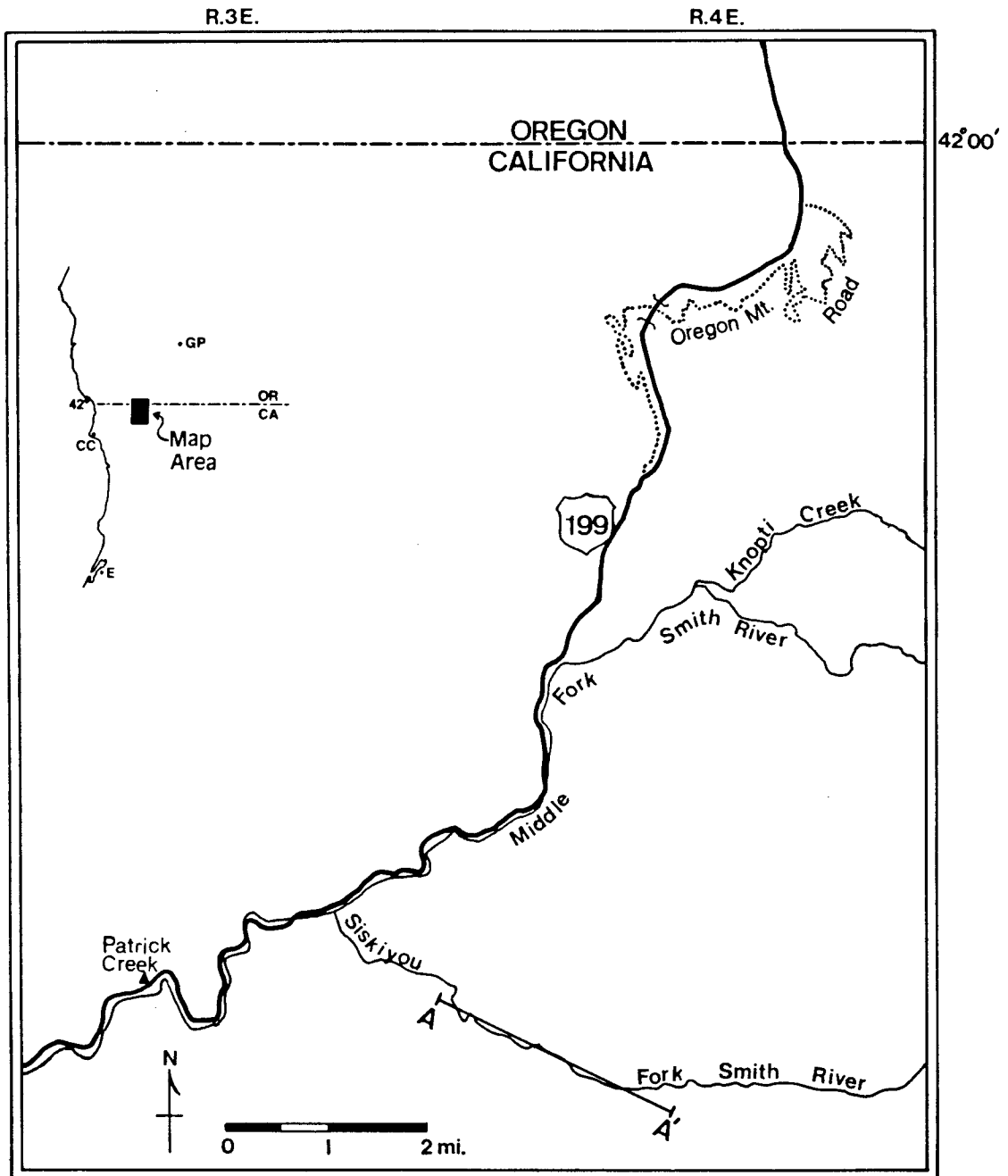
Figure 1.9 Reference map for study locations in northern California. A-A' is the location of the vertical cross-section discussed in chapter 4.

Field work leading to this thesis was conducted for six weeks during June and July, 1986. A structural map (Plate 1) was prepared from detailed observations and data collected along logging roads in the area immediately east of Kerby, Oregon. Structural data for the map was recorded on 1985 aerial photographs from the Bureau of Land Management (USDI). Enlarged quadrants of the USGS 15' Cave Junction topographic quadrangle provided the base map. Field data from traverses in the northern California field area were recorded on the USGS 7.5' Hurdygurdy Butte, Devils Punchbowl, and Broken Rib Mountain topographic quadrangle maps.

1.6 Objectives

This project was originally undertaken to approach several structural problems in the Galice Formation noted by previous workers. These are discussed below:

1. Whether or not the Galice was deformed in a partially lithified state.-- There is evidence that deep water sediments are strongly deformed in an unconsolidated state at many convergent margins (Cowan, 1982; Westbrook et al., 1982; Byrne, 1984). Chapter 3 is a discussion of early structures in the Galice and their possible significance.

2. An apparent scarcity of F_1 folds, and the ubiquitous parallelism between bedding and the S_1 cleavage.-- These problems are emphasized by Harper (1980a) and Wyld (1985).

An important objective of this study is to determine whether the strata constitute limbs of large, overturned folds, or whether they are largely upright and only rarely folded. This problem has not been fully resolved in previous structural studies of the Galice Formation.

3. The direction of Nevadan thrusting and vergence.-- Studies of Nevadan vergence from folds and tectonic lineations in the Galice and along the basal thrust of the Josephine ophioite have produced conflicting interpretations (Harper and Wright, 1984; Roure, 1984; Cannat and Boudier, 1985; Gray, 1985).

4. The extent and relative timing of defomations which post-date the main-phase Nevadan deformation (D_1).-- Are F_2 folds a continuation of the main-phase Nevadan episode, or are they "post-Nevadan" structures? A solution depends on how "Nevadan" structures are defined. Some aspects of what is termed "late Nevadan" deformation are examined in chapter 6.

A more general question to be addressed is, "Do structures in the Galice Formation reflect the kinematics of underthrusting and emplacement of the Josephine/Galice thrust sheet during the Nevadan orogeny?" In rocks deformed by regional thrusting or shearing, it is important to determine whether penetrative fabrics record coaxial or non-coaxial strain histories. In chapter 5, syntectonic fibers in pressure shadows of pyrite framboids are examined and discussed in light of the above questions. Fibers have

proven to be a useful tool for stuctural geologists in the determination of strains accumulated during tectonic transport and emplacement (Durney and Ramsay, 1973; Beutner et al., 1983; Sample and Fisher, 1986). Fiber growth in Galice slate clearly reflects a north-south variation in finite strain during Nevadan cleavage development.

Chapter 2: THE NEVADAN OROGENY

2.1 Regional Extent

The Nevadan orogeny was first defined as plutonism, metamorphism and deformation affecting Cordilleran rocks from Alaska to Mexico (Blackwelder, 1914). Blackwelder (1914) assigned a Jurassic age to the Nevadan. Subsequently, three phases of Middle and Late Jurassic arc-type plutonism have been interpreted as Nevadan events (Lanphere et al., 1968). The Nevadan was more recently restricted to Late Jurassic deformation and metamorphism in the Sierra Nevada foothills (Bateman and Clark, 1974); a Late Jurassic age for the Nevadan in the Klamath Mountains is consistent with recent age data from syn- and post-Nevadan plutons (Harper et al., 1986). The Nevadan is best documented in the western Klamath Mountains (Harper and Wright, 1984) and in the foothills of the Sierra Nevada range (Schweickert et al., 1984; Tobisch et al., 1987).

2.2 The Western Klamath Mountains

The Nevadan orogeny mainly affected rocks in the western Jurassic belt of the Klamath province. However, further to the east, the Rattlesnake Creek Terrane (RCT) in the upper plate of the Orleans thrust probably experienced

Nevadan deformation (Snoke, 1977). Gray (1985) suggested that melanges in the RCT were "remixed" during the Nevadan. Nevertheless, Nevadan-age structures may be indistinguishable from the deformational and metamorphic effects of a recently documented Middle Jurassic (ca. 170 Ma) orogenic event (Snoke, 1977; Fahan and Wright, 1983; Gorman, 1984).

The regional-scale effect of the Nevadan in the Klamath Mountains, shown in figure 2.1 (from Wyld and Wright, 1988), was westward thrusting of the Late Jurassic Josephine ophiolite and Galice Formation over the coeval volcanoplutonic Rogue-Chetco island arc subterrane (Harper and Wright, 1984; Wyld and Wright, 1988). Thrusting of the Josephine ophiolite and peridotite over the Late Jurassic arc occurred along the Madstone thrust (Dick, 1976). To the east, the ophiolite and overlying Galice flysch were underthrust at a low angle beneath the western Paleozoic and Triassic belt (WPTB) along the Orleans fault (Klein, 1977; Jachens et al., 1986). These regional thrusts are shown in figure 1.2. Intense deformation in the Galice, and locally in the upper portion of the Josephine ophiolite, accompanied Nevadan thrusting. Large flattening strains (chapter 5) are evident from flattened pillow lavas in the southern Josephine ophiolite and foliated pebble conglomerates in the Galice. Small-scale thrusting, folding and penetrative cleavage development are prevailent in the Galice Formation

A.

ACTIVE MIDDLE
JURASSIC ARC

TRENCH

RCT   WHT

B.

ACTIVE LATE JURASSIC ARC   REMNANT ARC

CHETCO   ROGUE FM.   GALICE FM.
COMPLEX

TRENCH

RCT   JOSEPHINE OPHIOLITE   RCT   WHT

C.

NEVADAN
OROGENY   WESTERN JURASSIC BELT

RCT

RCT
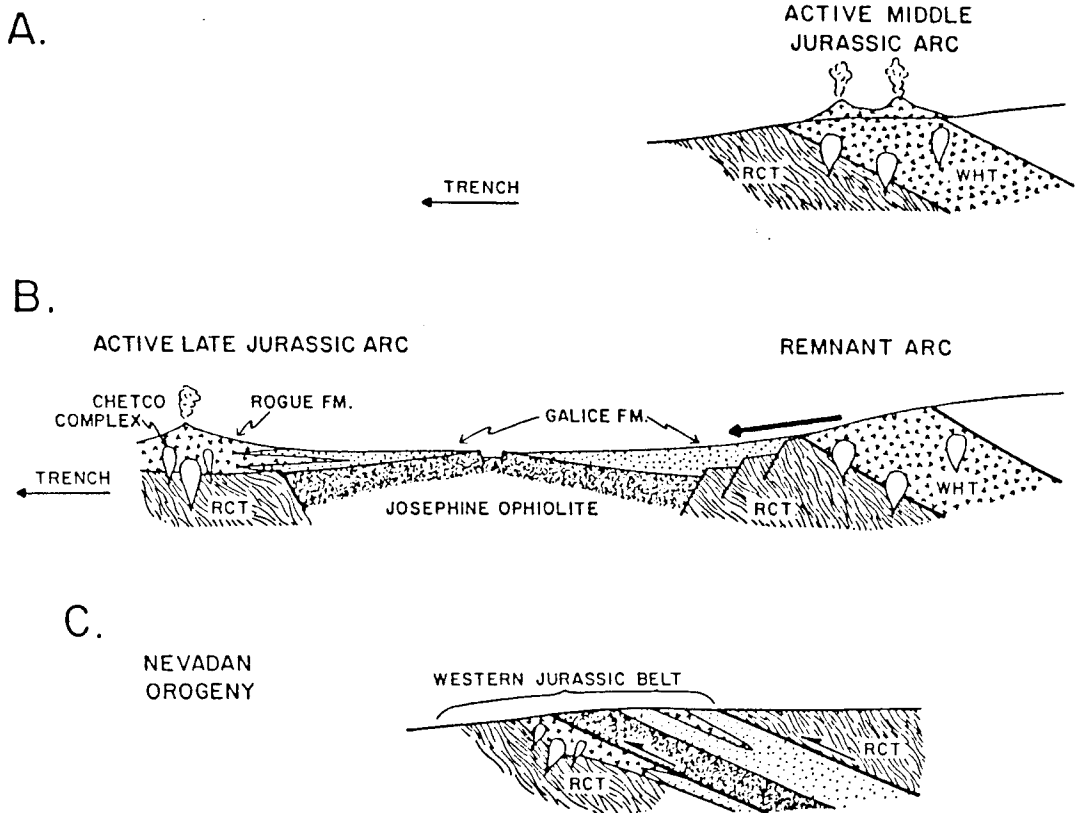
Figure 2.1   Illustration of Middle to Late Jurassic
tectonism in the western Klamath Mountains.   A. Middle
Jurassic arc (western Hayfork terrane, WHT) is built on
continental margin (Rattlesnake Creek terrane, RCT).
B. Formation of the Josephine ophiolite and Late Jurassic
arc following rifting of the older arc and its basement.
C. Following cessation of the Late Jurassic arc, imbrica-
tion of the arc, ophiolite and remnant arc occurred during
the Nevadan orogeny.

overlying the Josephine ohiolite, as well as the type-Galice and underlying Rogue Formation.

All lithologies in the western Jurassic belt experienced regional prehnite-pumpellyite to lower greenschist facies metamorphism during the Nevadan Orogeny (Harper, 1980a). Metamorphic grade increases from north to south. The transition between the prehnite-pumpellyite and lower greenschist facies occurs about 25 kilometers south of the Oregon border, roughly at the latitude of Crescent City, California (Harper and Wright, 1984).

The age of the Nevadan is well-constrained as Late Jurassic. An upper age bracket is the Oxfordian-Kimmeridgian Galice Formation, the youngest formation involved in the orogeny. Middle Jurassic plutons intruding the western Paleozoic and Triassic belt are older than the cross-cutting Orleans thrust (Gray, 1985; Jachens et al., 1986). Small calc-alkaline plutons intruding the Galice and underlying ophiolite have yielded Ar^{40}/Ar^{39} dates of 148 +/-1 Ma and 150 +/-1 Ma, respectively, and are interpreted as syn-emplacement plutons (Harper et al., 1986). 150 million-year-old dikes and sills (Saleeby et al., 1982) intruding the Galice (fig. 2.2) are typically deformed and metamorphosed along with the host rock. Two plutons intruding the Orleans thrust provided Pb/U ages of 150 +/-2 Ma and 146 +/-4 Ma (Harper et al., 1986). Plutons in the western Klamaths that are younger than 147 Ma are largely unaffected by Nevadan deformation and metamorphism.

Figure 2.2 Three meter wide felsic sill intruding vertical
slates of the Galice Formation. Exposure along Middle Fork
Smith River at intersection with Knopti Creek (fig. 1.9).
Sills in the Galice are folded with their sedimentary host
rocks.

Other important Nevadan age-constraints are the previously discussed outliers of early Cretaceous shallow marine sedimentary rocks which unconformably overlie the Galice and older terranes in the Klamaths. These rocks have been correlated with various formations of the Great Valley sequence in California, and may be as old as latest Tithonian, or about 145 Ma (Imlay et al., 1959). The above age relationships suggest that Nevadan thrust emplacement and peak metamorphism occurred in the Klamaths between 151 Ma and 147 Ma. Whole-rock metamorphic K/Ar ages of 148 +/- 2, 151 +/-4, and 153 +/-4 Ma from metagraywackes in the southern Galice are consistent with these age limits (Lanphere et al., 1978).

2.3 Nevadan Orogenesis in the Sierra Nevada

Much parallelism exists between Nevadan orogenesis in the western Klamaths and the western foothills of the Sierra Nevada range in northern and central California. The Late Jurassic Mariposa and Logtown Ridge formations, which may be southern extensions of the Galice and Rogue, were strongly deformed and metamorphosed in the Late Jurassic. The Smartville ophiolite, with published magmatic ages of 161-155 Ma (Saleeby and Moores, 1979; Saleeby, 1981), was emplaced during the Nevadan orogeny. A northwest structural trend in the northern Sierra Nevada is parallel to the structural trend in the southern Klamaths; however, the two

provinces are offset along a roughly east-west disjuncion, the "Sierra-Klamath tear". An apparent difference between the provinces is that Nevadan deformation and low-grade metamorphism affected rocks as old as middle Paleozoic in the Sierra Nevada foothills (Varga, 1985).

Nevadan structural development was more complex in the foothills of the Sierra Nevada than in the western Klamaths. West-vergent high-angle reverse faults and upright folds with a steep slaty cleavage are interpreted as the dominant Nevadan structures (Bogen et al., 1985). However, Day and others (1985) document earlier east-directed thrust faults, and interpret them as Nevadan. The direction of Nevadan thrusting and emplacement is less clear in the Sierra than in the Klamath province.

Another important difference between the Klamaths and Sierra Nevada is the age of the Nevadan orogeny. The Nevadan may be older in the Sierra Nevada (Schweickert et al., 1984; Bogen, 1984). Stratigraphic ages and ages of cross-cutting plutons constrain the Nevadan as 158 Ma to 152 Ma in the northern Sierra Nevada (Schweickert et al., 1984).

2.4 Tectonic Models for the Nevadan Orogeny

The Nevadan orogeny has been suggested to have involved the collision of one or more island arcs with the Late Jurassic continental margin (Schweickert and Cowan, 1975; Schweickert, 1981; Schweickert et al., 1984; Day et al.,

1985). Schweickert and Cowan (1975) envisioned the Nevadan as a collision of an arc/ back-arc basin/ remnant arc system with an early Mesozoic arc built on the continental margin. Their model requires the closure of an ocean basin at oppositely-dipping subduction zones, similar to modern arc convergence in the Molluca Sea, south of the Phillipine Islands (Hamilton, 1979; Silver and Moore, 1979). This model was recently simplified to involve collision of a single arc with the basement of an older continental arc (Schweickert et al., 1984). Collision during the Nevadan is proposed to be the cause of extensive shortening in pre-existing rocks along or near the Late Jurassic continental margin.

The Nevadan orogeny in the Klamath province was a short-lived event involving collapse of a Late Jurassic island arc, closure of a back-arc basin, west-directed thrust imbrication and accretion of the Late Jurassic arc and ophiolite to the continental margin (Harper and Wright, 1984). Harper and Wright (1984) proposed that this entire process took place proximal to the continental margin, within a single west-facing arc system.

It has been suggested that the Late Jurassic ophiolites in the Sierra and western Klamaths were generated by oblique spreading, roughly parallel to a truncated continental margin (Harper et al., 1985). This model is consistent with the east-west orientation of sheeted dikes in the Josephine ophiolite (Harper, 1980a), and evidence for major north-

south paleo-fracture zones beneath the Great Valley and in the Sierra and western Klamaths (Harper et al., 1985). The Late Jurassic paleotectonic setting of the Sierra-Klamath orogen is illustrated in figure 2.3. Nevadan convergence at a high angle to the continental margin may have resulted from an abrupt change in relative plate motion between the Farallon and North American plates. Large magnitudes of crustal shortening in the Klamaths and Sierra Nevada orthogonal to the continental margin favor high-angle convergence rather than a strike-slip dominated transpressive regime, as suggested by Saleeby (1981).

The expression of the Nevadan orogeny apparently differs significantly in the Klamaths and Sierra Nevada. Ingersoll and Schweickert (1986) note several important discrepencies:

1. There may be a significant age difference as noted above.

2. The Mariposa Formation, unlike the Galice, is interpreted as synorogenic flysch that was deposited in an active trench (Bogen, 1984).

3. Different litho-tectonic terranes were accreted in the Sierra region during the Nevadan orogeny. For example, the Nevadan apparently involved accretion of two island arc systems with intervening ophiolite and marine basinal sedimentary/volcanoclastic rocks (Schweickert and Cowan, 1985).

Figure 2.3 Late Jurassic paleotectonic setting of
northern California showing inferred orientations of
spreading centers, subduction zones and transform faults
with respect to the continental margin. (after Harper
and others, 1985, fig. 5)

4. It is highly uncertain whether Middle to Late Jurassic terranes in the western Sierra Nevada were obducted onto, or thrust beneath, the continental margin.

Strict parallelism between the Late Jurassic tectonic history of the Sierra Nevada and the Klamath Mountains remains controversial. Clear definition of a "Sierra-Klamath link" awaits better geochronologic control on accretionary and deformational events, particularly in the northern Sierra Nevada.

This thesis examines the deformational effects of regional convergence during the Nevadan orogeny. Although the focus is on the structure of a single formation, the deformational succession in the Galice has an important bearing on models for Late Jurassic accretion of island arc and ophiolite terranes in the Klamath Mountain province (Dick, 1976; Harper and Wright, 1984; Gray, 1985; Wyld and Wright, 1988).

Chapter 3: PRE- AND EARLY TECTONIC STRUCTURES

This chapter includes a discussion of those structures in the Galice Formation that appear to pre-date Nevadan folding, cleavage development and thrusting. These structures formed while the sediments were unlithified or incompletely lithified. Various lines of evidence in support of this conclusion are presented throughout this chapter. Although most of the structures are considered "pre-tectonic", the possibility of an early, pre-D_1 phase of tectonic deformation is also considered.

3.1 Penecontemporaneous Deformation

In the Galice Formation, as in most other tectonically deformed sedimentary sequences, it is important to make a distinction between hard-rock and soft-sediment or "penecontemporaneous" structures. Mistakenly interpreting soft-sediment folds as tectonic in origin introduces obvious errors into structural analysis of folding. For this reason, geologists have introduced several criteria, based on field observations, which help in this distinction (Rettger, 1935; Nevin, 1949; Potter and Pettijohn, 1963; Hobbs et al., 1976). From a lengthy list, Hobbs and others (1976) cite three criteria which, when used singly, provide

conclusive evidence for either soft-sediment or hard-rock folding:

(1) Existence of undeformed animal burrows in folded rocks implies soft-sediment folding.

(2) Bending of a metamorphic foliation around fold closures is evidence for hard-rock folding.

(3) A systematic relationship between strain of fossils and their position in the folds (e.g. Geiser, 1974) provides conclusive evidence for hard-rock folding.

Penecontemporaneous folds are defined as those which form in a sedimentary environment at approximately the same time as deposition. Thus, their development is thought to precede lithification. There could, however, be a complete gradation between folds formed in unlithified sediment and those formed in hard rock (Williams et al., 1969; Hobbs et al., 1976). The common conception that soft-sediment folds are non-tectonic may also be questionable (Potter and Pettijohn, 1963).

Penecontemporaneous folds are sometimes equated with "slump folds"--those which presumably form by sliding of a layer down an inclined surface with eventual crumpling at the base. Another type of penecontemporaneous structure is convolute lamination. This chaotic feature results from seismic disturbance of unconsolidated bedding laminae. However similar disruption may be produced as currents flow over the sediments (Potter and Pettijohn, 1963).

Slump features are often restricted to a single bed, or group of beds, within a particular stratigraphic horizon (Williams et al., 1969; Helwig, 1970). Folds may be truncated by undeformed beds parallel to a planar erosional surface (Potter and Pettijohn, 1963). Slump folds are commonly found in highly disturbed packets of strata, separated from undeformed beds by "planes of sliding" (Helwig, 1970). Groups of chaotic folds in which neighboring folds have different orientations and geometries have been cited as evidence for penecontemporaneous deformation (Rettger, 1935).

Soft-sediment Folds

Folds which satisfy some of the criteria mentioned above are found in the Galice Formation, particularly in the structurally complex outcrops along the Illinois River (fig. 1.7). Figure 3.1 is interpreted as a slump fold in which thinly-laminated shale is sharply truncated against part of a graywacke bed. The fold is intrafolial, as it is contained between two graywacke beds, and appears to be restricted to a specific bedding horizon.

Figure 3.2A is a hand sample of other intrafolial folds contained within a single bed. The sample's position in the bed, as well as the relative attitude of the regional S_1 cleavage, is shown in figure 3.2B. Bedding is highly disrupted, particularly in the core of the synform. Dark

Figure 3.1 Slump fold in shale beds and graywacke along West Fork Illinois River. The shale beds are truncated against the graywacke bed at the arrows. Younging direction from adjacent beds is "upwards" in the photo. Lens cap is 5 cm wide.
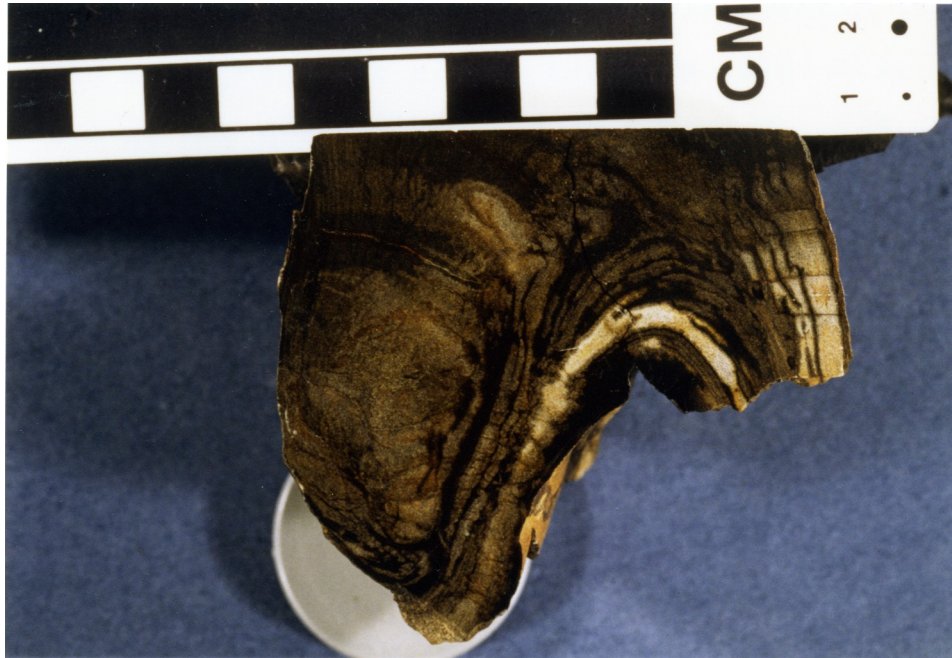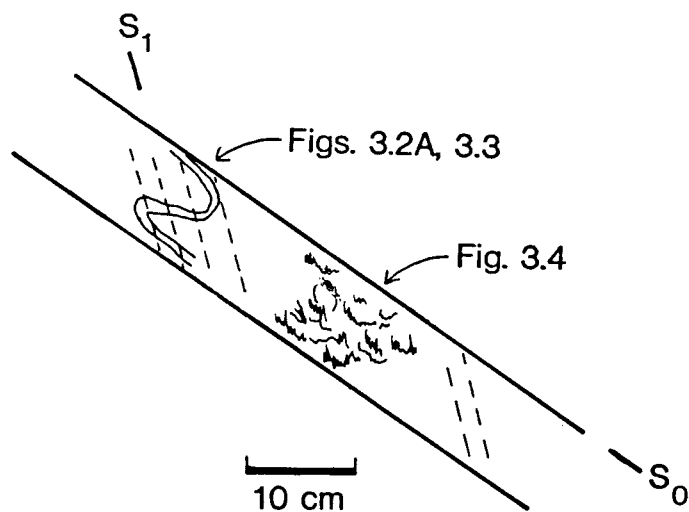
Figure 3.2 A. Hand sample of internally disrupted soft-sediment folds of bedding laminae. B. Sketch showing relative positions of samples shown in figures 3.2A, 3.3 and 3.4 in a single bed from an exposure approximately 6 km northeast of Kerby, Oregon. Bedding and cleavage (S_o, S_1) are indicated. View is to the north.

pelitic laminae are chaotically dispersed and cross-cut more quartzose layers. This cross-cutting relationship is more obvious in a thin-section of the antiform (fig. 3.3). Figure 3.3 is cut normal to the fold axis and axial plane. The foliation in the pelitic zones is parallel to, and morphologically resembles, the S_1 cleavage observed at the sample locality. An adjacent sample from the same bed (fig. 3.4) shows no folding, but contains irregular, discontinuous pelitic laminae which appear "stylolitic". The stylolitic spikes are, in fact, S_1 cleavage folia. These relationships are illustated in figure 3.2B. The Nevadan cleavage transects the axial planes of the folds; thus, the folds are interpreted as pre-Nevadan.

Axial-planar cleavages are known to occur with penecontemporaneous fold structures (Williams et al., 1969; Newell et al., 1972; Woodcock, 1976). However, no preferred orientation of mineral grains or cleavage folia were found parallel to the axial planes of soft-sediment folds in the Galice Formation. Furthermore, a regional tectonic cleavage, S_1, transects the early folds, similar to the findings of Helwig (1970) from penecontemporaneous folds in Newfoundland. More recently, however, the choatic zones of folding studied by Helwig (1970) have been interpreted as tectonic zones of detachment (P.F. Williams, fide W.S.F. Kidd).

Dispersed pelitic material and contorted beds (fig. 3.3) probably suggest that the rocks were not completely

Figure 3.3 Thin-section showing detail of the antiform in figure 3.2A. The section is cut normal to the fold axis and axial plane. S1, oriented upper left to lower right, apparently transects the axial plane. Photograph is about 2 cm wide.

Figure 3.4 Hand sample taken from the same bed as the folds in figure 3.2A (see fig. 3.2B for relative position). Bedding, subparallel to the top and bottom edges, is internally disrupted. S1 is present as "pseudostylolitic" spikes in thin, discontinuous pelitic laminae.

lithified at the time of folding. Furthermore, the folds are strictly local, and small-scale intrafolial folds, with wavelengths on the order of a few centimeters, were not observed in any other graywacke beds. Internal disruption of bedding laminae could have resulted from local sediment liquefaction and injection.

3.2 High Fluid Pressure and Early Deformation Mechanisms

Overpressuring occurs in thick sedimentary sequences when the pore-fluid ratio (λ) is greater than about 0.46 (Hubbert and Rubey, 1959). The λ ratio, not to be confused with a principal strain, is defined as P_f/σ_n, where P_f is the pore-fluid pressure, and σ_n is the total normal stress exerted by the rock (+ fluid) column. Hubbert and Rubey (1959) first recognized that overpressuring can greatly reduce basal sliding friction along large thrust detachments, allowing horizontal movement of thick rock masses over great distances. This concept has been incorporated into many recent models for development of foreland fold-and-thrust belts and accretionary complexes (Cowan and Silling, 1978; Davis et al., 1983). Chapple (1978) predicted that structural thickening in a thrust belt would halt basal sliding if the pore-fluid pressure across the surface did not significantly exceed the hydrostatic pressure. Pore-fluid pressure has the effect of weakening the rock (reducing basal shear stress) by decreasing the

effective confining pressure. The Galice Formation had the following characteristics which, according to Hubbert and Rubey (1959), would have favored high fluid pressures:

(1) Compactible pelitic beds serving as impermeable caps, interlayered with permeable sandstone (fluid reservoirs).

(2) A total sedimentary thickness in excess of 2,000 meters. While the Galice may not have been this thick immediately after deposition, it was probably structurally thickened by thrusting prior to complete dewatering.

(3) Periods of rapid sedimentary or tectonic loading. Massive graywacke and pebble conglomerate units probably indicate high depositional rates during short time intervals.

The onset of underthrusting of the Josephine ophiolite and overlying Galice flysch probably occurred while pore-fluid pressures were reasonably high. Geochronological evidence suggests that the Galice was deformed shortly after deposition (Harper et al., 1986). Calc-alkaline dikes, as young as 150 Ma, intruded poorly lithified sediments in the Galice (Harper, 1980a).

Late Jurassic underthrusting of the Galice and its ophiolitic basement is broadly analogous to underthrusting beneath an overriding plate at low-angle subduction zones. A modern analogue is the Lesser Antilles subduction complex. Rapidly deposited turbidites, transported from Venezuelan river deltas, are presently being subducted at a very low angle beneath older rocks of the Barbados accretionary

complex (Karig and Sharman, 1975). A zone of overpressured sediments occurs beneath a basal decollement of the the overriding plate (fig. 3.5). Fluid is interpreted to be migrating in advance of the wedge causing overpressuring and formation of decollements and mud volcanoes (Westbrook and Smith, 1983). Seismic profiles suggest that deformation within the underthrust sediment pile is restricted to sliding along bedding-parallel detachment faults connected by a small number of ramps (Biju-Duval et al., 1982).

The Galice Formation probably behaved similarly during early stages of Nevadan underthrusting. Layer-parallel sliding along overpressured horizons connected by ramps is suggested to be the dominant deformational mechanism. Thrusting relatively impermeable rocks (the diverse assemblages of the western Triassic and Paleozoic belt) over the Galice Formation could have had the effect of <u>increasing</u> its pore-fluid pressure, further retarding dewatering of the sediments. Early thrust-related structures are not recognized in the Galice, although they may be confused with later thrusts. The following section is a discussion of pre-tectonic structures which formed in response to high pore-fluid pressures.

3.3 Sediment Dewatering

The concept that regional slaty cleavage forms during tectonic dewatering of poorly lithified sediment was first
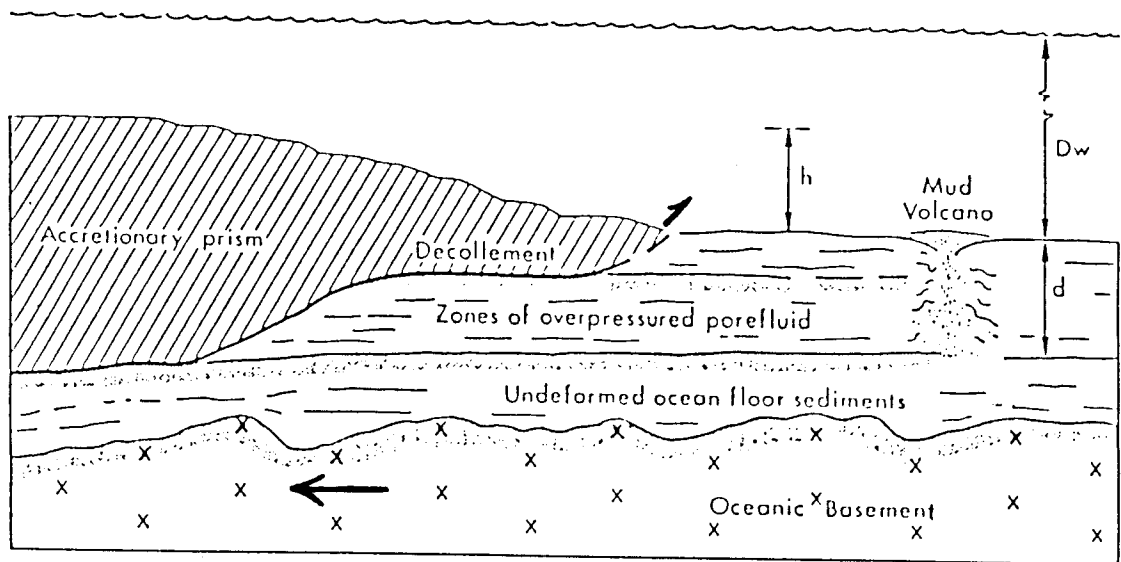
Figure 3.5 A speculative modern analogue for early under-
thrusting of the Galice Formation beneath the Late Jurassic
continental margin. Sketch shows low-angle thrusting of
a thick turbidite sequence beneath the older accretionary
prism forming the Barbados ridge in the Caribbean. (after
Westbrook and Smith, 1983) See text for details.

suggested by Maxwell (1962). This paper has sparked perhaps the largest controversy among structural geologists studying slaty cleavage development. Maxwell (1962) proposed that slaty cleavage is produced by preferred alignment of detrital mica grains during unidirectional tectonic dewatering of sediments. The strongest premise of Maxwell's (1962) argument is that clastic (sand) dikes are always strictly parallel to slaty cleavage, thus the two are coeval and genetically related. A host of geologists have supported this theory, citing evidence from various slate belts (see Geiser, 1975, and Beutner, 1980, for extensive reference lists).

Harsh criticism of the "dewatering hypothesis" has risen from findings that clastic dikes are generally not parallel to cleavage when viewed in three dimensions (Geiser, 1975; Beutner, 1980). Clastic dikes are soft-sediment structures, and are commonly folded by strains associated with cleavage development (Boulter, 1974; Geiser, 1975; Gregg, 1979). Near-parallelism of some dikes and cleavage can result from rotation of the dikes by tectonic strains (Groshong, 1976; Borradaile, 1977). Furthermore, Beutner and others (1977) showed that slaty cleavage and related folds deform laminated fault-veins which formed during hard-rock folding. A causal relationship between clastic dikes and slaty cleavage is further invalidated in light of detailed studies on the origin of slaty cleavage (e.g. Holeywell and Tullis, 1975; Groshong, 1976; Beutner,

1978; Wright and Platt, 1982; and many others). Therefore, strong evidence suggests that clastic dikes in pelitic flysch sequences were injected prior to complete lithification, before regional penetrative cleavage development.

Clastic Dikes and Liquefaction

Sandstone dikes are relatively uncommon in the northern Galice; only three outcrop-scale dikes were observed. Clastic dikes mark locations of fissures that filled with sediment either by forceful injection of a sediment/water mixture (Smith and Rast, 1954), or by penecontemporaneous sediment in-filling (Smith, 1952). The variable morphologies and modes of occurrence of clastic dikes has produced contoversy over their origin (see discussions in Powell, 1969; Dionne and Shilts, 1974). In the Galice, as in many other flysch belts, clastic dikes appear identical in composition to other graywacke beds.

All dikes, when viewed in two-dimensional exposures, are oblique to the S_1 cleavage (figs. 3.6, 3.7). One of the dikes is folded (fig. 3.6); the axial trace of the folds is approximately parallel to the trace of S_1. The dike in figure 3.6 begins as a clastic sill and cuts up-section as a dike. Clastic dikes are known to be folded by differential sedimentary compaction between the dike and its host sediment (Donovan and Foster, 1972; Boulter, 1974; Boulter,
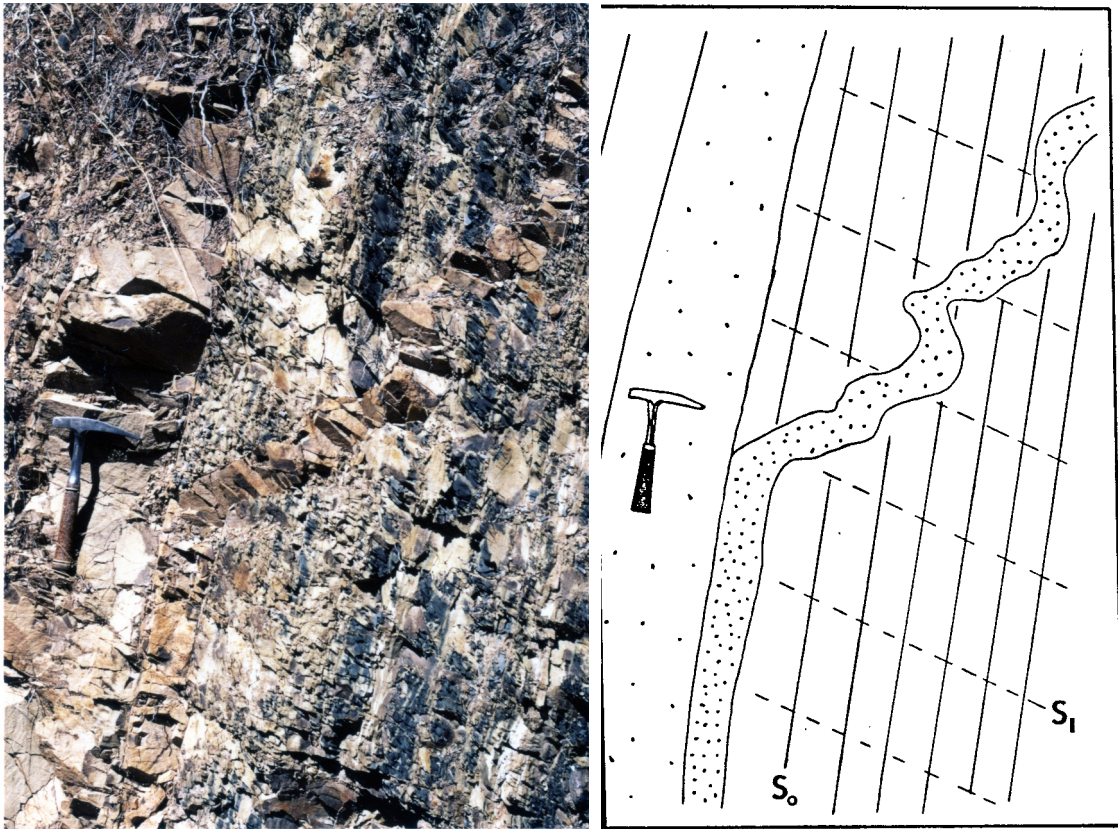
Figure 3.6   Photograph and sketch of a folded graywacke
dike/sill.   The dike cuts up-section into pelitic beds
near the hammer.   Younging direction is to the right.   Ex-
posure near Reeves Creek Road.

Figure 3.7 30 centimeter-wide clastic dike transecting vertical bedding and the bedding-parallel cleavage in an exposure along Reeves Creek Road. As in most large wacke beds in this area, the dike is unaffected by Sl.

1983). However, the orientations of folds in the dike shown in figure 3.6 suggest that the dike was probably folded during S_1-related shortening. The dikes observed near Kerby, Oregon are "isotropic", in that they do not possess primary or secondary foliations.

Small-scale disruption of bedding is frequently encountered in thinly-laminated rocks. Figure 3.8 shows obliteration of bedding laminae, presumably where sediment liquefaction occurred. The disrupted regions in figure 3.8 have a greater pelitic content than the adjacent graywacke layers. This suggests local mixing of thin, pelitic laminae with the more quartz-rich sandstone layers. S_1 clearly overprints the disrupted zones in figure 3.8. These may be soft-sediment injection features formed by local migration of a sediment/fluid mixture or "liquefaction". However, because of the small size and weakly-defined boundaries of the structures in figure 3.8, they may be have formed by bioturbation.

Other soft-sediment features commonly found in the Galice Formation are isolated round blobs or "pseudonodules" of coarse-grained graywacke in pelitic beds. They are interpreted as sedimentary load features which separated from the bases of wacke beds prior to lithification. The blobs possess a weak foliation that is parallel to S_1 in the pelitic beds; therefore, separation and isolation of the pseudonodules preceded S_1 development.
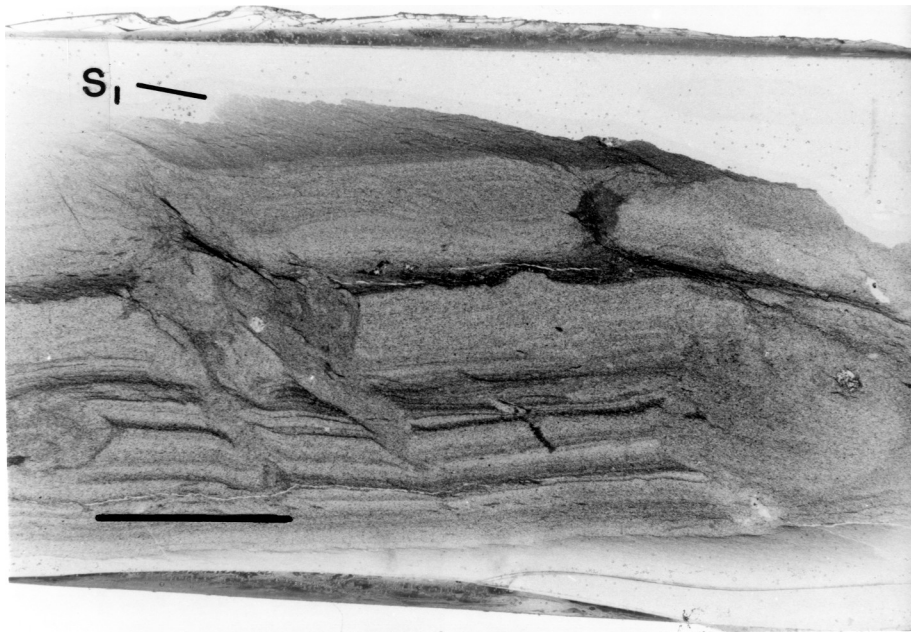
Figure 3.8 Local obliteration of bedding (horizontal in photo) by sediment liquefaction and injection or bioturbation (?) in interlaminated shale, siltstone and graywacke. S1 is developed in pelitic bed at top of photo. Younging direction is upwards. Scale bar=1 cm.

3.4 Melange Zones

Narrow zones of intense stratal disruption are typical in some exposures in the Galice Formation. The best examples are in the horizontal outcrops along the West Fork Illinois River, approximately 0.5 kilometers north of Pomeroy Dam (see ref. map- fig. 1.6). In these zones, subrounded blocks of graywacke are surrounded by shale (fig. 3.9). Tight small-scale folds are sometimes found in the shale matrix. The zones are 2-5 meters wide, and are bounded on each side by coherent strata. Individual graywacke beds in the zones are difficult to reconstruct from the isolated blocks. The term "melange" has frequently been used in descriptions of similar block-in-matrix geometries (Hsu, 1968; Silver and Beutner, 1980).

The zones of stratal disruption in the Galice Formation are comparable to "type 1" melange (Cowan, 1985) observed in the Franciscan assemblage of western California and Oregon. Type 1 melange consists of dismembered beds of sandstone in a pelitic matrix ("broken formation" of Hsu, 1968). Sandstone blocks tend to be crudely aligned parallel to original bedding, and the melange contains no exotic fragments. Blocks are either completely isolated or show pinch-and-swell structure. Type 1 melange generally occurs in tabular zones; they are grossly parallel to, and bounded by, less deformed or undeformed beds. Type 1 melange has
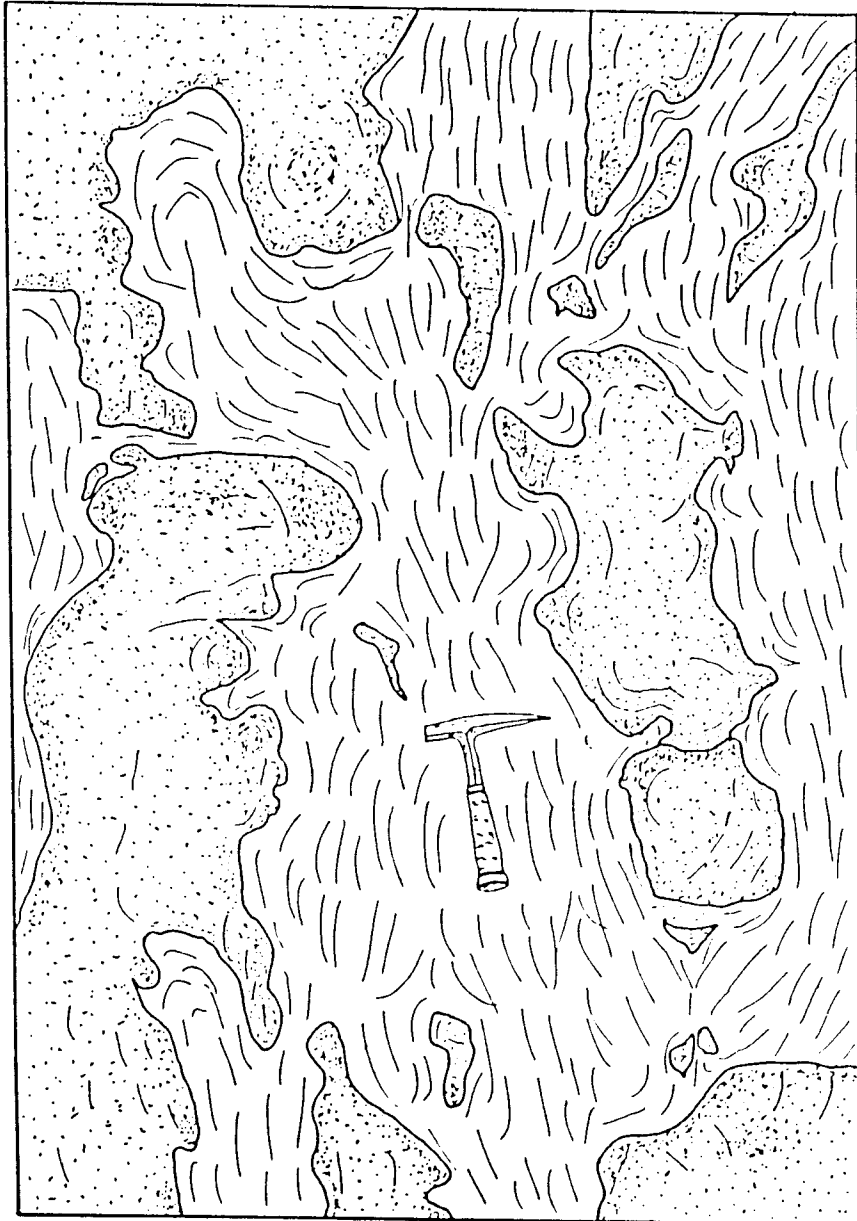
Figure 3.9 Tracing from a photograph of a horizontal
exposure of subrounded graywacke blocks in a shaly matrix
(type 1 melange of Cowan, 1985). The foliation in the
matrix (vertical in this outcrop) appears to be an
original bedding-plane fissility that was disrupted during
melange formation. Exposure located along West Fork
Illinois River, 0.5 km north of Pomeroy Dam.

been attributed to in-situ disruption of poorly-lithified
sediments by extensional processes (Cowan, 1985).

The absence of extensional faults or veins in the
Galice melange shown in figure 3.9 suggests that it formed
at a time when the sediments were insufficiently lithified
for brittle fracture. In the northernmost Galice Formation,
such ductility cannot be attributed to extension under
metamorphic conditions. The strong fissility in the shaly
matrix is interpreted as a disrupted equivalent of primary
bedding.

Melange in the Galice Formation, a largely ductile
feature, is sometimes distinguishable from layers disrupted
by fault-accomodated extension (fig. 3.10). It is difficult
to determine the relative timing of these brittle
extensional structures in the northern Galice. They may be
related to regional post-Nevadan normal faulting.
Alternatively, they may have formed soon after
lithification.

Some possible explanations for bedding-parallel
extension (see figure 3.11 A-D), assuming an early stage of
development, include the following:
(1) Gravitationally-induced lateral spreading. Beds are
pulled apart radially during rapid episodes of load-induced
dewatering. While pelitic layers may be rapidly compacted,
the presence of pore-fluid in graywacke beds delays
compaction, and serves to weaken the layers.

Figure 3.10 Layer-parallel extension by boudinage and
extensional faulting in an exposure along West Fork Illinois
River. Note well-defined faults in laminated pelites.
Length of photo is approximately 1 meter.
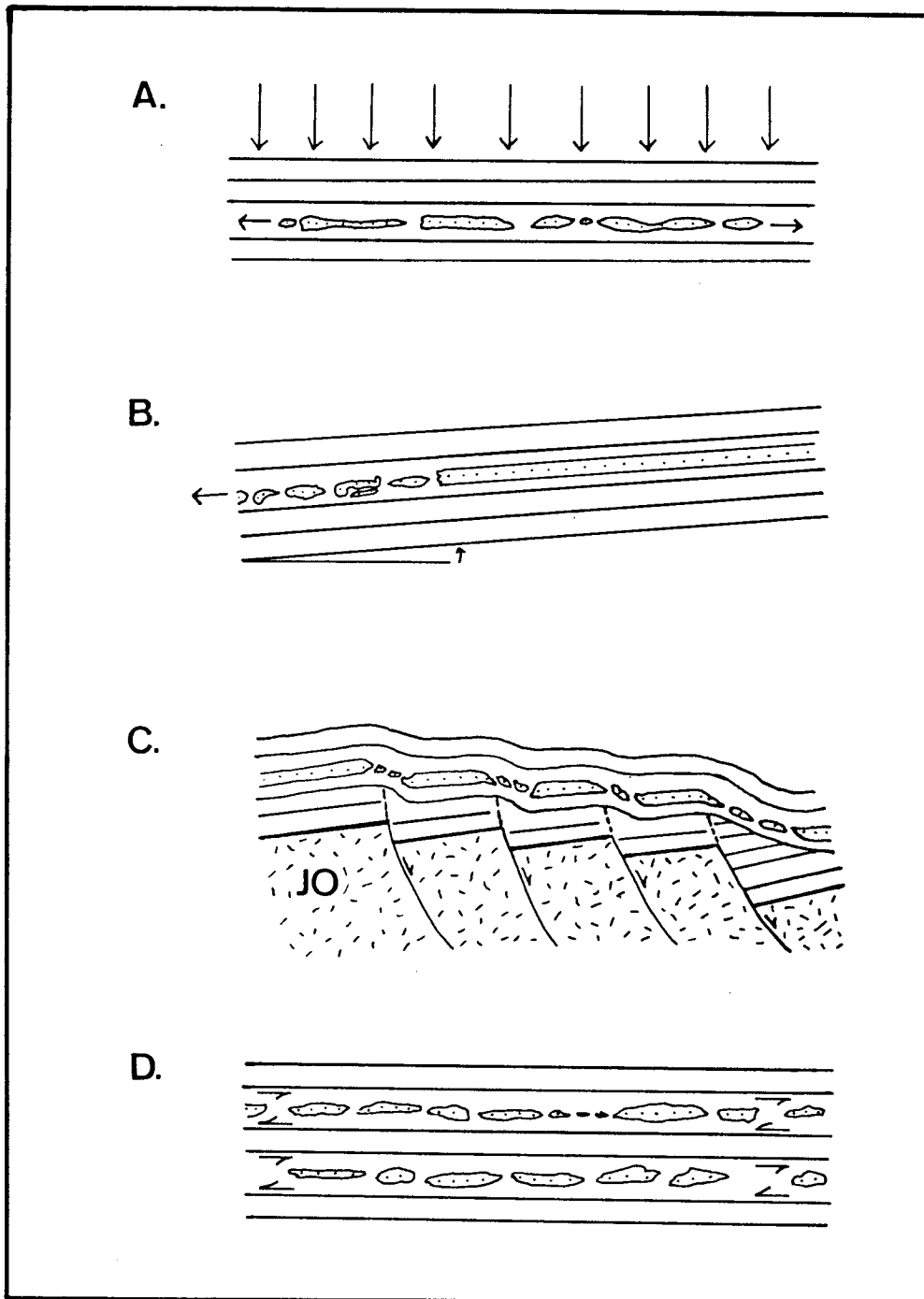
Figure 3.11 Schematic sketches showing four possible settings for early boudinage and melange development. A. Lateral spreading from sedimentary and/or tectonic loading. B. Down-slope gravitational sliding. C. Extension above oceanic normal faults in ophiolitic basement. D. Layer-parallel shearing. See text for discussion.

(2) <u>Gravitational</u> <u>sliding</u> or slumping. Contrasts in density and fluid content cause disruption of layers by differential down-slope movement.

(3) <u>Normal</u> <u>faults</u> in ophiolitic basement. Oceanic normal faults in the Josephine ophiolite cause local extension of overlying sediments. Extension in the Galice possibly occurred as a result of gravitational instability (draping effect) above large normal faults. If the faults did not appreciably cut through the Galice, extension of some beds may have resulted from compactional variations directly above fault offsets in the ophiolitic basement.

(4) <u>Layer-parallel</u> <u>shearing</u>. Early tectonic bedding-parallel sliding results in boudinage of some beds.

These concepts are schematically illustrated in figure 3.11 A-D. It is uncertain whether local extension of bedding occurred during an early stage of underthrusting of the Josephine ophiolite and Galice Formation. Fisher and Byrne (1987) describe similar extensional structures in an ancient sequence of underthrusted turbidites exposed on Kodiak Island, Alaska, which formed by layer-parallel shear (fig. 3.11 D) <u>combined</u> with vertical loading (fig. 3.11 A). Nevertheless, pre-tectonic, syn-sedimentary origins for early extension in the Galice (figs. 3.11 A,B) are equally plausible. Extension of horizontal strata by load-induced radial spreading is not favored in the Galice, as there is an apparent room-problem unless compressional structures develop simultaneously.

3.5 Discussion

Structures that are unequivocally soft-sedimentary (folds, disrupted bedding) are not widespread in the Galice Formation. They were only observed in the northern field area (fig. 1.6). The "hard rock" nature of D_1 structures (discussed in chapter 4) suggests that the Galice was completely lithified at the time of Nevadan deformation.

It is conceivable, however, that initial Nevadan shortening occurred while the sediments were incompletely lithified. Pre-cleavage injection structures like clastic dikes (figs. 3.6, 3.7) suggest fluid/sediment mobility and locally high pore-fluid pressures. Early underthrusting of the Galice beneath the western Paleozoic and Triassic belt may have involved layer-parallel sliding along overpressured decollements in the Galice. Based on evidence from multi-channel seismic profiles, sliding along layer-parallel decollements was interpreted as an early deformation mechanism in a young turbidite sequence underthrust beneath the Barbados accretionary complex (Biju-Duval et al., 1982; Westbrook and Smith, 1983).

The Galice Formation largely consists of coherent strata; melange (fig. 3.9) is rare and restricted to bedding-parallel zones. Early deformational structures observed in accretionary complexes such as "web" structure, shear foliations defined by microfaults and mappable melange

zones (Byrne, 1984) are absent in the Galice Formation. This suggests that initial shortening in the Galice was not accompanied by intense shearing. Indeed, as emphasized in chapter 6, shearing occurred <u>late</u> in the deformation history.

Chapter 4: MAIN-PHASE NEVADAN STRUCTURES

4.1 F_1 Folds

F_1 folds in the Galice Formation have been defined as those possessing a weak to strong axial-planar S_1 cleavage (Snoke, 1977; Harper, 1980a). They are clearly the first generation of widely-distributed folds. Snoke (1977) termed F_1 folds "metamorphic folds" to distinguish them from a second generation of folds, F_2, which lack a penetrative axial-planar slaty cleavage. The S_1 foliation is folded in F_2 hinge zones, while it is always axial-planar to F_1 folds. Most F_1 folds are observed at the outcrop scale, although a few larger-scale folds were identified from bedding-cleavage relationships.

F_1 in the Northern Study Area

F_1 folding is widespread in exposures of the northern Galice in the vicinity of Kerby and Cave Junction, Oregon (fig. 1.6). The folds are, however, localized in small groups or fold-pairs. Fold styles vary widely, as evident from figures 4.1 and 4.2. In the Cave Junction area, F_1 folds range from open to very tight. The open folds (fig. 4.1) are parallel folds, geometrically resembling class 1C folds of Ramsay (1967). They have rounded profiles and
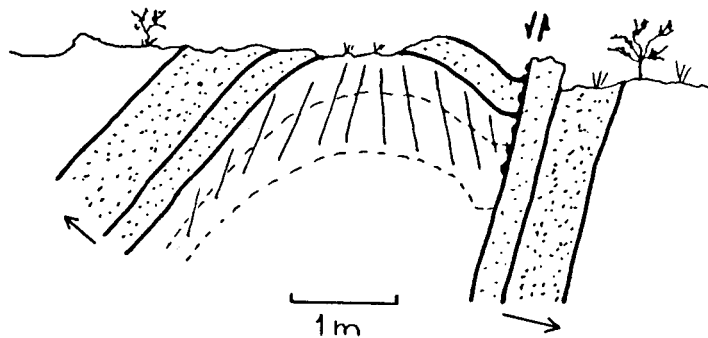
Figure 4.1 Open Fl anticline exposed along East Fork Illinois River near Cave Junction, Oregon. Sl forms a weak pencil structure in the shale beds and shows weakly divergent fanning. Pencil long axes are parallel to the fold axis. Note that the anticline is cut by a normal fault to the right of the hammer. Load casts indicate that the steeply-dipping graywacke beds are overturned. Arrows show the younging direction.
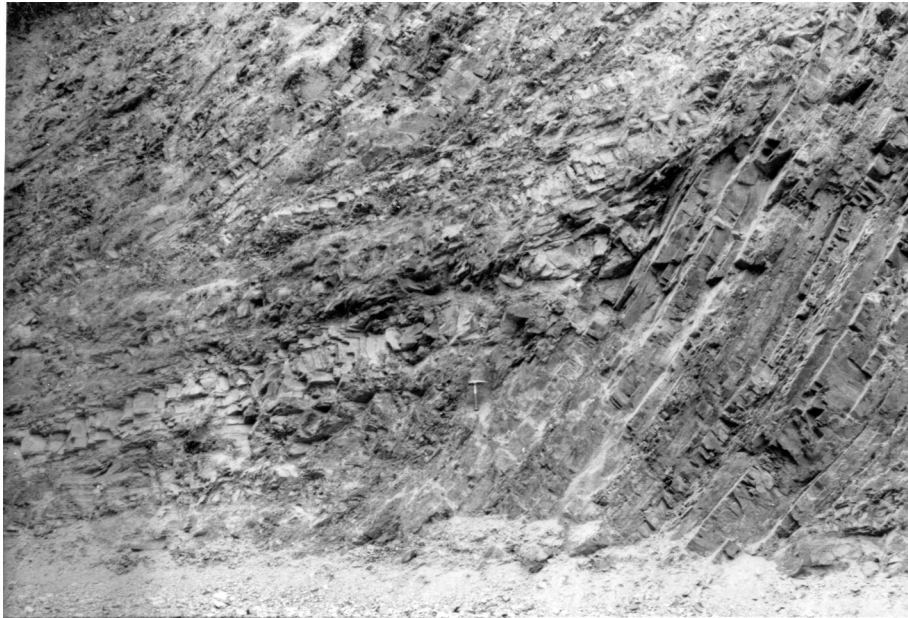
Figure 4.2 (top) Tight, angular F1 folds in a steep road-cut, 3 kilometers south of Lake Selmac, Oregon. Folds are overturned to the northwest. Hammer in center of photograph for scale.

Figure 4.3 (bottom) Slightly overturned F1 syncline exposed along Siskiyou Fork Smith River, 4 kilometers west of the Preston Peak thrust. Note ideal similar fold geometry. Parasitic folds are seen to the immediate left of the hammer.

frequently exhibit weakly-developed pencil structure in pelitic beds (fig. 4.1). In contrast, the majority of F_1 folds in the northern field area are tight or isoclinal, asymmetric, and have angular profiles with interlimb angles of less than 70° (fig. 4.2). S_1 is weakly to moderately developed in folded pelitic beds. Graywacke beds do not normally possess the S_1 cleavage in the northernmost Galice Formation, but rather have spaced fractures perpendicular to bedding. Moderate hinge thickening occurs in most pelitic beds in F_1 fold hinges.

$\underline{F_1}$ $\underline{in}$ $\underline{the}$ $\underline{Southern}$ $\underline{Study}$ $\underline{Area}$

South of Oregon Mountain Road in northern California (see fig. 1.9), F_1 folds are predominantly tight to isoclinal. In profile, they range from class 2 to class 3 similar folds (Ramsay, 1967), showing substantial hinge thickening and limb attenuation in most beds. Strong S_1 development, combined with an absence of bedding markers, frequently obscures the presence of tight F_1 folds in Galice slates. F_1 fold closures are rarely observed in exposures south of Oregon Mountain Road (Harper, 1980a; Wyld, 1985; this study). Figure 4.3 is one of few F_1 fold closures observed in the southern field area.

F_1 folds are typically overturned or show asymmetry to the west or northwest. Western limbs of the folds are normally shorter, and dip steeper, than the eastern limbs.

At least 70% of outcrop-scale F_1 folds in the Galice are northwest facing, in the sense of Shackleton (1958). All folds face upwards; that is, no F_1 axial planes have been rotated past horizontal by refolding or other modes of rotation. "Upside down" folds could conceivably exist, as several nearly recumbent F_1 folds were observed in both northern and southern field areas.

Stereographic projections of poles to bedding (fig. 4.4) show that overturned beds are evenly distribbuted among upright beds and are much less common. With few exceptions, beds have northeast-southwest strikes and dip southeast. Rotation of beds around F_1 fold axes (fig. 4.6B) did not cause extensive dispersal of points into eastern quadrants. The near coincidence of maxima of poles to upright and overturned beds (fig. 4.5) suggests that large-scale F_1 folds are, in a large part, tight to isoclinal with southeast-dipping axial surfaces. Like bedding, S_1 cleavage planes generally dip to the southeast, further suggesting tight, asymmetric F_1 folding (fig. 4.6A). Post-F_1 rotation is evident from north-south and northeast-southwest scatter in poles to bedding (fig. 4.4), poles to S_1 (fig. 4.9A) and F_1 fold axes (fig. 4.6B).

F_1 Fold Axes

Figure 4.6B is a stereographic projection of F_1 fold axes measured from bedding-cleavage intersections (L_{OX1}),

⊥ S_o CONTOURED

N

⟨⟩ UR
⟨⟩ OT

>6% DATA PTS. PER 1% AREA
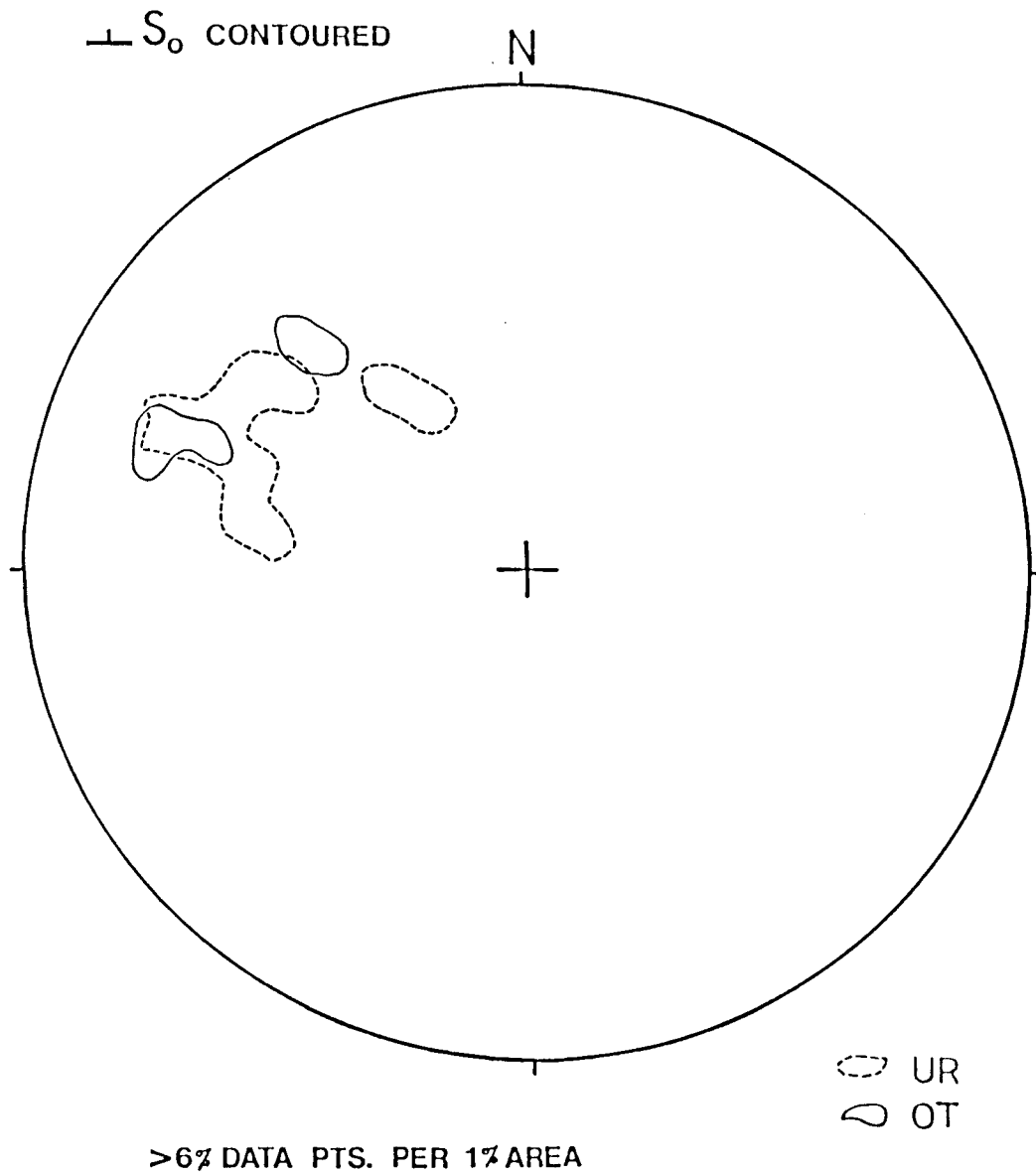
Figure 4.5 Contoured maximum concentrations of poles to upright (dashed) and overturned (solid) beds. Data from northern and southern field areas are combined. Two separate maxima occur in both upright and overturned beds. Total number of points contoured is 271--230 are upright, 41 are overturned.

and directly from outcrop-scale F_1 hinges. The axes are widely dispersed in the northeast and southwest quadrants. A weak concentration of points has a south-southwest trend, and an average plunge of 30°. Figure 4.6B is a combination of F_1 fold axes from the northern and southern field areas. No distinct groupings of points were found in data from either field area. Groupings of axes from certain regions or "domains" are not apparent from F_1 data.

Northeast-southwest dispersal of F_1 fold axes may be the result of rotation by northwest-trending post-Nevadan folds; however, there is no field evidence from this study to support this suggestion. Furthermore, F_2 fold axes, discussed in chapter 6, have similar orientaions to F_1 axes, so that refolding of F_1 axes is improbable. Small F_1 folds at a single locality sometimes have axes which plunge northeast and southwest in the absence of later folds, suggesting primary non-cylindrical geometries.

Rotation by northwest-trending high-angle faults is an equally plausible explanation for dispersal of F_1 axes. Tilting or flexure along post-Nevadan faults could have caused dispersal of pre-existing Nevadan structures. A tight grouping of early fold axes is not expected over a large, multi-deformed region. F_1 axes were undoubtedly reoriented by Post-Nevadan faulting in the northern area shown in Plate 1. The orientations of F_1 axes are, however, somewhat consistent across small, unfaulted sections of the Galice. From figure 4.6B, it can be presumed that F_1 folds

A.

⊥ S₁   N

n=50

B.

F₁   N

n=65
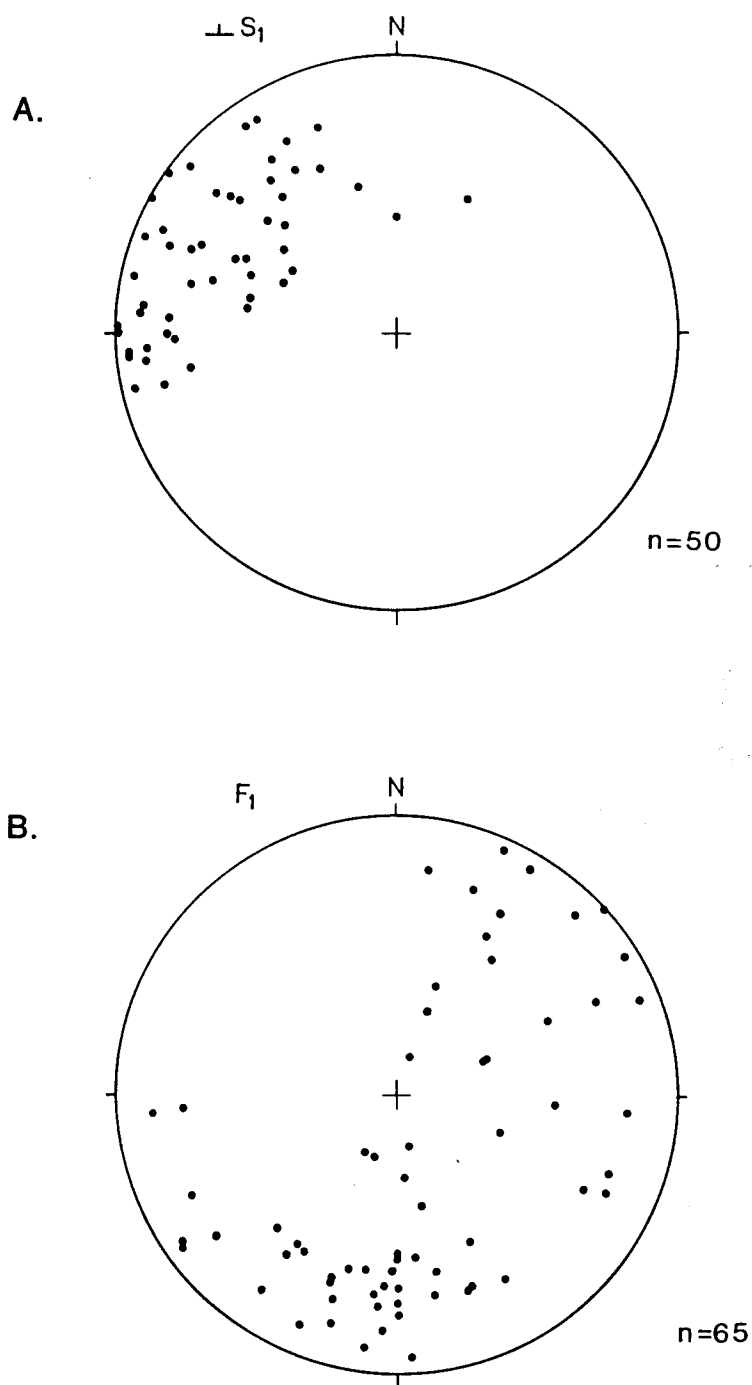
Figure 4.6 A. Lower hemisphere projection of poles to S1.
B. Projection of F1 fold axes. Data from both field areas
are combined on each stereonet.

and directly from outcrop-scale F_1 hinges. The axes are widely dispersed in the northeast and southwest quadrants. A weak concentration of points has a south-southwest trend, and an average plunge of 30°. Figure 4.6B is a combination of F_1 fold axes from the northern and southern field areas. No distinct groupings of points were found in data from either field area. Groupings of axes from certain regions or "domains" are not apparent from F_1 data.

Northeast-southwest dispersal of F_1 fold axes may be the result of rotation by northwest-trending post-Nevadan folds; however, there is no field evidence from this study to support this suggestion. Furthermore, fold axes, discussed in chapter 6, have similar orientations to F_1 axes, so that refolding of F_1 fold axes is improbable. Small F_1 folds at a single locality sometimes have axes which plunge northeast and southwest in the absence of later folds, suggesting primary non-cylindrical geometries. Alternatively, the northeast-southwest dispersal of F_1 axes may reflect reorientation of the axes during thrusting (e.g., Vollmer and Bosworth, 1984).

Rotation by northwest-trending high-angle faults is an equally plausible explanation for dispersal of F_1 axes. Tilting or flexure along post-Nevadan faults could have caused dispersal of pre-existing Nevadan structures. A tight grouping of early fold axes is not expected over a large, multi-deformed region. F_1 axes were undoubtedly reoriented by faulting in the northern area mapped in Plate

1. The orientations of F_1 axes are, however, somewhat
consistent across small, unfaulted sections of the Galice.
From figure 4.6B, it can be presumed that F_1 folds formed by
east-west or southeast-northwest compression, and were
dispersed by subsequent deformation. Similar conclusions
were reached in previous studies of the Galice Formation
(Snoke, 1977; Harper, 1980a; Gray, 1985; Wyld, 1985).

Large-scale F_1 Folds

Across-strike traverses along logging road exposures in
the area east of Kerby, Oregon, show the existence of tight
to isoclinal F_1 folds with wavelengths of more than 0.5
kilometers (Plate 1, in back flap). These first-order F_1
folds were identified from bedding (S_0)-cleavage (S_1)
relationships and sedimentary younging information. The
folds cannot generally be traced through their hinge zones
due to breaks in the exposure and intense faulting. Pelitic
rocks, particularly in faulted sections of logging road
exposures, have usually weathered to reddish clay-rich
saprolite. Large F_1 folds are, therefore, partially exposed
in "pieces" between highly-weathered fault zones and breaks
in the exposure. Location of F_1 hinge zones is thus
dependent upon recognition of abrupt transitions between
continuous sequences of upright and overturned beds.

Large-scale F_1 folds mapped in this study are
overturned to the north or northwest, as shown in the map

and cross-sections in Plate 1 and figure 4.7. Abrupt
reversals in the younging direction of uniformly-dipping
stratigraphic sequences is evidence that the folds are
isoclinal. An example is found along McMullin Creek Road
(see fig. 1.6) where a younging reversal is coincident with
a narrow zone of brecciation (fig. 4.8). An isoclinal F_1
fold was probably sheared-out in its hinge zone. Plate 1
shows the ubiquitous occurrence of fault zones along
overturned limbs of large F_1 folds. These zones are usually
10-20 meters wide, and are interpreted as Nevadan thrusts,
along which nappe-like north or northwest-directed movement
occurred.

Large-scale F_1 folds were also observed in continuous
across-strike exposures along Siskiyou Fork Smith River in
northern California. Figure 4.7 is a structural map and
cross-section of a six-kilometer traverse across much of the
exposed width of the Galice Formation (see fig. 1.9 for
location of section). Two large-scale F_1 folds were located
from bedding-cleavage relationships and a few preserved
graded beds. Snoke (1977) mapped a large overturned F_1
anticline near the Preston Peak thrust, immediately east of
the cross-section in figure 4.7. Part of the overturned
limb of this fold is exposed in the southeastern portion
(right side) of figure 4.7.

Figure 4.7 (following 3 pages) Structural map and cross-section constructed from data collected along Siskiyou Fork Smith River in northern California. Refer to figure 1.9 for location of cross-section (A-A). Cross-sectional view is N25E. Note major reverse faults and large-scale F1 folds. A small, fault-bounded sliver of Josephine ophiolite pillow lavas and overlying hemipelagic chert are exposed at the 2.3 km mark in the cross-section.
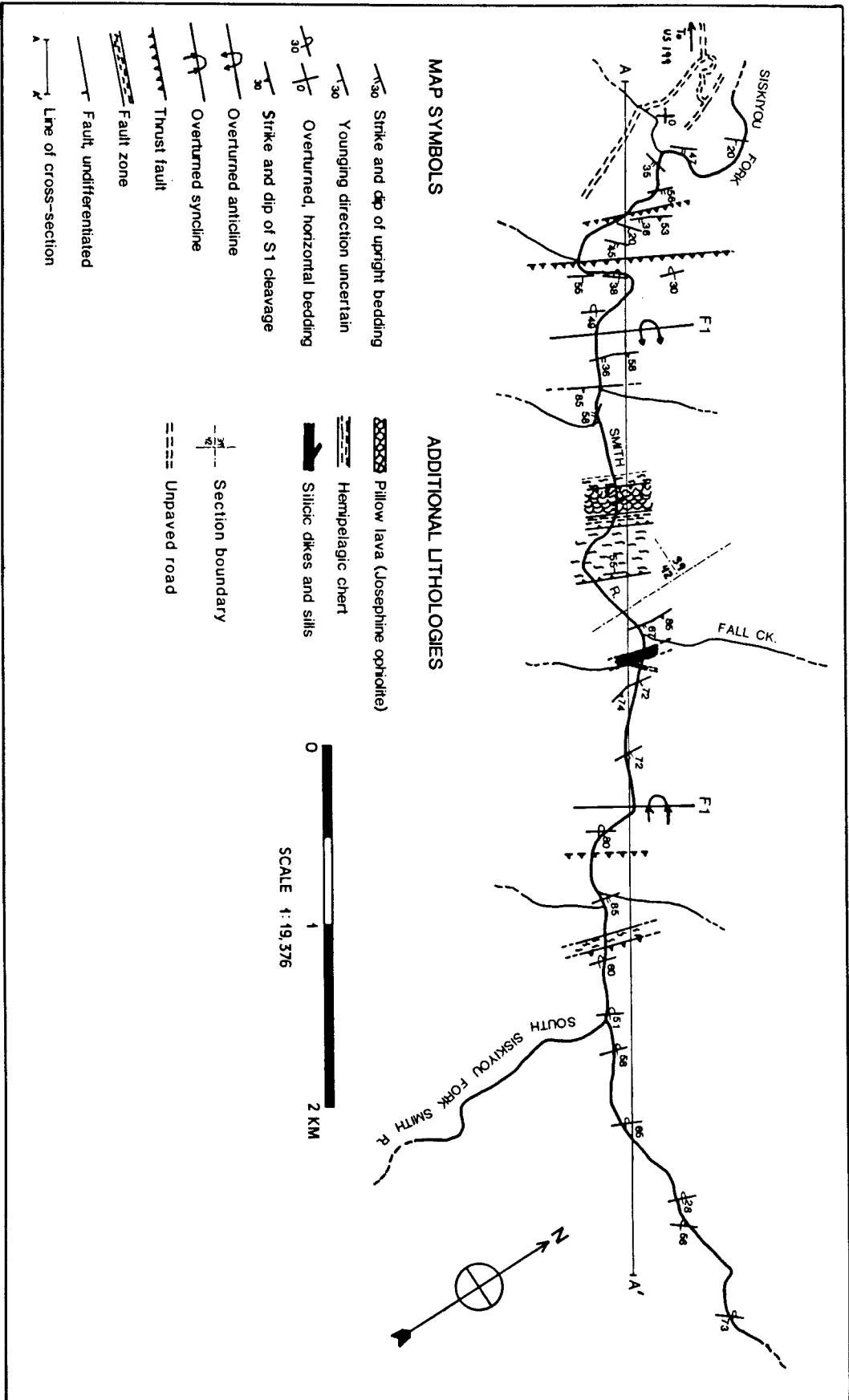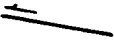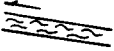
CROSS-SECTION SYMBOLS

Bedding

Nevadan cleavage

Stratigraphic younging direction

Fault

Brittle fault zone

Silicic dikes and sills

Hemipelagic chert

Pillow lava (Josephine ophiolite)

VERTICAL CROSS-SECTION: SISKIYOU FORK SMITH RIVER
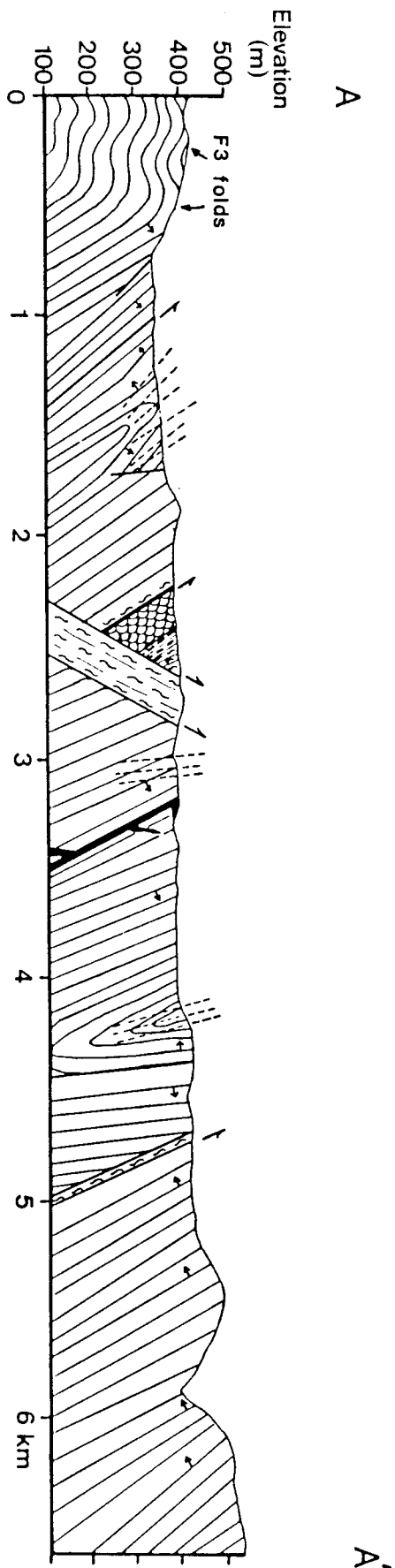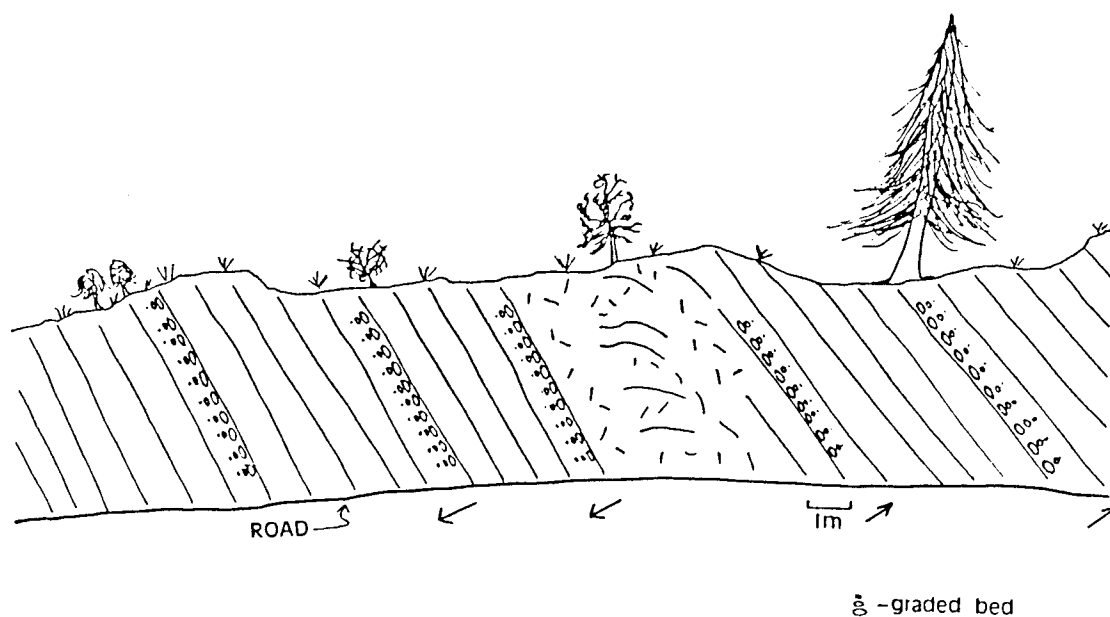
Figure 4.8 Sketch of the hinge zone of an isoclinal over-
turned anticline. A narrow zone of brecciation with a few
subhorizontal beds coicides with an abrupt reversal in the
younging direction, shown with arrows. Logging road
exposure located 8 kilometers east of Kerby, Oregon.
View is due-north.

Fold Mechanisms

F_1 folds in the Galice probably formed by buckling in some combination with flexural-slip along bedding surfaces. Stiff graywacke beds experienced extension in outer arcs, and compression in inner arcs of some F_1 fold hinges (fig. 4.9). Pelitic beds were shortened by pressure-solution (Chapter 5) sub-perpendicular to the S_1 cleavage. Weak cohesion between alternating graywacke and shale layers favored folding by flexural-slip and the resultant chevron fold geometries (Ghosh, 1968). In the northernmost Galice, tightening of F_1 fold limbs beyond approximately 60° was aided by fracturing in fold cores, presumably when flexural-slip was no longer operable.

In contrast, cleavage-related shortening contibuted significantly to F_1 fold tightening in northern California. Folding occurred under more ductile conditions in the southern Galice. Unlike F_1 folds in southern Oregon, parasitic folds are observed along F_1 limbs; note the small folds of thin laminae near the hammer in figure 4.3. The kinematics of Nevadan cleavage development and bulk shortening are addressed in chapter 5.
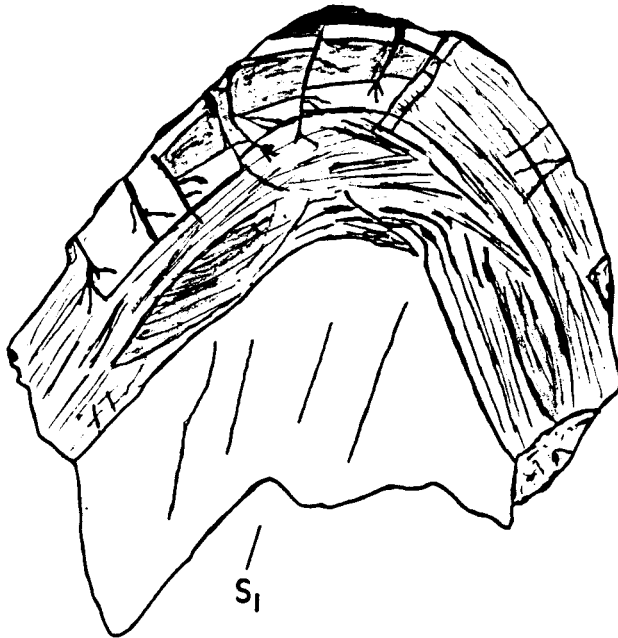
Figure 4.9 Photo and sketch of an F1 fold hinge from
Reeves Creek Road. Note excellent preservation of cross-
laminae in the graywacke bed. Buckling of the wacke bed
was accomodated by "normal faulting" along peculiar dendri-
tic zones and inner-arc "thrusting". A very weak S1
cleavage is observed in hand sample as irregular axial-
planar fractures in the shale bed.

4.2 The S_1 Cleavage

S_1 is a regionally penetrative foliation which ranges from a slaty cleavage or schistosity in the southern Galice Formation to a very weak, discontinuous cleavage in the northern Galice. In exposures near Cave Junction, Oregon, S_1 is only apparent in hinge zones of F_1 folds, where it is seen as irregular, crudely axial-planar parting surfaces in shale beds. In thin-section, S_1 is defined by the subparallel alignment of thin, opaque cleavage lamellae or pressure-solution seams (fig. 4.10). The cleavage lamellae are locally accompanied by a weak grain-shape fabric. In the northern study area, S_1 is sometimes a stronger anastomosing cleavage, or locally, a true slaty cleavage.

A strong slaty cleavage is the dominant fabric in pelitic rocks south of the Oregon-California border. Galice slates are typically dark gray to black and posses a strong planar fissility. Cleavage planes are commonly polished and contain one or several sets of slickenside lineations. A reasonably well-developed mineral lineation can be observed on some cleavage planes. In this and subsequent chapters, this mineral lineation will be referred to as "L_1", not to be confused with the L_{OX1}, the bedding-S_1 intersection lineation.
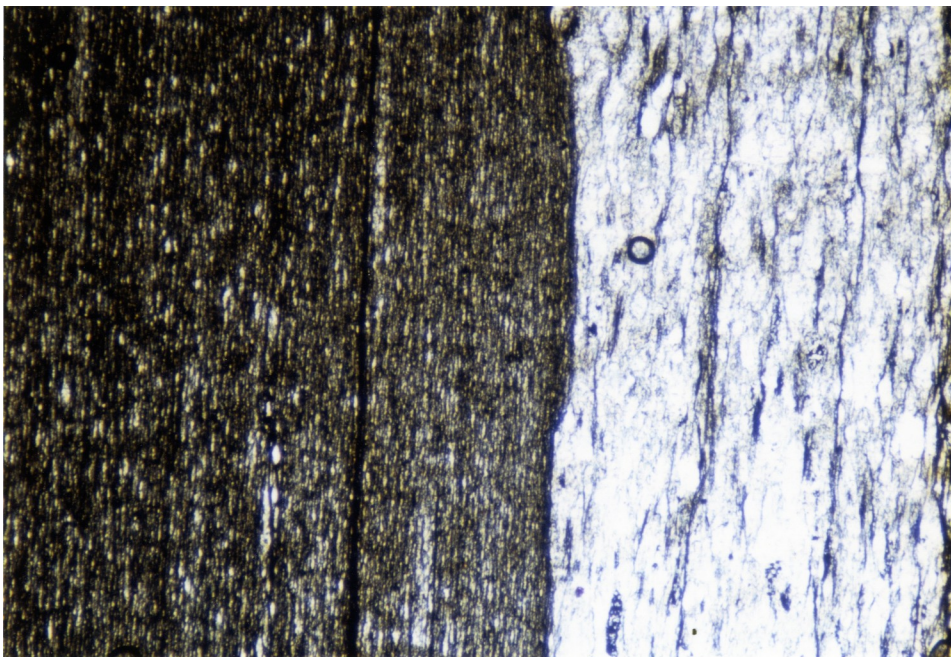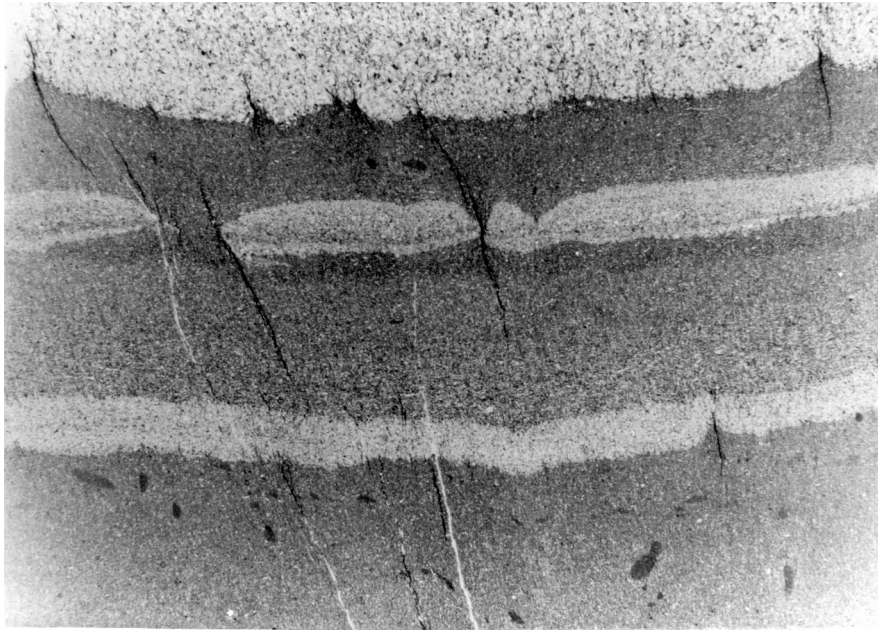
Figure 4.10 (top) Discrete opaque folia define S1 in the northern Galice. Sample from an F1 hinge zone near Reeves Creek Road. Length of photograph equals 2 centimeters.

Figure 4.11 (bottom) Strict parallelism of S1 and a well-defined bedding horizon. Sample from Siskiyou Fork Smith River, 5 km southeast of US 199. Length of photo= 6mm.

The Problem of Bedding-Parallel Cleavage

Galice slates and metagraywackes generally possess a weak to strong foliation parallel to bedding, particularly where F_1 fold hinges are not observed. Figure 4.11 shows thin-section-scale parallelism between the S_1 slaty cleavage and a sharply-defined bedding horizon. This section is oriented normal to S_1 and parallel to the L_1 lineation.

No explanations have been offered by previous workers for this widespread phenomenon. S_1 is commonly parallel to bedding in F_1 fold limbs and approximately normal to bedding in the immediate hinge zone. This pattern reflects strong fanning of S_1 across F_1 folds. S_1 folia form a strongly-divergent cleavage fan across the shale bed in figure 4.9; the folia are parallel to bedding on the limbs, gradually becoming axial-planar to the fold (parallel to mesoscopic fractures sketched in figure 4.9) in the immediate hinge zone. Therefore, it can be argued that the occurrence of S_1 parallel to bedding is not restricted to the limbs of isoclinal folds. Note that divergent fanning was also observed in the core of the anticline shown in figure 4.1.

With the exception of areas having F_1 folds, S_1 is consistently parallel to bedding over large regions. This is most evident in the exposures along Oregon Mountain Road, near the Oregon-California border, although it is a regional phenomenon (observed in both field areas and further to the south). S_1 is parallel to bedding over several kilometers

of exposure, without any evidence of F_1 folding. Bedding and S_1 are gently warped by large F_3 folds in this area.

Similar regionally-penetrative bedding-parallel tectonic foliations have been attributed to large-scale isoclinal folding (Holst, 1985) and to small-scale transposition of thinly-bedded rocks (Hobbs et al., 1976). While there is some evidence for regional isoclinal folding (discussed above in section 4.1) and transposition in the Galice Formation (Snoke, 1977; this study), a strong bedding-parallel cleavage exists even in areas where these structures are clearly absent.

An alternative explanation to isoclinal folding or transposition is that bedding-parallel fabrics are inherited from an original depositional fabric (Williams, 1972; Maltman, 1981). A strong sedimentary fabric may lead to subsequent static recrystallization parallel to bedding. Maltman (1981) proposed that some depositional fabrics are intensified during burial metamorphism or diagenesis in the absence of tectonic stress. This process would normally require a lengthy period of very deep burial and minimal alteration of the fabric by later tectonic foliation development. Alternatively, strong alignment of detrital grains parallel to bedding may be produced during rapid compaction related to dewatering, as suggested by Alterman (1973).

A strong depositional (+compactional?) bedding-parallel fabric is preserved in some Galice pelites where S_1 is

weakly developed. This fabric is probably <u>not</u> tectonic in origin, as the well-aligned detrital grains are truncated by S_1 cleavage lamellae where S_1 is oblique to bedding. In contrast to the observation of Williams (1972) in similar low-grade rocks at Bermagui, Australia, there is no evidence in the Galice for metamorphic mineral growth parallel to an earlier detrital bedding fabric.

In the northern Galice, a bedding-parallel S_1 pressure-solution cleavage appears to have been imposed on an earlier depositional fabric. It remains unclear why the regionally-penetrative tectonic foliation (S_1) preferentially developed parallel to bedding. In the southern Galice, where penetrative strains were much higher, transposition or isoclinal folding may be more likely origins of bedding-parallel cleavage.

Microstructure of Slaty Cleavage

S_1 in the southern field area (fig. 1.9) is a domainal slaty cleavage, possessing lenticular domains separated by cleavage lamellae (terminology of White and Knipe, 1978; Weber, 1981). Figure 4.12 is a photomicrograph of the typical domainal slaty cleavage. Lenticular domains consist of monocrystalline quartz, chlorite-mica stacks and framboidal pyrite grains flanked by fibrous pressure shadows. The darker cleavage lamellae are 2-4 microns wide and contain phyllosilicates with fine carbonaceous and
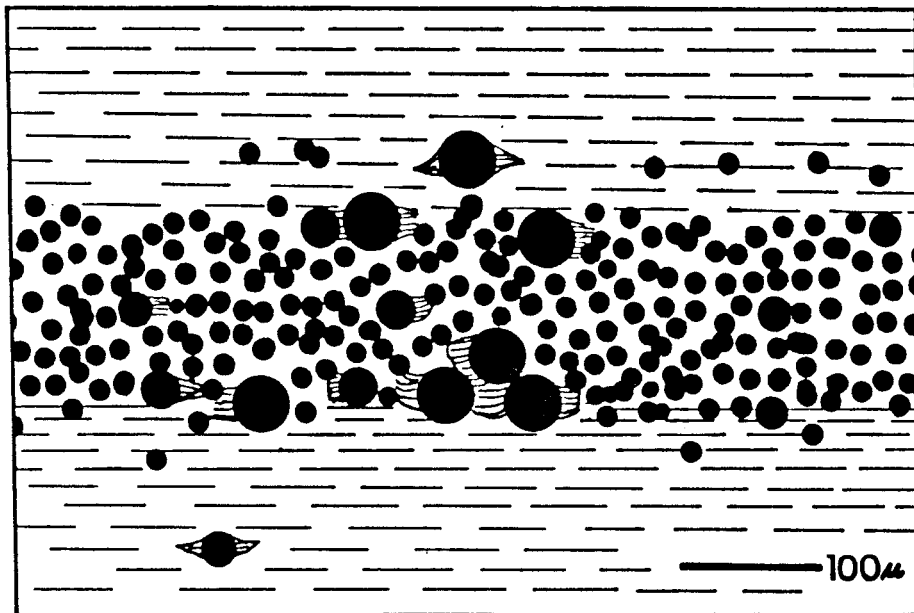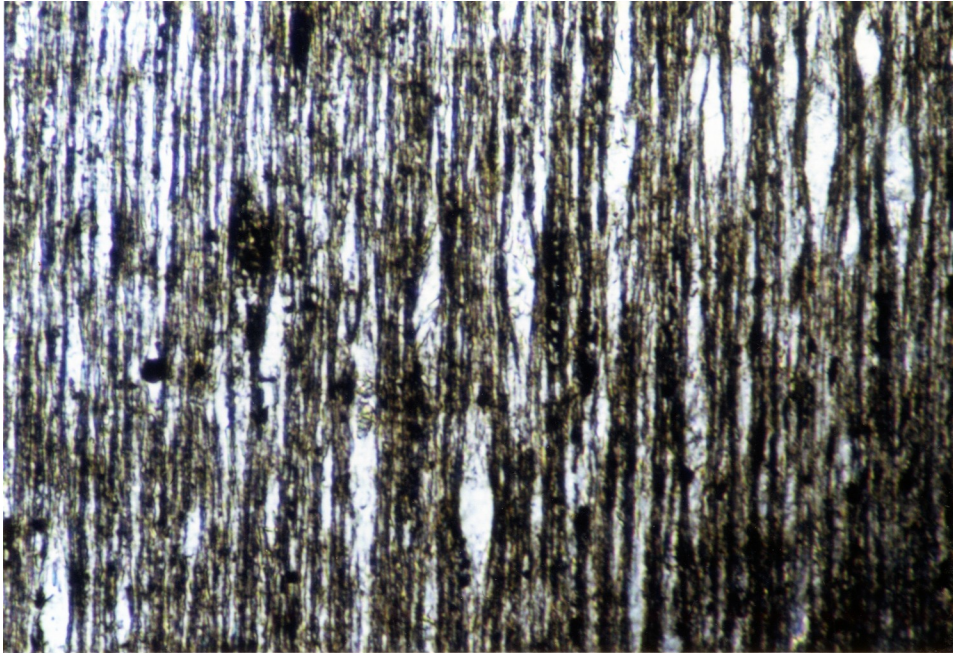
Figure 4.12 (top) Photomicrograph showing dark cleavage lamellae and lenticular domains which define slaty cleavage. Lenticular domains are 10-20 microns wide. Section cut normal to Sl and parallel to Ll (XZ Section). From Middle Fork Smith River, 4 kilometers northeast of Patrick Creek Resort. Figure 4.13 (bottom) Sketch of a bedding-parallel framboidal pyrite layer in slate. Bedding and Sl are horizontal.

pyritic material. Minor carbonate is also interspersed between the cleavage lamellae. Pyrite framboids sometimes occur in long lenses, where they have been disaggregated into constituent pyrite spherules. In many cases, they form long pods or thin bedding-parallel layers (fig. 4.13). In these layers, each spherule is connected to other pyrites by fibrous quartz, or occasionally, white mica. Framboidal pyrite is commonly a major constituent of the rock.

A weakly to moderately-deveoloped lineation (L_1) is observed in thin-sections cut parallel to the slaty cleavage. L_1 is defined by weak alignment of elongate "patches" of quartz, micas and carbonate with patches of pyrite and carbonaceous material. This crude alignment of light and dark-colored (in plane light) "domains" gives the S_1 planes a streaky appearance. Fibrous overgrowths and pressure shadows of pyrites and detrital grains also help to define the lineation. Note that dimensional alignment of <u>individual</u> grains does not contribute significantly to this lineation.

Most Galice pelites contain thin, discontinuous laminae which are distinctively darker than the surrounding rock. They are clearly transected by S_1 in slates and appear to have been folded passively during cleavage-related shortening, showing hinge thickening and limb attenuation (fig. 4.14). They are normally parallel to bedding, where bedding and S_1 are distinguishable. These features are probably organic-rich feeding trails of bottom-dwelling
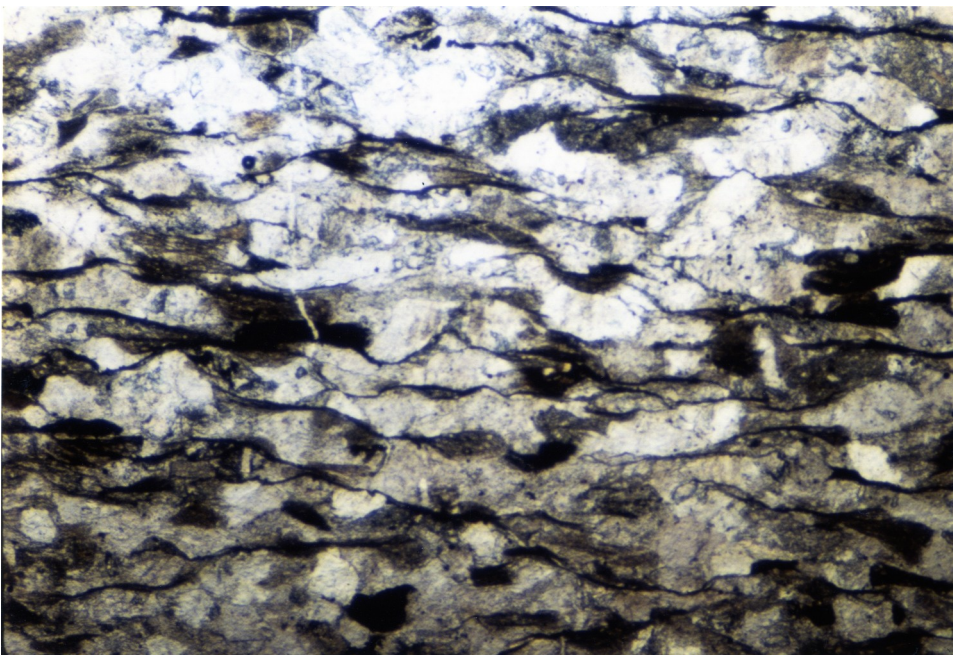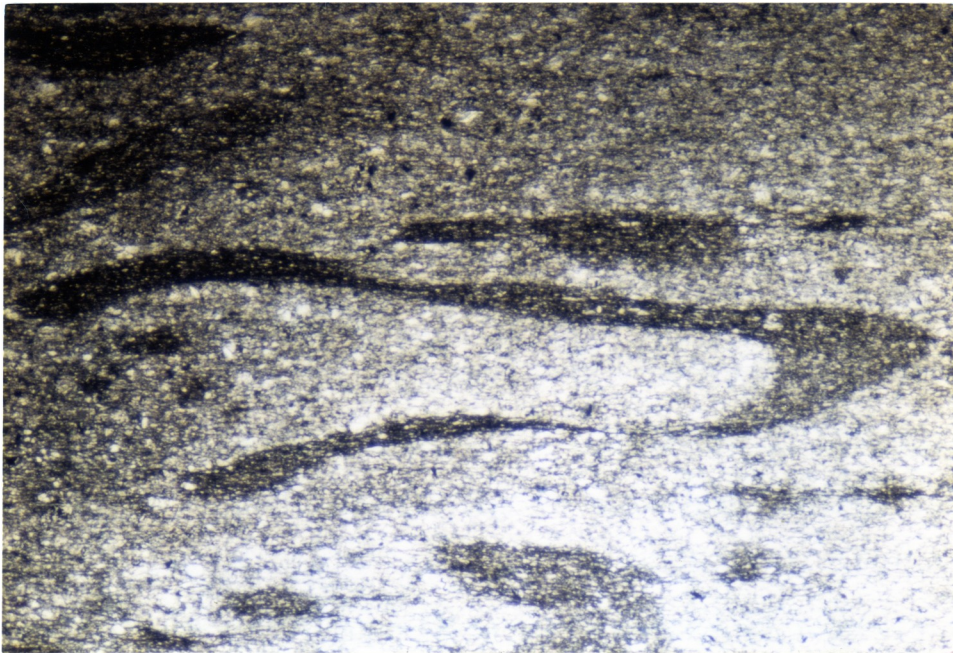
Figure 4.14 (top) Dark fold-like forms presumed to be trace fossils. Sample from Knopti Creek, near its intersection with Middle Fork Smith River. Length of photo is 6mm.

Figure 4.15 (bottom) Foliated metagraywacke from an exposure along Knopti Creek (near sample locality of fig.4.14). Cleavage folia separate domains of detrital clasts. Average spacing of the folia is 50 microns. Detrital clasts are mostly quartz, chert and plagioclase.

organisms. Sinuous trails are observed on bedding-parallel
cleavage surfaces of some slates.

S_1 in Metagraywacke

The S_1 cleavage in metagraywacke is a domainal fabric
(fig. 4.15). It is similar to the "rough cleavage"
described by Gray (1978) and interpreted as the psammitic
equivalent of slaty cleavage in interbedded pelites. Thin,
opaque cleavage folia surround domains containing large
grains of detrital origin which average 50 microns in width.
Mica and chlorite occur as secondary overgrowths and fibrous
beards on the detrital grain margins. Subgrain development
and undulatory extinction observed in detrital quartz grains
are evidence for intracrystalline deformation; these
features, however, may have been inherited from the original
source-rock.

Well-foliated metagraywackes and pebble conglomerates
possess a strong lineation on cleavage surfaces. In these
coarse-grained rocks, the lineation is largely defined by
preferred dimensional alignment of quartz, phyllosilicates,
lithic clasts, patches of fine-grained quatzose matrix and
fibrous overgrowths of detrital grains. In thin-sections
cut normal to this lineation, S_1 lamellae anastomose around
flattened detrital grains. In contrast, the lamellae are
more planar in sections cut parallel to the lineation and
normal to S_1; lensoidal detrital grains are elongated

parallel to the trace of S_1, and are connected by fibrous overgrowths and a fine-grained recrystallized quartzose matrix. This lineation is interpreted as the equivalent of the L_1 mineral or "stretching" lineation in slates.

Quartz-Calcite Veins

Veins consisting of recrystallized quartz and calcite are locally present in slates. The veins occur in several sets which intersect S_1 at various angles. The larger veins (0.5-2.0 mm wide) have central cores of strongly-twinned calcite and polygonal quartz grains. When viewed normal to S_1 and parallel to L_1 (XZ sections), marginal zones consist of finer-grained quartz and possess a foliation parallel to the trace of S_1 in the wall-rock. Since the outer quartz "fringes" do not appear to be fibrous overgrowths, they are interpreted as outer zones of large composite veins which attained a foliation during S_1 development (i.e., they are pre-cleavage or early syn-cleavage). In addition to being partially transected by S_1, the veins are frequently buckled and offset parallel to S_1 (figs. 4.16, 4.17). Pre-cleavage quartz veins are extensively shortened, particularly when they were originally at high angles to S_1 (fig. 4.18). Intracrystalline deformational features in the veins include subgrain development and sutured grain boundaries.

Although many of the veins were probably deformed during S_1-related shortening, initial vein-opening may have

Figure 4.16 Quartz vein (vertical) deformed by buckling
and offset along pressure-solution seams. The deformed
vein cuts older calcite veins which lie at a low angle to
S1 (horizontal in photo). Section cut normal to the vein
and S1, and parallel to L1. Sample from a slate exposure
along Middle Fork Smith River, 4 kilometers northeast of
Patrick Creek Resort. Horizontal dimension of photo-
micrograph= 1.5mm.
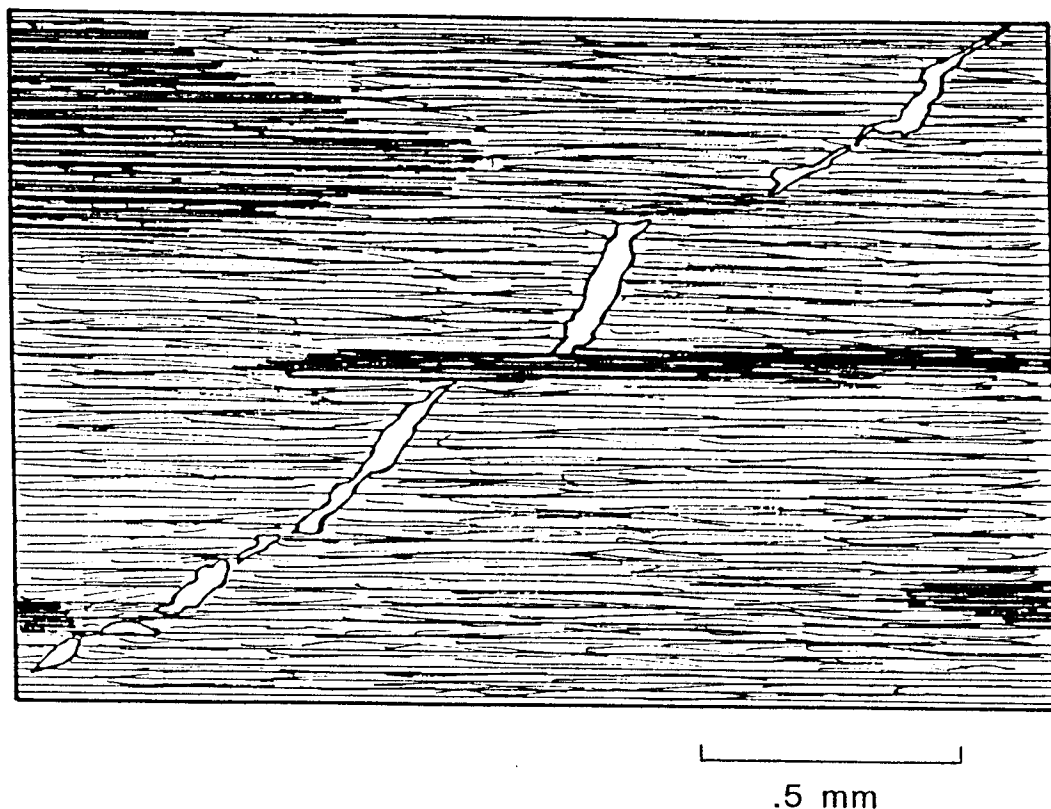
Figure 4.17 Quartz vein offset along a residual zone of
dissolution in slate. Tracing from a photomicrograph with
S1 horizontal. Enhanced dissolution occurred along the
darker zones, presumed to be remnants of trace fossils
(see fig. 4.14). Sample from same exposure as figure 4.16
along Middle Fork Smith River. Section cut normal to S1
and parallel to L1.
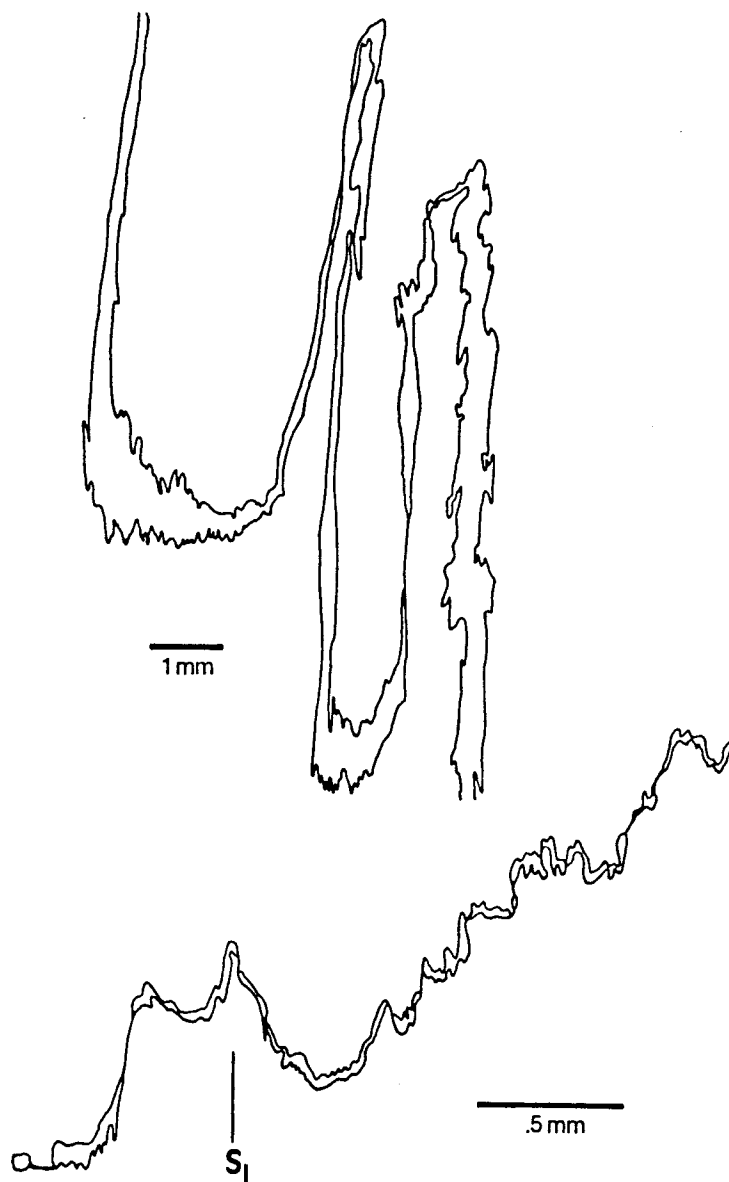
Figure 4.18 Thin quartz veins shortened by folding.
Tracings from magnified images of a thin-section. Sample
from same exposure as figures 4.16 and 4.17, also cut
normal to S1 and parallel to L1.

been during an early stage of S_1 development. The largest veins, commonly perpendicular (+/-10°) to S_1, are consistently normal to the L_1 lineation on cleavage surfaces. This relationship is especially apparent in a slate exposure along the Middle Fork Smith River and US 199, about 4 kilometers northeast of the Patrick Creek Resort. The orthogonal relationship between the large veins and L_1 at this outcrop (fig. 4.19) suggest that the two may be coeval; the extension parallel to L_1 was probably responsible for vein dilation. This conclusion is, however, somewhat tenuous, as a temporal relationship between the veins and L_1 is not firmly established.

F_1 Axes and L_1

The three fold axes plotted in figure 4.19 from a slate exposure along Middle Fork Smith River lie at various angles to the mean L_1 orientation. This is consistent with variable dihedral angles between F_1 axes and L_1 measured from other Galice slates in this study. Ramsay and Huber (1983) note that local variations between fold axis orientations and co-generational X-direction lineations are quite common in slate belts. However, few measurable F_1 axes and younger slickensides on S_1 planes contributed to a paucity of L_1 data obtained in this study.

Other workers have found L_1 to be generally parallel to F_1 fold axes, especially in metagraywackes (Hartper, 1980a;
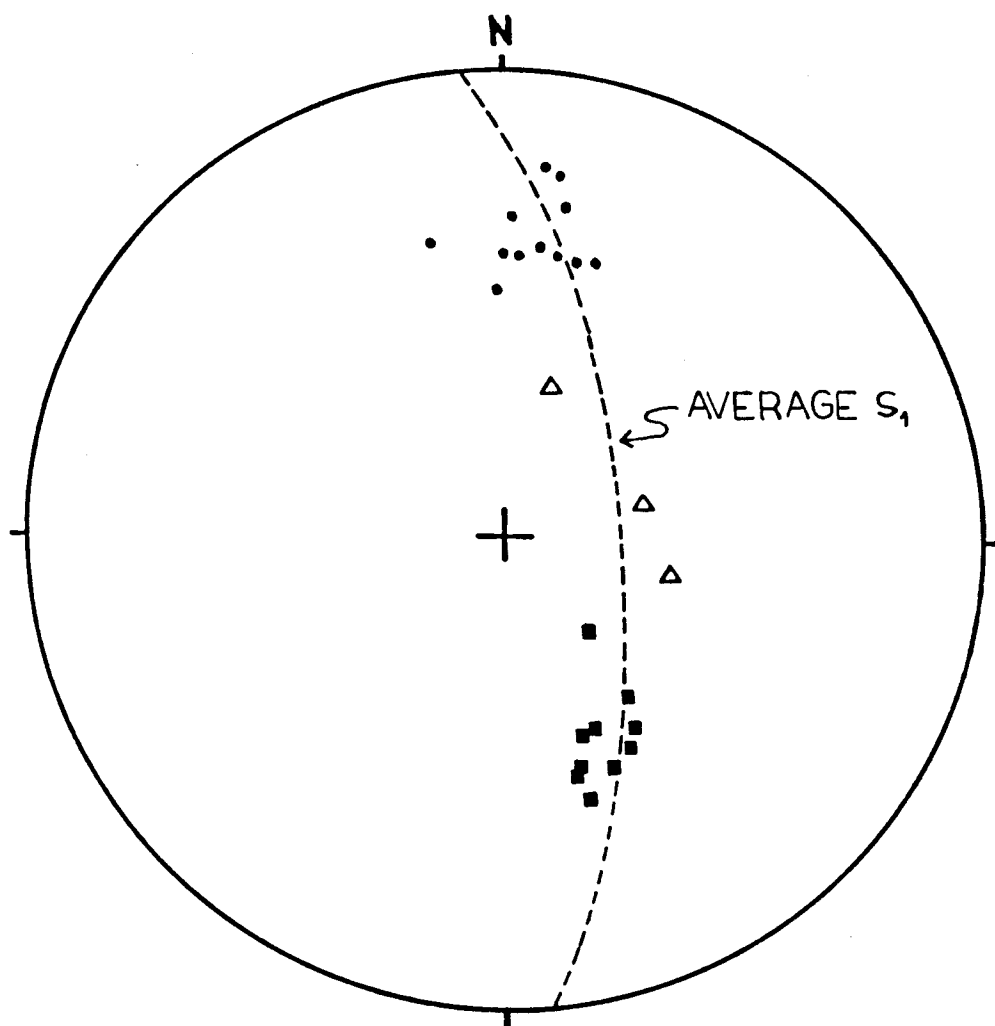
Figure 4.19 Stereographic projection of structural elements measured from a slate exposure along Middle Fork Smith River in northern California, 4 kilometers northeast of Patrick Creek. L1 lineations lie at 90° to extensional vein traces on S1 planes. See text for discussion.

Wyld, 1984). Large non-coaxial strains during during a progressive shear deformation may cause rotation of pre-existing fold axes into parallelism with an X-direction lineation (Bryant and Reed, 1969). However, large penetrative ductile shear strains are not recorded by post-F_1 structures in the prehnite-pumpellyite facies rocks examined in this thesis. Furthermore, it is unusual that extensive elongation, as large as 300% (determined from syntectonic fibers grown parallel to L_1, chapter 5) would occur parallel to the north-south Nevadan structural trend. F_1/L_1 relationships provide an interesting structural problem in the southern Galice that could be approached in a well-focused future study.

4.3 Transposition

Local transposition of beds into parallelism with S_1 was a result of tight folding, combined with cleavage-parallel extension. Transposition is especially apparent in thin, alternating beds of slate and fine-grained metagraywacke. Snoke (1977) also described transposition in thinly-bedded "laminites" (interlayered siltstone metagraywackes and slates) along the Siskiyou Fork Smith River. One line of evidence for transposition is the frequent pinching-out of thin graywacke beds in the laminites. Fold closures are generally missing completely.

Figure 4.20 is a rare example where isolated fold hinges can be observed in transposed laminites.

A second example of transposition is shown in figure 4.21. This photograph shows isolated graywacke lenses (light color) which are elongated parallel to S_1. Wispy trails of graywacke protrude from the larger beds in a direction parallel to the trace of S_1. It is uncertain whether this sort of transposed layering was a ressult of isoclinal F_1 folding, as is evident from the laminites in figure 4.20. Pressure solution along spaced cleavage planes probably contributed to the offset and ultimate isolation of individual segments of graywacke beds.

All examples of transposition in the Galice Formation occur in thinly-bedded rocks with strong slaty cleavage. No evidence of transposition was observed in exposures north of the California-Oregon border. It is thus intrinsically related to strong S_1 development. A case can be made that Nevadan transposition occurred on a regional scale by isoclinal folding. Reversals in the younging direction occur in the absence of fold closures, as isoclinal hinge zones are narrow and may be obscured by faulting (fig. 4.7).

The main-phase Nevadan deformation involved substantial extension parallel to S_1. Cleavage-parallel extension is necessary for the separation of graywacke beds and isolation of fold hinges in transposed rocks (fig. 4.20). Sills showing boudinage parallel to S_1 observed near Patrick Creek (fig. 1.9) are further evidence for large Nevadan extensions

(following page)

Figure 4.20 (top) Transposition of bedding into parallel-
ism with S1. Tracing of silty beds from a photograph
showing isoclinal folding and lensing-out of the beds.
Non-shaded portions are black slate. Several large pyrite
framboids with quartz pressure shadows are also shown. In
this outcrop, S1 dips gently to the southeast. Exposure
along Middle Fork Smith River, 3 kilometers northeast of
Patrick Creek.

Figure 4.21 (bottom) Transposition of graywacke beds (light
color) into parallelism with S1 in slate. Note offsets and
lensoidal appearance of transposed graywacke beds. Large
offsets are faults. Siskiyou Fork Smith River, 3 kilo-
meters west of the Preston Peak thrust.
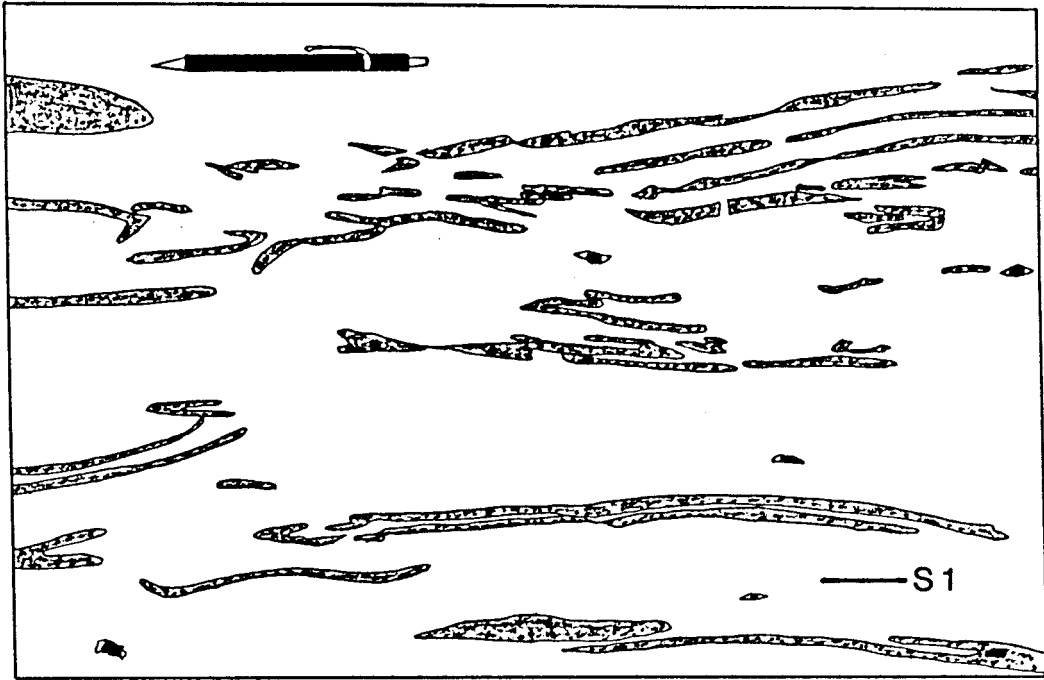
(Harper, 1980a). Measurement of extension parallel to L_1 using syntectonic fibers in Galice slates will be discussed in the next chapter.

4.4 The Preston Peak Thrust

The Orleans fault is a regional thrust fault along which the western Paleozoic and Triassic belt was displaced westward over the western Jurassic belt (see figure 1.1). The fault juxtaposes the Galice Formation with older rocks along nearly the entire north-south length of the Klamath province. It is considered to be a Nevadan-age thrust in light of cross-cutting relationships with several well-dated plutons and regional structural relationships (Klein, 1977; Snoke, 1977; Wyld, 1985; Harper et al., 1986). I will use the name assigned by Snoke (1977), the Preston Peak thrust, as a local name for the Orleans thrust in the northern Klamath Mountains.

In the field areas of this study, the Galice Formation is faulted against either: 1) Metasedimentary and metavolcanic rocks of the western Paleozoic and Triassic belt (mapped as the Applegate Group in Oregon by Wells and others, 1949), or 2) A serpentinite-matrix melange forming the lowest exposed portion of the Preston Peak ophiolite (Snoke, 1977). These rocks have been correlated with the Rattlesnake Creek terrane (Irwin, 1966) to the south (Gorman, 1985). The Preston Peak thrust exposes rocks of

different ages and structural levels in the upper plate. In the area near Cave Junction, Oregon, the upper plate primarily consists of strongly foliated siliceous argillites of the Applegate Group. Irregular bodies of greenstone and serpentinite melange are found sporadically along the thrust. Inclusions in the melange include red chert, metagabbro, metasedimentary rocks and large blocks of massive marble (e.g. "lime Rock" shown on Plate 1). In northern California, the Galice Formation is thrust beneath serpentinite-matrix melange containing tectonic inclusions of amphibolite and, locally, blocks of the Galice Formation.

The Preston Peak thrust has been interpreted as a high-angle reverse fault along its exposure in southwestern Oregon (Wells et al., 1949; Ramp, 1979). Although it strikes roughly north-south along the entire extent of the Klamaths, the trace of the fault curves abruptly toward the west near Cave Junction, where it passes underneath Illinois River alluvium for several kilometers. This unusual curvature was probably produced by large-scale post-Nevadan folding or oroclinal flexure, and is not an artifact of a low-angle fault trace curving around topography (based on mapping by Wells et al., 1949; Ramp, 1979; and field observations from this study). Structural trends in the Galice such as bedding, cleavage and F_1 fold axes are parallel to the curved trace of the thrust (Plate 1). The Preston Peak thrust is cut by numerous small high-angle

faults, which were previously interpreted as transcurrent tear faults (Snoke, 1977; Gray, 1985).

A large re-entrant, in which the Galice is exposed in northern California (fig. 1.1) suggests at least 110 kilometers of displacement along the Orleans fault (Jachens et al., 1986). Where unaffected by post-Nevadan folding, the thrust is relatively flat, dipping 10° to 30° to the east (Wyld, 1985; Jachens et al., 1986). Nevadan displacement along this thrust produced approximately 40% shortening across the Klamath province (Jachens et al., 1986). Ages of plutons intruding the fault suggest that thrusting ceased between 150 Ma and 148 Ma (Harper et al., 1986; Wyld, 1985).

Rocks in the upper plate of the Preston Peak thrust were deformed to some extent during the Nevadan orogeny. Nevadan thrusting reportedly caused remixing of serpertinite melange in the Rattlesnake Creek terrane of the upper plate (Snoke, 1977; Gorman, 1985; Gray, 1985). An east-dipping shear foliation in ultramafic rocks of the Preston Peak complex was interpreted as Nevadan (Snoke, 1977). Siliceous argillites and metaconglomerates of the Applegate Group in Oregon possess a penetrative anastomosing foliation. Interestingly, this foliation is often subparallel to the S_1 cleavage in the Galice Formation. Clasts in pebbly mudstones are strongly flattened, the least competent being smeared-out in the plane of foliation. Polished foliation surfaces and the locally phacoidal nature of the foliation,

is evidence that the rocks were strongly sheared. It is unclear, however, whether the deformation suffered in the upper plate of the Preston Peak thrust was Nevadan or earlier. These older rocks were probably deformed during a Middle Jurassic deformational event (Fahan and Wright, 1983). Brittle shearing in the upper plate was certainly an important Nevadan effect (Snoke, 1977; this study).

4.5 Nevadan Thrusting and Vergence

Nevadan thrusts in the Galice commonly dip east or southeast and are subparallel to bedding and the typically bedding-parallel cleavage. In the northern Galice, Nevadan thrusts are brittle structures, generally occurring parallel or slightly oblique to bedding (fig. 4.22). With few exceptions, main-phase Nevadan structures pre-date Nevadan thrusts. Truncated F_1 folds are widespread in the Galice (see figs. 6.9, 6.10, 6.11).

The relative age of thrusting in the Galice Formation is considered "late Nevadan", as it occurred after the cessation of the main-phase deformation and regional Nevadan metamorphism. No changes in the attitude or intensity of S_1 were observed in the vicinity of Nevadan thrusts. This observation contradicts the findings of some previous workers. For example, Kays (1967) documented mylonitization and chlorite-zone recrystallization along Nevadan thrusts in the type-Galice Formation. However, he also notes the

(following page)

Figure 4.22 (top) Nevadan thrust intersecting bedding
(and bedding-parallel S1 cleavage) at a low angle. View
is to the southwest. Exposure along Knopti Creek Road,
approximately 1 kilometer west of the Preston Peak thrust.
Note that bedding is discontinuous and lensoidal above and
below the hammer, possibly indicating smaller splay thrusts.
Down-dip slickensides were observed along the underside of
the hanging wall.

Figure 4.23 (bottom) Small-scale thrusts offsetting silty
beds. White zones are sigmoidal quartz veins. View is
north. Sample from a slate exposure, 4 kilometers north-
east of Patrick Creek. See text for additional details.

occurrence of drag folds and other evidence of brittle
detachment along Nevadan thrusts. In the southernmost
Galice, the dip of S_1 steepens progressively away from the
Orleans thrust (Wyld, 1985). In the southern extent of the
Galice, Nevadan thrusting and S_1 development may have been
related aspects of the same event.

Some thin section- scale thrusts (fig. 4.23) were at
least partially coeval with S_1 development. The thrusts in
figure 4.23 are generally parallel to S_1, the graywacke beds
showing offset and thinning between the small thrusts. The
faults are marked in places by crudely-sigmoidal polygonized
quartz veins. The S_1 fabric is intensified against portions
of the veins and some veins are cut by cleavage lamellae.
Furthermore, the relatively rigid veins and offset wacke
beds created triangular-shaped strain shadows where the S_1
fabric is substantially weaker. In this particular case,
the thrusts may be considered "main-phase" or syn-S_1
structures.

In the present study, no systemmatic variations of
main-phase Nevadan structures were observed near the Preston
Peak thrust. Thin-sections of slates from within a few
meters of the thrust are typical of most Galice slates,
showing no evidence for unusually high strains.

The typical southeastward dip of S_1 (see poles to S_1 in
figure 4.6A) suggests dominantly northwestward vergence
during the Nevadan orogeny. Nevadan folds and thrusts are
also northwest-vergent. Westward thrusting along the

regional-scale Orleans thrust is suggested by increased westward vergence of F_1 and F_2 folds and associated cleavages in the Galice as the thrust is approached (Gray, 1985; Wyld, 1985). This structural vergence is evident from the cross-sections in figure 4.7 and Plate 1. The possibility of dominantly eastward Nevadan thrusting (Roure, 1984) is not supported by data in this thesis or most previous studies of the Galice (Snoke, 1977; Harper, 1980a; Wyld, 1985; Gray, 1985; Jachens et al., 1986).

4.6 Summary

The Galice Formation is a uniformly-dipping (fig. 4.4) package of deep water turbidites that were deformed into west and northwest-vergent tight to isoclinal folds during the Nevadan orogeny. Approximately 15% of all measured beds in the Galice are overturned, although some overturned beds were certainly overlooked in rocks lacking younging indicators. Large-scale F_1 folds are probably controlled by the most competent stratigraphic intervals--those dominated by massive graywacke beds. Smaller outcrop-scale F_1 folds are preferentially developed in thinly-bedded rocks.

The three previous sections of this chapter have been devoted to description of structures which formed during a D_1 or "main-phase" Nevadan deformation. F_1 folds, S_1 cleavage and transposition are clearly associated with an initial stage of shortening in the Galice Formation.

Characteristics of the main-phase structures are summarized in figure 4.24. Development of these structures probably coincided with Nevadan regional metamorphism; however, the exact timing of peak metamorphic conditions with respect to deveolopment of S_1, L_1 and syntectonic veins is uncertain.

A strong bedding-parallel cleavage is found over large regions of the Galice where there is no evidence for extensive F_1 folding. Although this may result from complete transposition in strongly deformed slates and laminites, the problem remains enigmatic in rocks of the northern Galice where transposition is absent due to low amounts of penetrative Nevadan strain. I suggest that the S_1 bedding-parallel cleavage may have formed parallel to an earlier depositional or compactional bedding-plane fabric.

Nevadan Structure	NORTH	SOUTH
S1	Very weak to moderately developed pressure-solution cleavage, locally slaty in pelitic rocks, often non-existent in graywacke	A strong slaty or pyllitic cleavage in pelites, a moderately developed schistosity in metagraywacke
F1	Open to tight folds with minor hinge thickening	Generally tight-to-isoclinal similar folds
Transposition of Bedding	None	Occurs in thinly-bedded slates and fine-grained metagraywackes

Figure 4.24 Characteristics of main-phase (D1) Nevadan structures in the northern and southern field areas (figures 1.6 and 1.9, respectively).

Chapter 5:   NEVADAN CLEAVAGE DEVELOPMENT

5.1 Pressure-solution Origin of Slaty Cleavage

The importance of the process of pressure-solution
during slaty cleavage development has been emphasized in a
number of detailed microstructural studies (e.g. Groshong,
1975; Holeywell and Tullis, 1975; White and Knipe, 1977;
Beutner, 1978). Grain-shape fabric analyses of slates
(Holeywell and Tullis, 1975; Beutner, 1978) demonstrate that
shortening normal to slaty cleavage may be dominantly by
corrosion, diffusion-transfer and neocrystallization of
quartz and phyllosilicate minerals. Dissolution of these
minerals results in the concentration of less mobile
components of the rock, typically carbonaceous material,
pyrite and fine micas in cleavage films or lamellae.

Large detrital quartz grains and chlorite-mica
aggregates are abruptly truncated by sub-opaque cleavage
lamellae or "selvages" in pelitic rocks affected by
pressure-solution. In contrast, similar grains that are not
enclosed between the lamellae are relatively equant
(Groshong, 1975). Dissolved components migrate either by
diffusional transfer, or in solution, to sites of active
deposition; generally, this will be in "strain shadows"
within lenticular domains, or in nearby syn-cleavage veins.

Some new grains may, however, grow <u>within</u> the cleavage lamellae (Beutner, 1978).

Pressure-solution is usually recognized by beds, veins and fossils which are offset along opaque cleavage lamellae or "seams". Beutner (1978) argued that originally rectangular detrital chlorites in the Martinsburg Slate (New Jersey) were aligned parallel to slaty cleavage, and attained lozenge and rhombohedral shapes by selective corrosion of each grain normal to cleavage. This mechanism is shown in figure 5.1B. Pressure-solution, combined with minor intracrystalline deformation, can account for the bulk shortening and preferred grain alignment related to slaty cleavage development (Beutner, 1978). Mechanical rotation of large platy detrital grains is demonstrably minimal in commercial slates such as the Martinsburg Formation (Holeywell and Tullis, 1975; Beutner, 1978; Morris, 1981).

Pressure-solution in the Galice Formation

Pressure-solution selvages consisting of opaque carbonaceous material and microcrystalline pyrite are typically intensified at bedding interfaces between slate and metagraywacke in the Galice Formation (fig. 4.10). Dissolution along the selvages causes beds to pinch-out (fig. 4.10) and leads to apparent offsets of pre-cleavage veins parallel to S_1 (figs. 4.16, 4.17). At interfaces between slate and wacke beds, pressure-solution selvages

A.

25μ

—S₁

(001)

B.

(after Beutner, 1978)
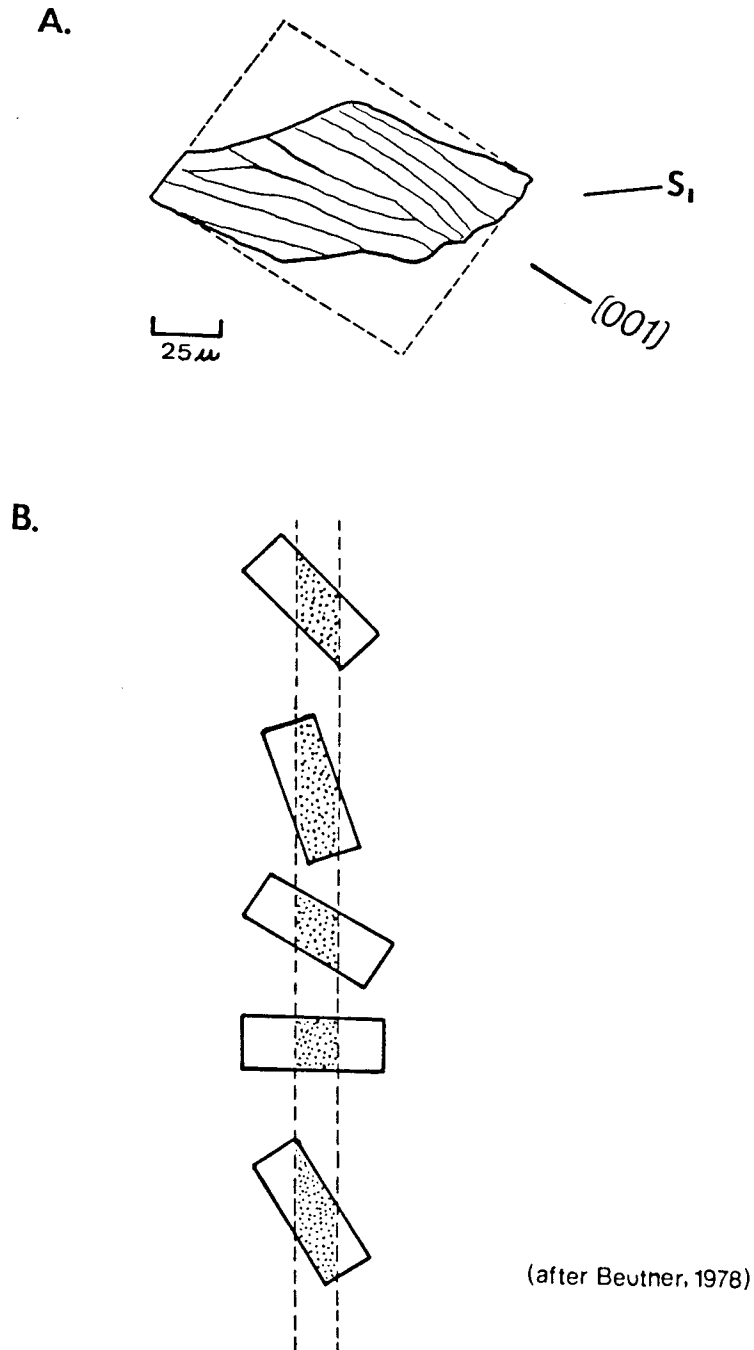
Figure 5.1 A. Tracing of a large chlorite stack from the Galice showing long axis alignment parallel to S1, and traces of the 001 mineral cleavage planes. Inferred original outline of the grain is dashed. B. Variously-shaped chlorites result from corrosion and removal of material outside of dashed lines (after Beutner, 1978, fig.4).

anastomose around lenses of wacke creating a transposed appearance at thin-section and outcrop scales (fig. 4.22). The dark folia forming the selvages bend markedly around impeding structures like graywacke blobs and large pyrites, suggesting strong mechanical influence by these structures.

Dark cleavage-parallel laminae, interpreted as deformed trails of bottom-dwelling organisms, appear to be sites where dissolution was particularly high. These features were isoclinally folded, probably by volume reduction along the "limbs" and dilational volume-gain in the "hinges". The final geometry of these mechanically passive features resembles a transposed foliation with isolated fold hinges and discontinuous dark laminae, which normally lie at low angles to S_1. Discontinuity of the laminae may also reflect original discontinuity of the fossils, as well as those laminae which curve in and out of the plane of the thin-section. Two probable original constituents of these zones, quartz and calcite, were almost entirely removed, leaving only fine micas, opaque material and minor quartz. Cleavage lamellae, defined by the residual material, are thicker and more closely-spaced in these zones, suggesting locally enhanced pressure-dissolution.

Large phyllosilicate grain aggregates or "chlorite-mica stacks" (Voll, 1960) are common in Galice slates. Their shapes resemble those recognized by Beutner (1978): diamonds, rhombohedrons and lozenge-shaped grains (fig. 5.1B). Various origins have been proposed for chlorite-mica

aggregates, such as growth as metamorphic porphyroblasts (Roy, 1978), early mimetic growth parallel to a bedding fabric (Craig et al., 1982) and deposition as detrital grains (Beutner, 1978). The latter suggestion is favored for two reasons. First, chlorite stacks are distinct, large rectangular grains which have 001 mineral cleavage traces subparallel to bedding in uncleaved pelites (Beutner, 1978; this study). Secondly, the aggregates are clearly pre-deformational and pre-metamorphic; their retangular detrital shapes were modified by pressure-solution (Beutner, 1978), and the stacks were not recrystallized during regional low-grade metamorphism.

Figure 5.2 is a photomicrograph of a parallelogram-shaped mica stack in a Galice slate. The 001 mineral cleavage trace is commonly oriented at a high angle to S_1. For this reason, chlorite-mica stacks have been termed "cross-micas".

Figure 5.1A is a large chlorite stack in a foliated graywacke siltstone. Intensified opaque cleavage folia along the upper and lower surfaces of the stack indicate selective corrosion along these surfaces. Dashed lines mark the probable original rectangular outline of the chlorite stack. At least 60% shortening by pressure dissolution probably occurred in the vicinity of this grain. Elongated grains with 001 normal to S_1 indicate significantly larger amounts of shortening normal to S_1.
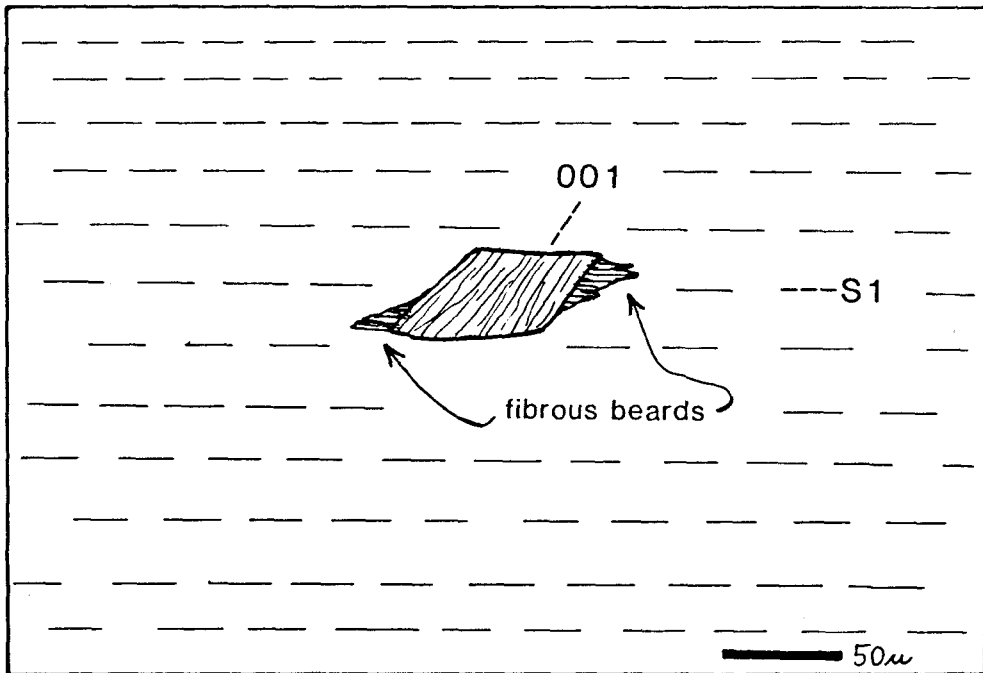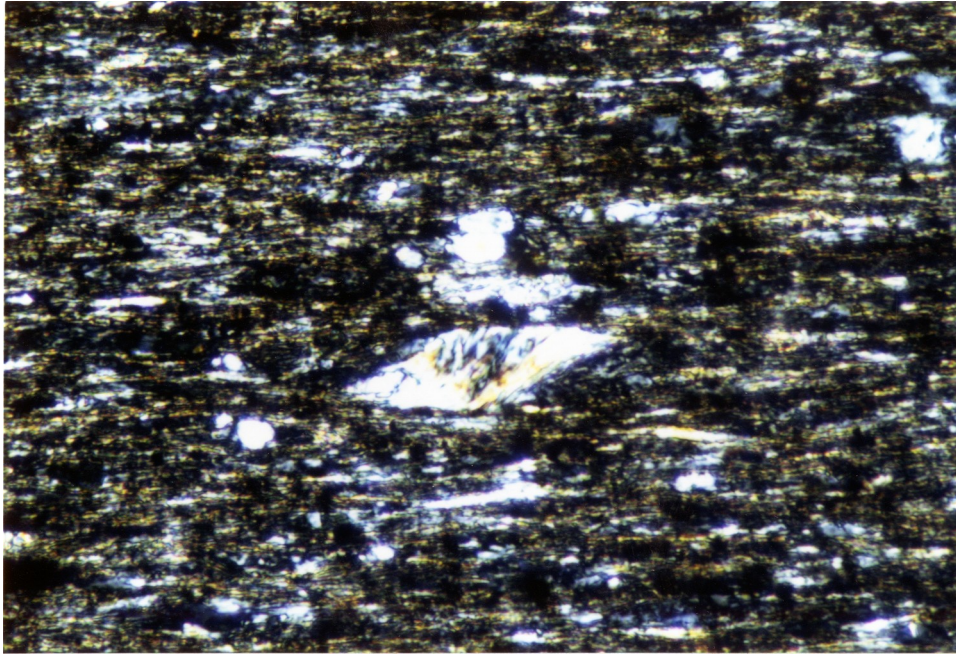
Figure 5.2 Photomicrograph and sketch of a parallelogram-shaped mica stack in slate. Sample from an exposure along Middle Fork Smith River, 4 kilometers northeast of Patrick Creek. Photo taken under crossed-nicols.

The phyllosilicates in the stacks are sometimes buckled or kinked when 001 planes are at high angles to S_1. This suggests the possibility of a small amount of shortening by intragranular deformation. However, kinking is not found in most of the stacks, and there is no microstructural evidence for preferential development of cleavage lamellae along microfolds or kink bands (e.g. White and Knipe, 1978).

In northern Galice pelites with a weaker S_1 cleavage, the 001 traces of fine-grained micas are moderately to strongly oriented parallel to <u>bedding</u>. S_1 cleavage folia truncate some of the detrital grains; however, a strong bedding-parallel preferred orientation persists.

Figure 5.3 is a different type of bedding-parallel fabric which is crenulated by F_1 microfolds. Examination of this thin-section, which is from an F_1 hinge zone, reveals buckled and fractured pyrite stringers which were originally parallel to bedding. S_1 pressure-solution selvages transect the bedding fabric along the limbs of the microfolds. The mechanical separation of the pyrite stringers from the matrix and other stringers produced dilational openings which were progressively filled with fibrous chlorite and white mica (fig. 5.3). The fibers are strongly curved, an artifact of fiber growth during buckling and rotation of the pyrite stringers. Assuming the fibrous zones represent all of the extended portions of the pyritic layer in figure 5.3, the layer is estimated to have experienced 400-500% bulk extension parallel to S_1. In light of the relatively weak
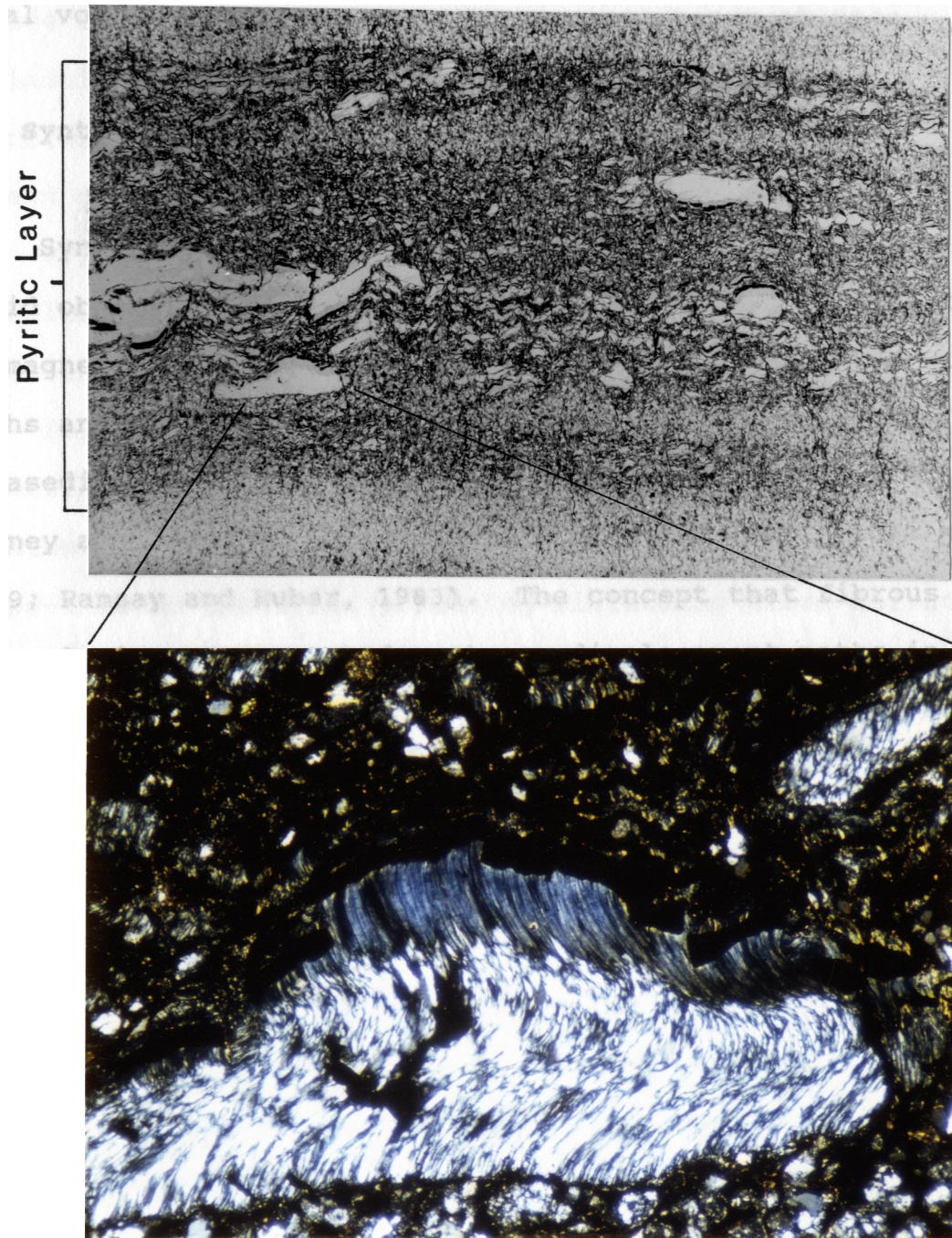
Figure 5.3 (top) Crenulated bedding-parallel pyritic layer in an F1 hinge zone. Bedding is horizontal; S1 is vertical. Sample from Siskiyou Fork Smith River, 3 kilometers east of US 199. Length of photo is 1cm. (bottom) Extension parallel to S1 caused dilation and fiber growth in zones between crinkled pyrite stringers. Fibrous zones consist of white mica and chlorite (blue fibers under crossed-nicols).

development of S_1 in this layer, extension was presumably by local volume-gain.

5.2 Syntectonic Fibers and Pressure Shadows

Syntectonic fibers in pressure shadows adjacent to rigid objects such as pebbles, fossil fragments and pyrite or magnetite grains are excellent indicators of deformation paths and incremental strains in low to medium grade metasedimentary rocks (Choukroune, 1971; Elliott, 1972; Durney and Ramsay, 1973; Wickham, 1973; Gray and Durney, 1979; Ramsay and Huber, 1983). The concept that fibrous minerals in pressure shadows trace displacement paths in a homogeneously deforming continuum has prompted development of techniques of directly measuring incremental strain (all above references plus Beutner and Diegel, 1985; Ellis, 1986). Incremental strain calculations involve measurement of the lengths and orientations of tiny fiber increments with respect to a reference line in the plane of section. Small lines or chords connecting these increments should mimic the curvature of the fibers. Some important pitfalls and sources of error in using syntectonic fibers to deduce strain paths are noted by several authors (e.g. White and Wilson, 1978; Gray and Durney, 1979; Beutner and Diegel, 1985; Ellis, 1986). They are briefly discussed below:

(1) Curvature of fibers must be established as occurring by growth, rather than by intracrystalline

deformation. Curvature by fiber growth is verified when the entire curved length of the fiber goes extinct at once. Extinction which sweeps along a fiber is common, and therefore caution is needed in interpretation of incremental strain data.

(2) Fibers must not curve out of the plane of section. As Ellis (1986) notes, non-Euclidean thin-sections have yet to be invented!

(3) Beutner and Diegel (1985) suggest that only rigid, essentially spherical objects should be considered in fiber studies. Euhedral or irregularly-shaped objects may undergo shape-induced rotations producing misleading fiber curvature patterns. Furthermore, in metamorphic rocks, euhedral minerals, such as magnetites, can grow during metamorphism, and may not record the total incremental strain history.

(4) Fibers must show a consistent, recognizable sense of growth--either towards or away from the object. For objects such as pyrite or magnetite grains, fibers always grow from the matrix toward the object (antitaxial growth), the latest growth increment occurring at the fiber-object interface (Durney and Ramsay, 1973). Evidence for antitaxial fiber growth in pressure shadows of pyrite/magnetite grains is presented in section 5.3.

Perhaps the most ideal rigid objects supporting fiber growth are pyrite "framboids". Framboids are subspherical, rasberry-like aggregates of smaller microcrystalline spherules. The individual spherules are normally on the

order of 1-4 microns in diameter, while the larger
framboidal aggregates range from 12 microns to several
millimeters in diameter. Pyrite framboids are products of
early diagenesis of sediments associated with activity of
sulfate-reducing bacteria (Berner, 1970). They form under
anaerobic conditions during diagenesis of highly
carbonaceous sediments (Berner, 1970). Framboids are most
common in carbonaceous pelitic rocks, although they are
present in some argillaceous limestones and graywackes.

Pyrite framboids in slates are generally flanked by
fibrous minerals in pressure shadows on opposite sides of
the pyrite. Fibers in slates consist of either quartz,
white mica, chlorite, or some combination of the three.
Pressure shadows represent sheltered, low-stress zones of
mineralization on opposite sides of the framboid. Unlike
passively deformed reduction spots, fibers in pressure
shadows of pyrite framboids probably do not record early
shortening by sedimentary compaction.

Figure 5.4 illustrates framboid-matrix interactions
which lead to pressure shadow development (Beutner and
Diegel, 1985). Figure 5.4A shows material flowlines or
particle paths for shape changes produced by a homogeneous
coaxial flattening, with the least principal stretch ($\sqrt{\lambda_3}$)
vertical. Figure 5.4B shows how flattening of the circle
centered at "0" will produce a strain ellipse, S, and
reciprocal strain ellipse, R, which contain the flowlines.
A deformation by mechanical flowage will produce particle
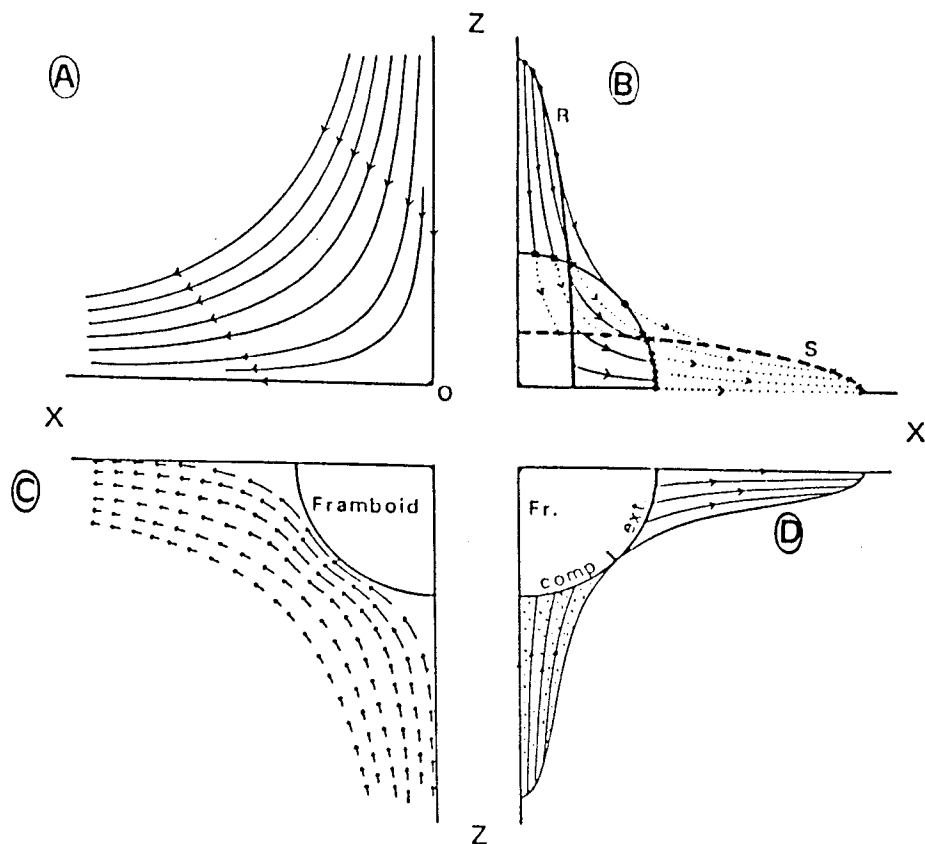
Figure 5.4 Framboid-matrix interactions during a deformation by pure flattening, where the maximum shortening direction is vertical and the maximum extension is horizontal. (after Beutner and Diegel, 1985, fig.4) See text for details.
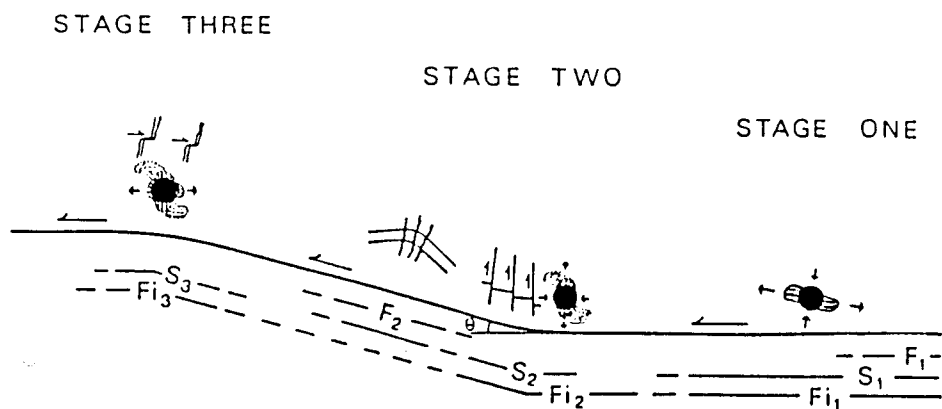
Figure 5.5 Schematic model showing three successive stages of fiber development (after Beutner and others, 1983, fig.16) Three generations of structures and associated fibers in pelites of the Hamburg sequence (Pennsylvania) record passage of a thrust sheet through a flat-ramp-flat thrust system. See text for discussion.

paths which are deflected around the spherical object (fig. 5.4C). Figure 5.4D represents a purely solutional mechanism by which material is dissolved in a quadrant of compression and reprecipitated in an extensional quadrant.

Crystal fibers grow incrementally in the extensional quadrant as the matrix is, in effect, pulled away from the framboid. Fibers grow progressively in the maximum direction of incremental extension (Durney and Ramsay, 1973). Pressure-dissolution and redeposition is the dominant mechanism contributing to fiber growth. However, mechanical flowage around large framboids can produce exceptionally long pressure shadows which misrepresent the bulk strain (Gray and Durney, 1979; Beutner and Diegel, 1985). Ideal framboid diameters are within the range of 25-75 microns (Beutner and Diegel, 1985).

Non-coaxial Fibers

One of the primary assumptions made in fiber analysis is that curved fibers record a non-coaxial strain history (Elliott, 1972; Durney and Ramsay, 1973). Non-coaxial fibers showing progressive reorientation can form under two general strain conditions. First, curved fibers can grow during bulk simple shear, or alternatively, during bulk simple shear in a spinning reference frame (Beutner and Diegel, 1985). Fiber growth under these conditions could occur in shear zones or on a rotating fold limb within a

shear zone, respectively. Secondly, curved fibers may develop by growth during two phases of flattening, separated by a rigid rotation. This second type of strain history is reflected by fiber curvature patterns in short, overturned limbs of folds in the Martinsburg slate (Beutner and Diegel, 1985). Rotation of the reference frame (bedding, e.g., Wickham and Anthony, 1977; Beutner and Diegel, 1985) with respect to relatively fixed axes of principal strain may explain sharply curved fibers associated with a cleavage that apparently formed by pure flattening.

Alternatively, central fibers in a pressure shadow which remain straight and parallel to cleavage record a coaxial strain history. Straight fibers imply that the direction of maximum incremental extension remained parallel to cleavage throughout cleavage development. Coaxial fibers form on fold limbs that did not experience substantial rigid rotations or shearing during cleavage development (Beutner and Diegel, 1985).

Syntectonic fibers uniquely record penetrative strains associated with the movements of thrust sheets (Beutner et al., 1983; Sample and Fisher, 1986). Figure 5.5 shows the progressive development of three discrete sets of fibers and associated structures within a single thrust slice of the Hamburg sequence in eastern Pennsylvania. Three cleavages with associated fiber sets formed in a sequence of deformational stages, each marked by unique strain conditions. The fiber geometries and associated structures

(fig. 5.5) record strains predicted as a thrust sheet encounters a closing bend, climbs a ramp and passes over an opening bend onto another flat (Beutner et al., 1983).

5.3 Fibers in the Galice Formation

Framboidal pyrite is a major constituent of most Galice shales and slates. The framboids are sometimes pulled apart into their constituent spherules, forming long quartz-pyrite lenses. In Galice slates, excellent fibrous pressure shadows are observed adjacent to spherical framboids. Most framboids have smooth surfaces, a result of the small diameters (1-2 microns) of the constituent spherules. Framboids within the 25-75 micron preferred range (Beutner and Diegel, 1985) are most common. The framboids in this range normally intersect at least several closely-spaced cleavage lamellae, thus recording an average local strain. Smaller individual spherules lie within cleavage lamellae; their pressure shadows probably misrepresent the bulk strain (Gray and Durney, 1979; Beutner and Diegel, 1985).

Pressure shadows in the Galice Formation consist of fibrous quartz, white mica, or intergrown combinations of the two. The distal ends of the fibers begin as overgrowths on grains in the matrix; however, the fiber-matrix interface usually marks a distinct break in optical continuity. In plane light, pressure shadows are easily discernible from the adjacent matrix, as they are conspicuously white. When

viewed under crossed-nicols, however, the fibers in the pressure shadows appear to merge with grains in the matrix.

Fibrous pressure shadows can have various geometries with respect to the pyrite framboid. The four geometries sketched in figure 5.6 are indicative of different strain conditions or deformation mechanisms. Figure 5.6A shows a pressure shadow with equal fiber lengths that preserves the outline of the spherical object ("rigid fiber" model of Ramsay and Huber, 1983). This geometry is indicative of unidirectional extension with negligible shortening in all other directions within the plane of section. Shadows resembling a strain ellipsoid (fig. 5.6B) form under moderate differential strain conditions, where the deformation mechanism is primarily pressure-solution (see fig. 5.4A,B). Figure 5.6C and D are attenuated pressure shadows. Distal portions of the shadows are compressed, no longer preserving the shape of original framboid-matrix boundary. Attenuated pressure shadows may form by dissolution of the most distal fibers, which are removed from the sheltering effect of the host object. Alternatively, they may indicate the influence of mechanical flow during the deformation (Beutner and Diegel, 1985; see fig. 5.4C).

Attenuated pressure shadows with triangular outlines are the most common geometries of pressure shadows in XZ sections of Galice slates. Eventhough some fibers pinch-out in the distal portion of the pressure shadow, a central
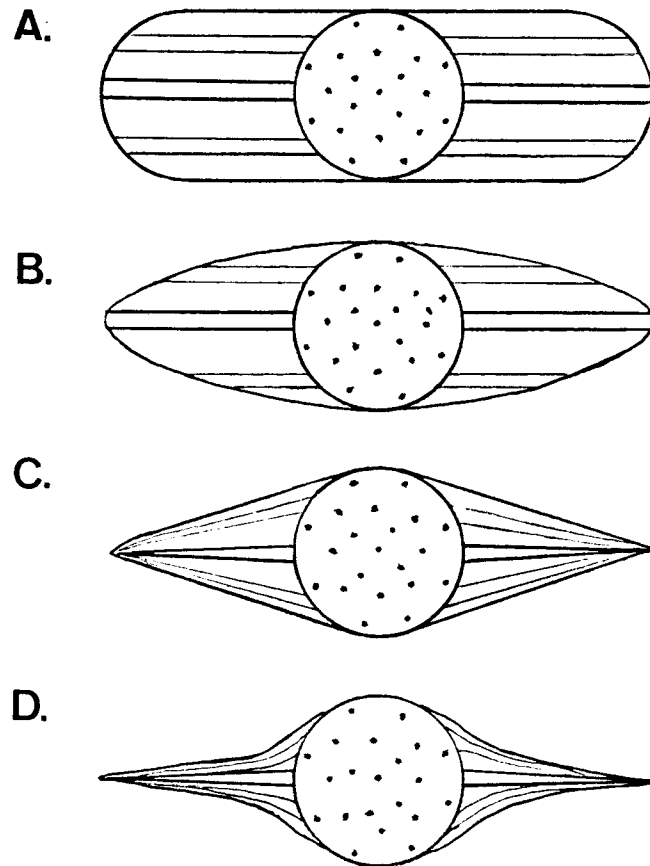
Figure 5.6 Geometries of pressure shadows adjacent to
rigid spherical objects. A. Rigid fiber model, B. Shadows
defining a strain ellipse, C. Triangular, attenuated
pressure shadows, D. Strongly attenuated pressure shadows.

fiber can usually be traced from the framboid to where it ends against, or passes into matrix.

Fiber growth is interpreted as antitaxial in pressure shadows of prites in Galice slates. The oldest material is at the distal end of the shadow; the newest fiber material is located at the pyrite-fiber interface. Several observations are consistent with antitaxial growth. First, the fibers are free of inclusions of matrix material, typically associated with syntaxially-grown fibers (Durney and Ramsay, 1973). Secondly, individual spherules are sometimes "plucked" off the framboid and included in distal portions of the pressure shadow. Finally, there are no solutional interfaces between the fibers and matrix that would suggest syntaxial growth (Ramsay and Huber, 1983).

Coaxial Fibers

One of the most important characteristics of fibers viewed in XZ sections of slates in the Galice Formation is that nearly all of them are straight, showing only slight asymptotic convergence from the framboid interface to the distal end of the pressure shadow (fig. 5.7). A few rare shadows with curved fibers probably reflect perturbational effects, as the fibers were forced to grow around large quartz grains or mica stacks. Consistent patterns of fiber curvature were not discovered in any thin-sections.
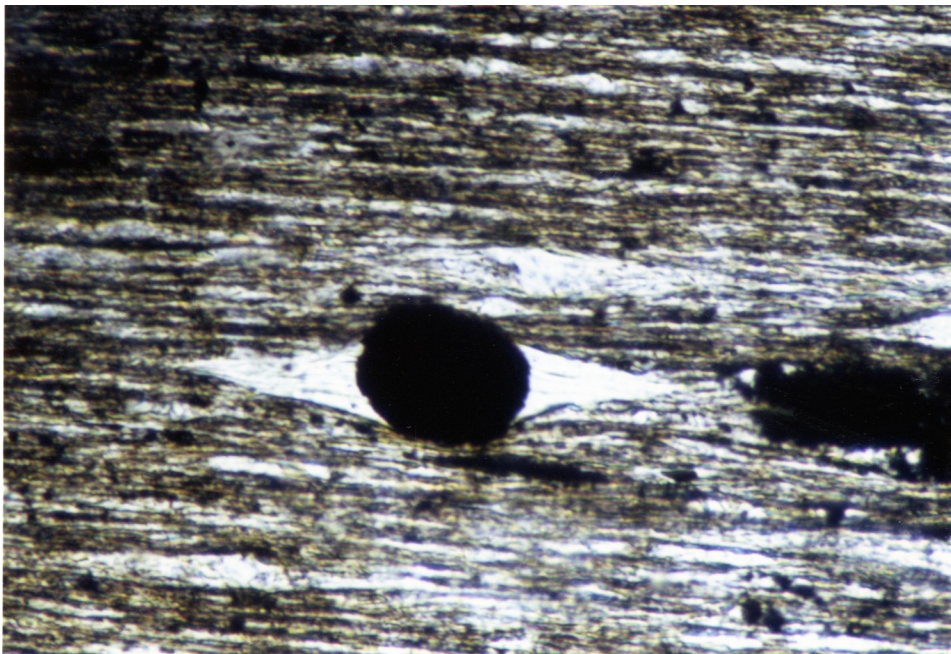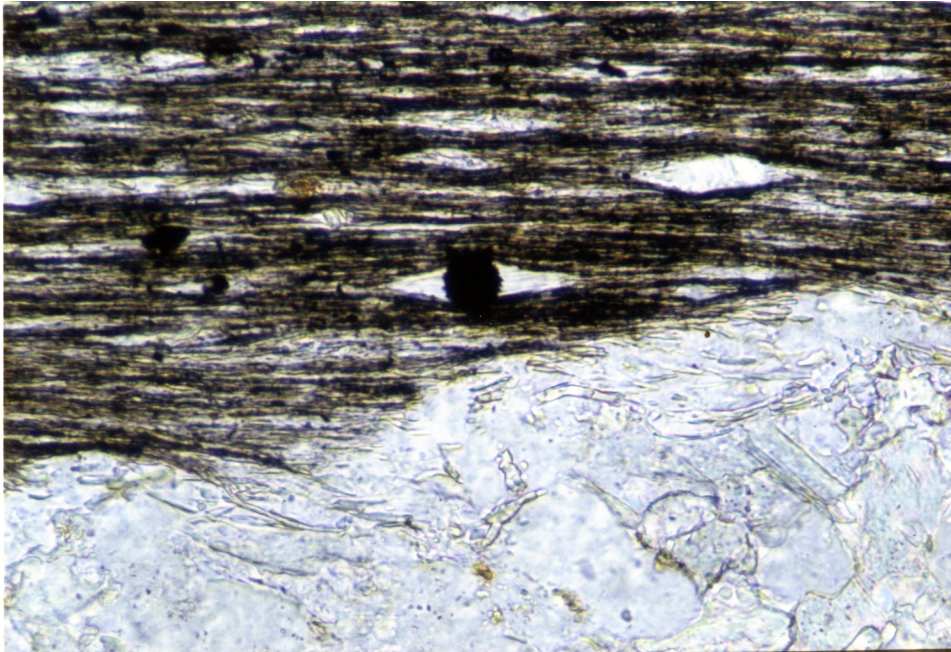
Figure 5.7 (top) Framboid with fibers adjacent to a large
quartz-calcite vein. Length of photomicrograph is 1.1mm.
(bottom) Slightly ovoid framboid with typical triangular-
shaped pressure shadows of fibrous white mica. Framboid
diameter is 70 microns. Photos taken in plane light.
Both samples are xz sections from an exposure along Middle
Fork Smith River (same location as figure 5.2).

In accordance with the findings of Beutner and Diegel (1985), fibers in sections parallel to S_1 (XY sections) are generally straight, parallel to the L_1 lineation and preserve the outline of the framboid. Since there is no evidence for shortening or extension normal to L_1 (Y direction), plane strain conditions are presumed to have prevailed during fiber growth. Additionally, the relatively strong L_1 stretching lineation observed in both hand samples and thin-sections is evidence that Galice slates were not in the flattening field of the Flinn (1962) diagram.

In one slate sample from near Kerby, Oregon, fibers in pressure shadows of large framboids viewed in the XY plane show optically-continuous curvature through an angle of approximately 30° (fig. 5.8). The fibers are sharply reoriented into parallelism with L_1 about half-way along their lengths; the youngest fiber increments (adjacent to the pyrite) are parallel to L_1. Fiber curvature in the XY plane was not observed in other slates exposed further to the south. It may be significant that the exposure containing this sample, a quarry northeast of Kerby, Oregon, is an unusual outcrop of strongly foliated slate. The rocks at this locality presumably experienced larger flattening strain than the weakly-foliated or non-foliated rocks exposed nearby. Fiber curvature was clearly related to a reorientation of the maximum direction of elongation (+L_1?) during penetrative deformation.
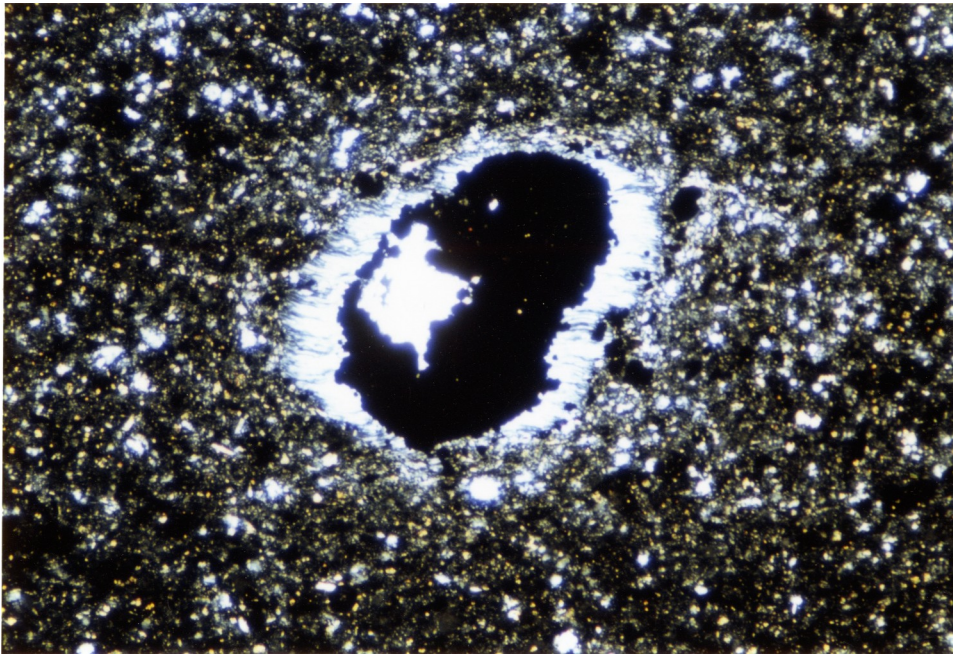
Figure 5.8 Large framboid in a section cut parallel to S1
(XY section). L1 is approximately horizontal in this
photo. Note that the pressure shadows preserve the shape
of the framboid. Horizontal dimension of the framboid is
4mm. THe sample is from an exposure along Reeves Creek
Road, 3 kilometers southwest of Lake Selmac, Oregon. Photo
taken with crossed nicols.

Selective Sampling

One of the primary objectives of studying fibers in the Galice was systematic sampling at localities likely to have experienced non-coaxial strains. Overturned F_1 fold limbs and areas adjacent to Nevadan thrusts are potential sites of non-coaxial penetrative strains. Figure 5.9 shows fiber patterns from the overturned limb of an F_1 fold in the northern field area. Curved distal portions of the fibers indicate an early reorientation (clockwise as shown) of the maximum extension direction with respect to S_1. This curvature is consistent with reorientation by rigid rotation of the overturned limb, as suggested for fiber curvature observed in the Martinsburg slate (Beutner and Diegel, 1985).

An overturned F_1 fold limb in more slaty rocks along Middle Fork Smith River unexpectedly contained coaxial fibers, showing no curvature. It is apparent that more samples from overturned limbs of F_1 folds are required to make any conclusions concerning strain states across the folds.

As previously noted, Nevadan thrusting did not involve intensification or reorientation of the S_1 cleavage in the northern Galice Formation. This is supported by observations of pressure shadows in slates adjacent to Nevadan thrusts, and particularly, the Preston Peak thrust. Fibers in these slates record <u>coaxial</u> strains, similar to

SE   NW

$\sqrt{\lambda_1} = 1.45$

10cm

100μ
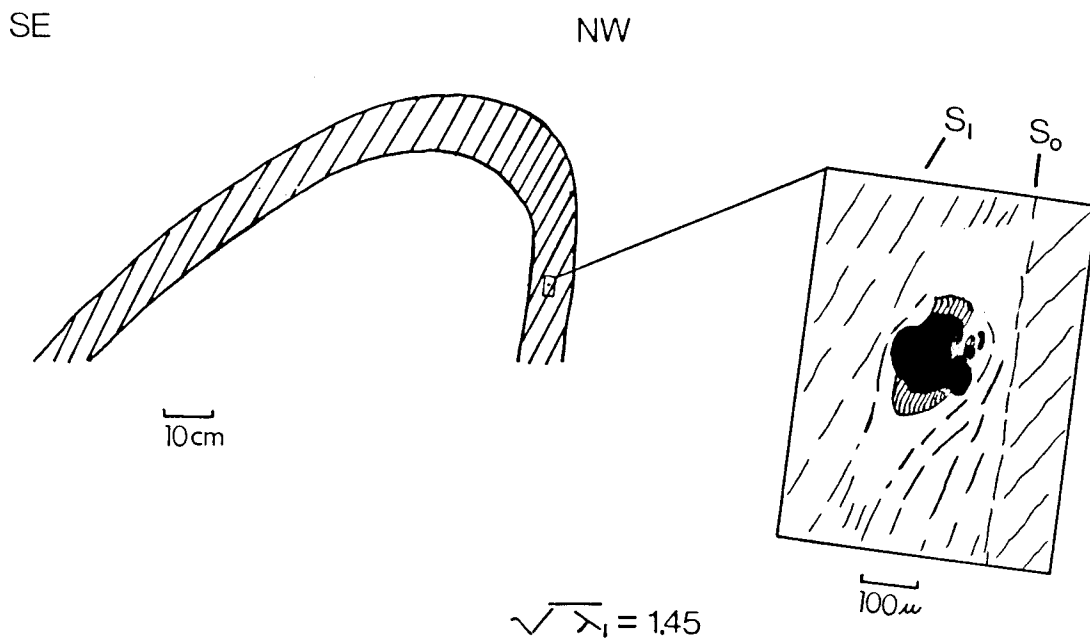
Figure 5.9 Thin-section sketch of fibers and sample local-
ity on the overturned limb of a northwest-vergent Fl fold.
Exposure near Reeves Creek Road. See text for details.

$$\sqrt{\lambda_1} = \frac{L_1}{L_o}$$
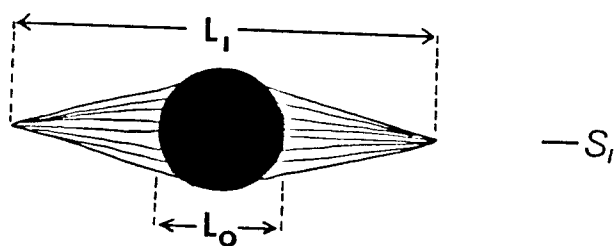
Figure 5.10 Determination of the maximum principal
stretch, $\sqrt{\lambda_1}$, as the tip-to-tip length of the pressure
shadows + pyrite diameter, divided by the pyrite diameter.

most other slates. Therefore, I suggest that shear strains related to Nevadan thrusting had no effect on S_1 development or fiber growth.

5.4 Finite Strain

The technique of measuring finite strain from fibers in pressure shadows of spherical objects is rather simple, and does not involve digitization or reiterated multiplication of strain matrices, normally required in incremental strain analysis. The maximum principal stretch, $\sqrt{\lambda_1}$, or 1+e, is equal to the tip-to-tip length of pressure shadows + framboid divided by the diameter of the framboid, as measured between the central fibers of the shadows (fig. 5.10). Assuming plane strain with no syn-deformational volume change ($\sqrt{\lambda_2}$ equals approximately 1.0), the least principal stretch, $\sqrt{\lambda_3}$, is simply $1/\sqrt{\lambda_1}$.

Fibers were measured from thin-sections of Galice slates cut normal to S_1 and parallel to L_1 (XZ sections), and parallel to S_1 cleavage planes (XY sections). Framboids with no pressure shadows, or very short ones, were observed in sections cut normal to S_1 and <u>normal</u> to L_1 (YZ sections). These minor fringes may represent off-center cuts through framboids (Beutner and Diegel, 1985). It is therefore assumed that there was no fiber growth parallel to the Y direction. The geometry of pressure shadows in XY sections, resembling the geometry shown in figure 5.6A, probably

indicates no lengthening or shortening parallel to the Y direction (i.e. plane strain during cleavage development). Pancake or disc-shaped pressure fringes (e.g. Williams, 1972b) were not observed in Galice slates.

Pressure shadows used for finite strain measurement were selected according to the following criteria:

(1) Spherical or subspherical framboids that intersect at least several cleavage lamellae were chosen; those larger than approximately 90 microns were omitted.

(2) Pressure shadows which posses a relatively straight central fiber which terminates against matrix at the distal end of the pressure shadow are optimal. This criterion is satisfied in nearly all pressure shadows observed in Galice slates.

(3) Fibers that are bent or deflected around other objects were not considered. Some fibers were forced to grow around large quartz grains, mica stacks or other framboids, resulting in curvature of the pressure shadow. In other cases, the distal portions of unusually short pressure shadows are juxtaposed against large grains. This phenomenon probably occurred by solution-removal of the intervening matrix, and possibly the oldest portion of the shadow. Measurement of these pressure shadows could potentially yield low finite strain values.

Pyrite Stringers

A sample taken along Reeves Creek Road contains long pyrite "stringers" that were stretched, the dilational gaps being filled with fibrous quartz (fig. 5.11). Since they are meandering features, and essentially parallel to bedding, they are interpreted as pyritized equivalents of trace fossils. They are constructed of smaller pyrite spherules, much like the microspherules in spherical framboids.

Quartz fibers filling the gaps in the stringers are curved when viewed in XY sections, and show characteristics of antitaxial growth (fig. 5.11). The pyrite stringers (fig. 5.11) are from the same sample as framboids with curved fibers discussed above (see fig. 5.8). Medial inclusions of pyrite and clots of carbonate are found in the vein-like openings. Fortuitously, the long axes of several stringers lie within 10° of the weak L_1 lineation (see fig. 5.11), allowing direct measurement of $\sqrt{\lambda_1}$. Stringers at moderate to high angles to L_1 are _not_ pulled apart, but rather possess fibrous pressure fringes along their lengths. Magnitudes of extension from the stringers are consistent with measurements of pressure shadows of pyrite framboids in the same section (e.g. fig. 5.8).

Values of $\sqrt{\lambda_1}$ measured in XZ and XY sections are shown in the table and histograms of figure 5.12 for thin-sections from the north and south field areas. Pressure shadows in
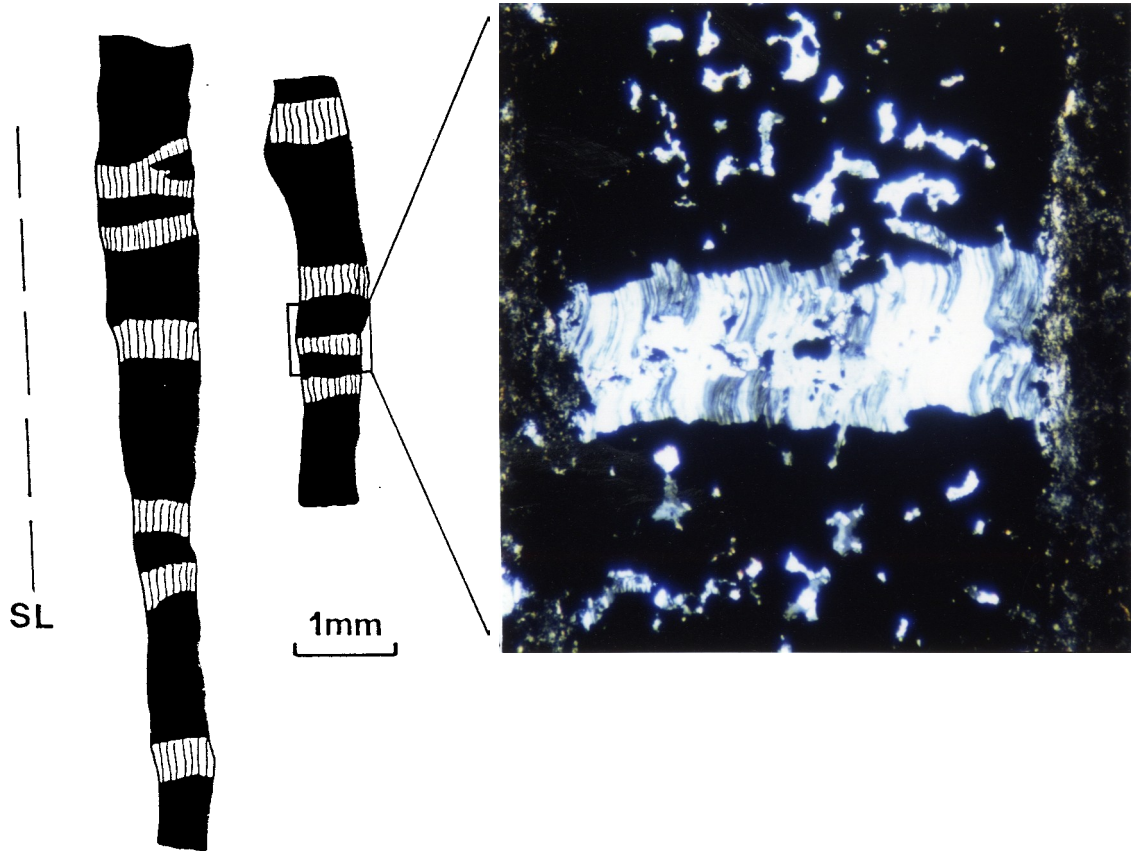
Figure 5.11 (left) Tracing from an S1-parallel thin-section showing stretched framboidal pyrite stringers and the orientation of L1. (right) Close-up view of a gap filled with sigmoidally-curved quartz fibers with medial clots of carbonate and pyrite. From same sample as figure 5.8.

	n	ave. (XZ)	range	n	ave. (XY)	range
North	22	1.63	1.32-2.21	5	1.40	1.32-1.50
South	41	3.20	2.20-4.21	9	2.81	2.49-3.51
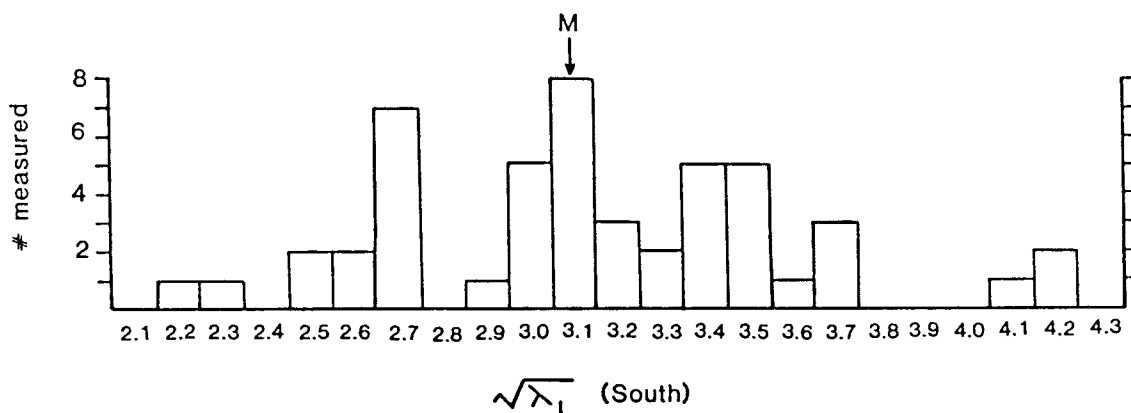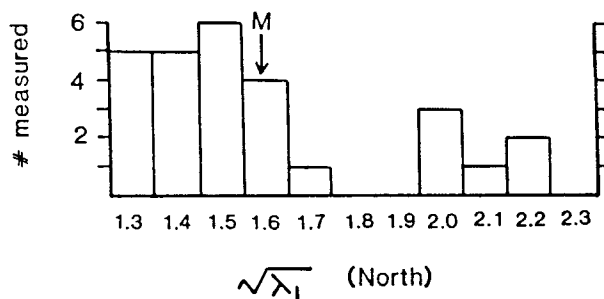
Figure 5.12 (top) Table showing $\sqrt{\lambda_1}$ values from fibers in slates from north and south of Oregon Mountain Road (see fig. 1.9). "n" is the number of framboids measured, "ave.(XZ), (XY)" are the mean $\sqrt{\lambda_1}$ values, and "range" shows the maximum and minimum values of $\sqrt{\lambda_1}$.
(bottom) Histogram showing #pressure shadows measured vs. extensional values from the northern and southern field areas. Measurements from XZ and XY sections are combined. "M" is the mean value.

Galice slates from the area south of Oregon Mountain Road show substantially higher values of $\sqrt{\lambda_1}$. The lack of measured pressure shadows from the northern field area reflects a paucity of pelitic rocks possessing slaty cleavage. Framboids in the typical weakly-foliated or non-foliated pelites of the northern field area rarely support pressure shadows. Furthermore, thin-sections cut parallel to S_1 in slates from the northern and southern Galice only rarely intersect framboid-rich layers. Framboids are usually scattered along discrete bedding/cleavage-parallel layers. Lower mean values from XY section may reflect this paucity of data. Nevertheless, the ranges of $\sqrt{\lambda_1}$ values in XY sections fall within ranges of $\sqrt{\lambda_1}$ in XZ sections. The data are rather dispersed throughout the ranges shown in the histograms in figure 5.12.

Assuming plane strain, apparent from XY sections of most Galice slates, the average value of $\sqrt{\lambda_1}$ from the southern area (combined data from both XZ and XY sections) corresponds to a finite strain ellipsoid with dimensions-- 3.1: 1.0: 0.3 and about 68% shortening normal to S_1. The lowest values in the range correspond to 55% shortening. Fibers from slates in the vicinity of Kerby, Oregon give an average shortening value of only 33%. These magnitudes of finite strain are schematically represented in figure 5.13.

Low values of $\sqrt{\lambda_1}$ in slates, such as those determined from fibers in the northern field area, can be attributed to tectonic volume-loss during cleavage development. Large
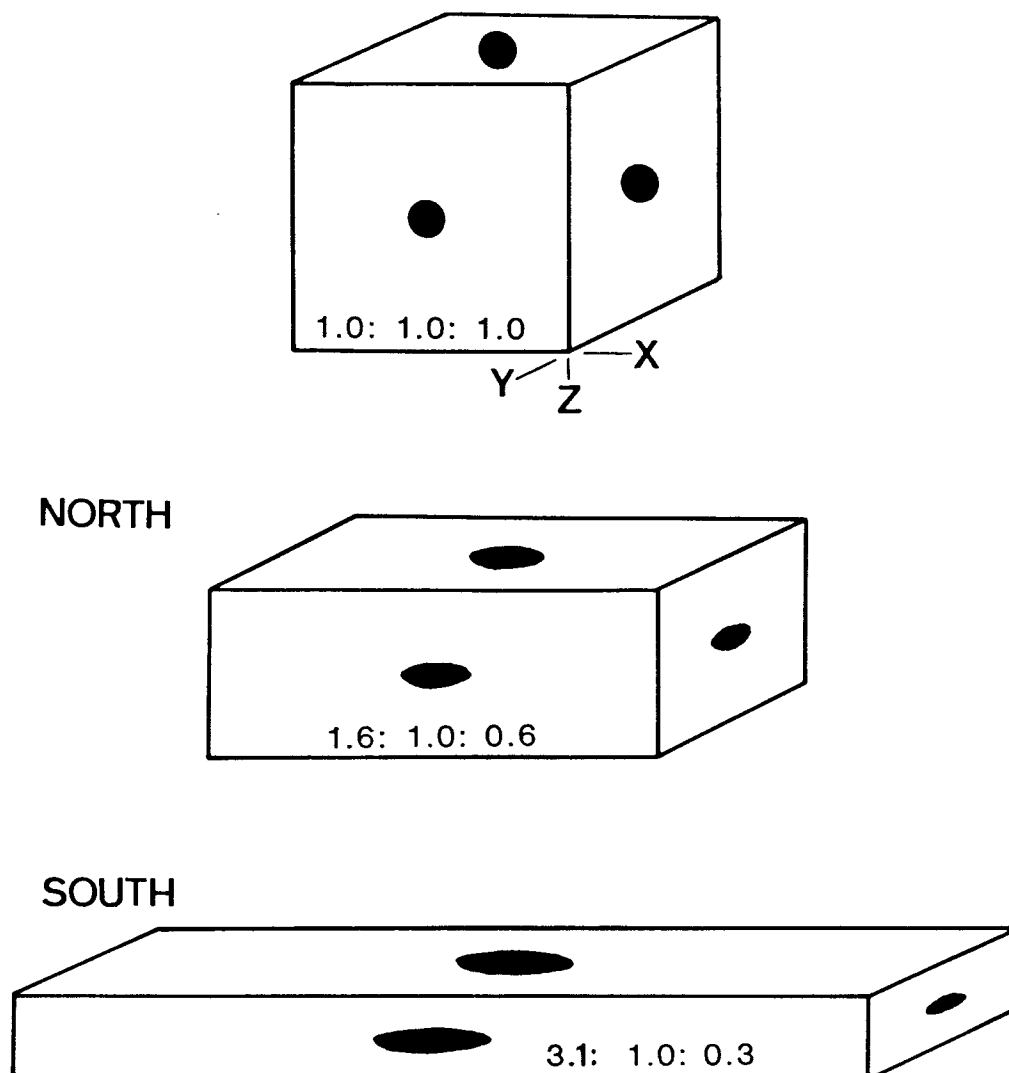
Figure 5.13 Deformation of a cube with passive spherical markers. X, Y and Z axes and magnitudes of principal stretches in those directions are shown for an undeformed cube, and cubes deformed by finite strains suffered in the north and south field areas (figures 1.6 and 1.9, respectively). Conditions of plane strain with no volume loss are assumed. Note that rocks in <u>both</u> field areas only experienced prehnite-pumpellyite facies metamorphism.

flattening strains normally expected during cleavage
formation (a minimum of 55%-60% based on finite strain
analyses--Wood, 1974; Beutner, 1978) were not fully
compensated by extension in the X direction of <u>northern</u>
Galice slates. Wright and Platt (1982) suggest that $\sqrt{\lambda_1}$ is
10% or less in Martinsburg slate that experienced 50%
tectonic volume-loss. Similarly, 29%-42% tectonic volume-
loss was calculated from a slate in the Hamburg sequence
(Pennsylvania), having experienced an extension of
$\sqrt{\lambda_1}$=1.41 (Beutner and Charles, 1985). Since some slates in
the northern Galice yield similar extensions ($\sqrt{\lambda_1}$=1.41),
29%-42% may be a reasonable estimate of local volume-loss
during S_1 development.

In northern Galice slates, relatively short fibers and
very few veins suggest that some proportion of material was
removed, rather than being deposited locally in pressure
shadows and veins. These slates may have experienced low
fluid pressures and open-system behavior during cleavage
formation (Beutner and Charles, 1985), possibly related to
their inferred higher structural position (relative to rocks
to the south) during main-phase Nevadan deformation and
regional metamorphism.

5.4 Strain Inhomogeneity

Outcrop to regional-scale variations in finite strain
are reflected in the intensity of folding and cleavage

development in the Galice Formation. In this section, finite strains from fibers are compared with those estimated from mesoscopic Nevadan structures.

Pencil Structure

The weak, anastomosing S_1 cleavage in the northern Galice is locally observed in the form of "pencil structure". Elongated linear fragments of shale or siltstone weather out of exposures where the rock is gently folded, possesses a weak S_1 cleavage and has a strong bedding-parallel fissility (Reks and Gray, 1981). Pencil structure is found in the cores of very gentle folds of bedding, the "pencils" having long axes parallel to the fold axis. Reks and Gray (1981) show that 9-26% shortening normal to cleavage is required for the development of pencil structure. Thus, the lowest amounts of penetrative strain in Galice pelites are probably associated with pencil structure. Massive graywackes without S_1 or any other signs of penetrative strain similarly experienced very low amounts of shortening by ductile processes.

F_1 Folding

Angular F_1 folds in the northern field area record as much as 62% shortening normal to the axial planes. This representative value was determined from a series of angular

folds, two of which are shown in figure 4.2. An original (unfolded) length of a graywacke bed was compared with a deformed length measured orthogonal to the axial plane. Folding was apparently by buckling and flexural-slip in graywackes and interbedded graywackes and shales. There is a clear north-to-south transition in the Galice from folding almost entirely by mechanical processes, to folding primarily accomodated by S_1-related shortening.

Nevadan strain in the northern Galice is strongly localized. For instance, the tightness and styles of F_1 folds, as well as the degree of S_1 development, are widely variable. Localized high-strain zones are evident in areas of particularly intense F_1 folding and strong cleavage development. Furthermore, large-scale F_1 folds (see Plate 1) may record Nevadan strains that are not apparent from outcrop-scale structures.

5.6 Interpretations

Syntectonic fibers in pressure shadows of pyrite framboids in Galice slates record a north-south finite strain gradient during the main-phase Nevadan deformation. Average shortening normal to S_1 in the northern and southern field areas are 33% and 68%, respectively. However, it is apparent from figure 5.12 that finite strain is quite variable in both field areas. Low amounts of penetrative finite strain in the northern field area are evident from

weak S_1 development and the local occurrence of pencil structure associated with gentle F_1 folds. However, relatively low extensions from fibers in slates in the northern field area could be misleading, as they may reflect substantial tectonic volume-loss.

Nevadan shortening in excess of 70% is possible further to the south, in light of strongly flattened pebble conglomerates in the Galice and deformed pillow lavas in the Josephine ophiolite. A comparison of pebbly wackes from Kerby, Oregon with those from Big Flat, California (20 kilometers south of the map area in figure 1.9) reflects extreme north-south variation in penetrative ductile strain (fig. 5.14). As previously noted, metamorphic grade also increases to the south (Harper, 1980a).

S_1 development occurred during a coaxial stage of flattening under plane strain conditions, dominantly by pressure-solution, combined with metamorphic recrystallization in rocks in the southern Galice. Although syntectonic fibers record coaxial deformation during S_1 development, the possibility of "pre-fiber" non-coaxial deformation cannot be excluded. Rigid rotations of bedding with respect to S_1 certainly occurred on limbs of overturned, asymmetric F_1 folds, but these large rotations are not recorded by syntectonic fibers observed in this study. Furthermore, there is no evidence from fibers that non-coaxial penetrative strains were experienced in slates near Nevadan thrusts. As will be discussed in the following

Figure 5.14 Comparison of pebbly wackes from Kerby, Oregon (top sample) and the Big Flat area in the southern Galice Formation (lower sample). The large grains are mostly chert, with lesser volcanic and argillaceous clasts. The local trace of bedding is horizontal in both samples.

chapter, Nevadan thrusts are largely post-kinematic, and were superimposed on earlier, main-phase structures.

Chapter 6: LATE NEVADAN DEFORMATION

Nevadan thrusting, which was briefly discussed in chapter 4, clearly occurred after Nevadan metamorphism and the main-phase Nevadan deformation in the northern Galice Formation. This chapter contains a more detailed discussion of the complex geometries resulting from Nevadan thrusting. Two important effects of thrusting were the truncation of F_1 folds and the development of angular discordance between sets of beds. F_2 folds, and their possible relation to Nevadan thrusting, are described in the first section.

6.1 F_2 Folding

A second generation of Nevadan folds, F_2, have been defined on the basis of the following characteristics:

(1) They fold the S_1 cleavage.

(2) They locally possess an axial-planar crenulation cleavage (S_2).

(3) They commonly have kink or chevron fold geometries.

F_2 folds in the northern Galice are outcrop-scale structures having wavelengths of less than three meters. They frequently have angular geometries with sharp hinges (fig. 6.1A,C,D), although open, concentric folds are equally abundant (fig. 6.1B). F_2 folds are typically found where S_1

145
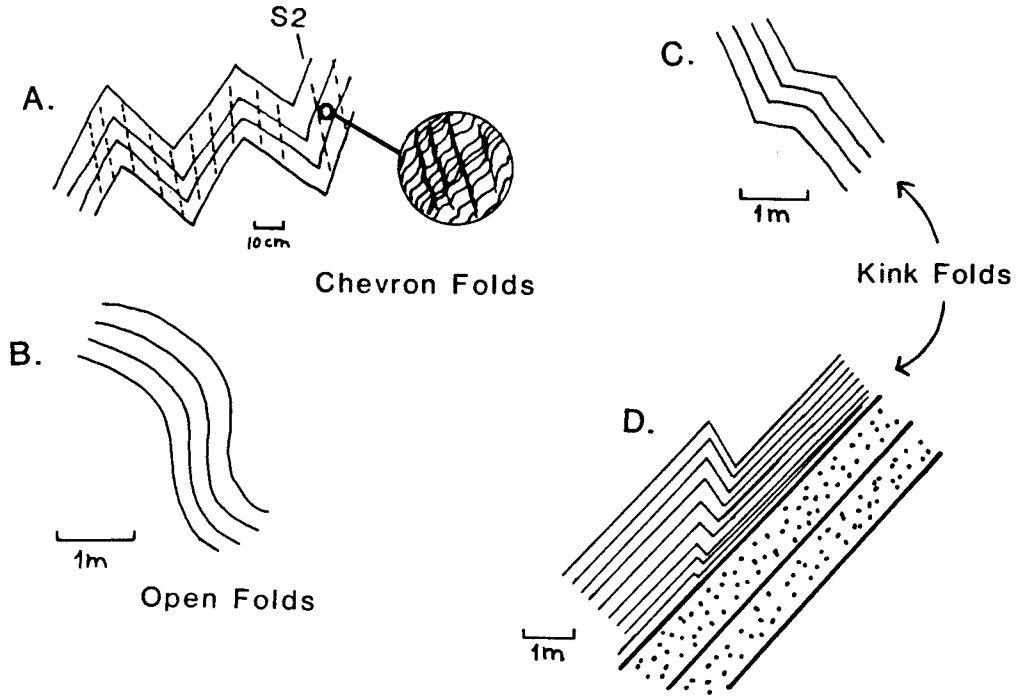
Figure 6.1 Outcrop sketches of F2 folds in exposures along Knopti Creek (fig. 1.9). See text for details.

Figure 6.2 The S2 crenulation cleavage defined by microfolds and kink bands, locally with discrete opaque folia along their shorter limbs. Length of photo is approximately 1cm. Sample from Knopti Creek, 2 kilometers east of the Middle Fork Smith River intersection.

is parallel to bedding. Apparently, strong anisotropy was a favorable condition for their development. Unlike F_1 folds, F_2 folds are normally upright, although somewhat asymmetric. Their variable styles, as well as the local nature of the S_2 crenulation cleavage in the northern Galice, suggest that the best criterion for identifying F_2 folds is that they fold S_1.

In northern California, the two fold generations can be distinguished by fold tightness, the degree of hinge thickening and the nature of the axial-planar cleavage. However, in the northernmost Galice Formation, there is a potential problem in distinguishing F_2 folds from F_1 folds, because the latter commonly have a very weak axial-planar S_1 cleavage. In the Kerby-Cave Junction area in Oregon, F_1 and F_2 fold styles (angularity, tightness) show significant overlap, and evidence of structural overprinting (e.g. Williams, 1970) is not always evident. A strong bedding-parallel fissility can generally be traced through the hinges of both F_1 <u>and</u> F_2 folds. It was essentially <u>bedding</u> that was folded during both F_1 and F_2 episodes in the northernmost Galice. Distinction between F_1 and F_2 folds in the area near Cave Juction was based on whether pelitic beds break along axial-planar fractures when struck with a hammer, particularly in water-polished exposures.

The S_2 Cleavage

S_2 is a crenulation cleavage that is axial-planar to F_2
folds. It is uncommon in the northern Galice Formation,
only being observed at two locations in this study-- near
McMullin Creek Road (fig. 1.6) and along Knopti Creek (fig.
1.9). S_2 has both discrete and zonal crenulation cleavage
morphologies (Gray, 1977). In slates, S_1 is normally kinked
in a stair-stepping fashion, with the local development of
discrete S_2 cleavage folia along short limbs of the kinks or
microfolds (fig. 6.2). In strongly-foliated metagraywackes
and phyllitic metasiltstones, S_2 occurs as spaced kink
bands, frequently in conjugate sets.

Other than the short limbs of microfolds and discrete
cleavage folia, no additional elements define the
crenulation cleavage in the northern Galice. There is no
evidence for recrystallization or mineral growth in
potential strain shadows of rigid objects such as pyrite
grains. Fibrous pressure shadows of pyrite framboids that
formed during the main-phase deformation are folded around
S_2 microfolds and are locally truncated by discrete S_2
cleavage folia. Even though S_2 cleavage development appears
to have involved shortening by pressure-solution,
neocrystallization of quartz or phyllosilicates in
dilational zones is not observed, possibly suggesting local
volume loss.

S_2 is a stronger, regionally-penetrative cleavage in southern exposures of the Galice Formation. To the south of the area in figure 1.9, S_2 is most commonly a discrete crenulation cleavage with extensive segregation of mineral phases. Recrystallized micas are oriented parallel to S_2, suggesting that the cleavage formed during Nevadan regional metamorphism (Gray, 1985). Gray (1985) notes that F_2 folds are cross-cut by dikes, similar to those to the west dated at 150 Ma (Saleeby et al., 1982), constraining the age of F_2 folding as Nevadan.

F_2 Kinematics

Gray (1985) observed a progressive transition from gentle, upright F_2 folds to tighter, west-verging folds near the Orleans thrust (fig. 6.3). This implies that F_2 folding was contemporaneous with Nevadan thrusting; the higher strains near the thrust produced tighter, west-vergent folds. A west-to-east transition from upright to strongly reclined F_2 folds may correlate with increased bulk simple shear as the thrust is approached (Sanderson, 1979).

F_1 and F_2 fold axes have similar orientations, although variations up to 30° in trend and plunge are observed (Harper, 1980a; Gray, 1985). At individual outcrops, F_1 and F_2 fold axes are commonly oblique to each other. Figure 6.4 is a plot of F_2 fold axes and poles to S_2 from this study. F_2 fold axis orientations are rather variable, although a
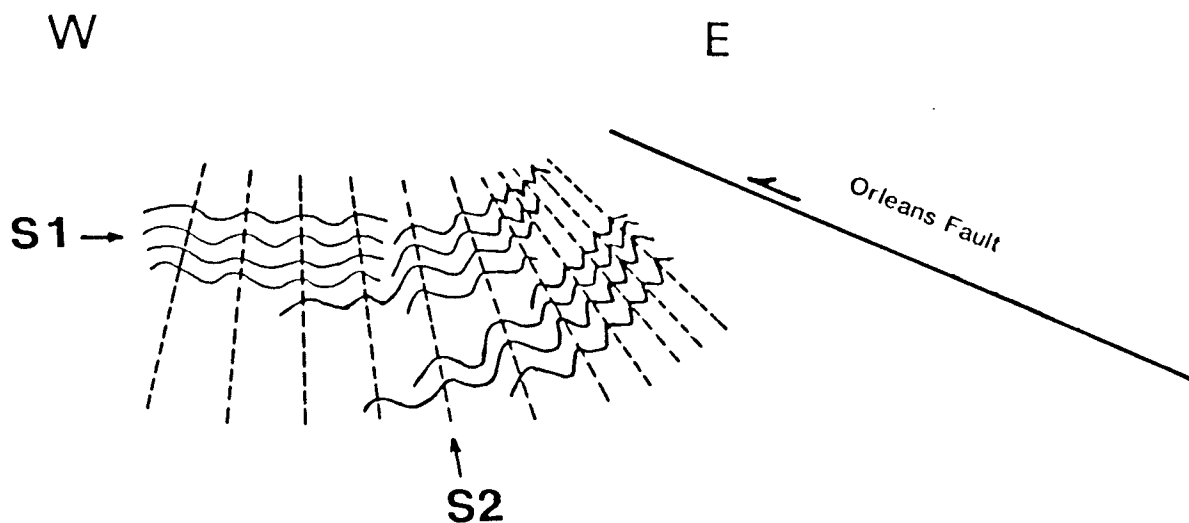
Figure 6.3 Schematic representation of the progressive rotation of F2 axial planes (locally defined by S2) towards the Orleans thrust in the southern Galice Formation. F2 folds become tighter and attain westward vergence near the thrust (based on data from Gray, 1985).
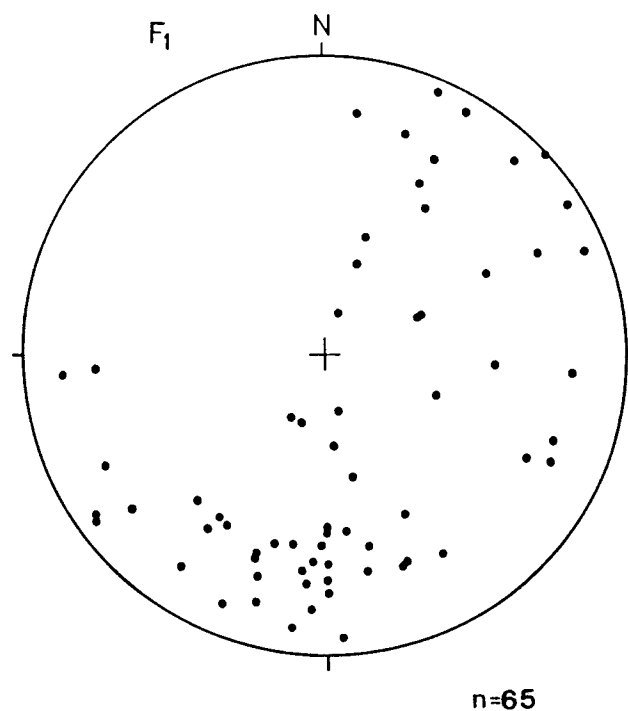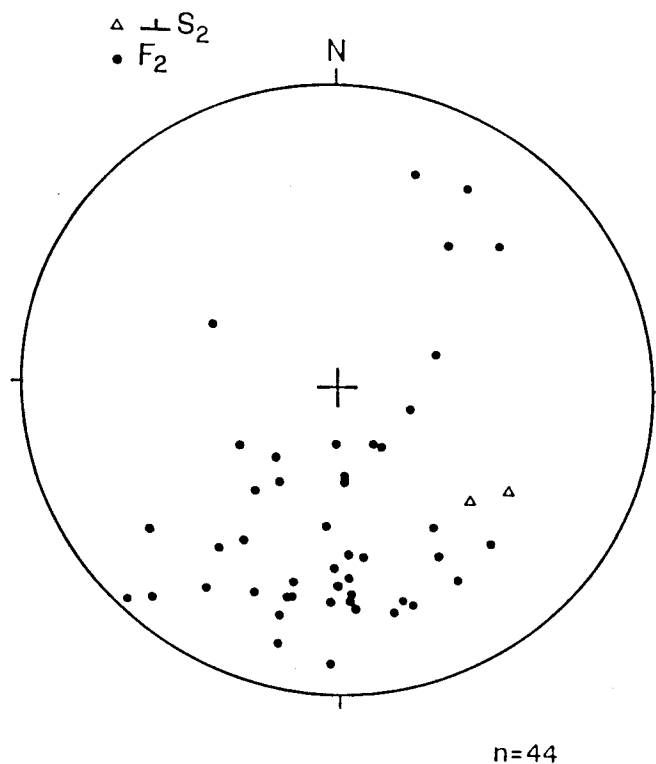
Figure 6.4 Stereographic projection of F2 fold axes (top).
Data combined from both field areas (figs. 1.6 and 1.9).
Similar to F1 fold axes, shown below, F2 axes generally
plunge to the south. Poles to S2 from two localities are
plotted with F2.

concentration of south-plunging F_2 axes is similar to the concentration of F_1 axes, shown below for comparison.

F_2 folds are found in association with thrusts and brittle shear zones. F_2 chevron folds tend to be confined to discrete, highly disrupted fault zones with boundaries roughly parallel to the local attitude of bedding. Some F_2 folds may have formed along bedding-parallel detachments, much like a rug is crumpled on a smooth floor. The kink folds sketched in figure 6.1D probably formed by sliding of the slate sequence (thinner beds) along the upper surface of the massive metagraywacke beds (stippled).

Other F_2 folds formed by flexure (fig. 6.5) along Nevadan thrusts (Wells et al., 1949; Kays, 1967; this study). The close association of F_2 folds with thrusting, and the nature of the S_2 crenulation cleavage discussed above, suggest that F_2 folding was a second generation Nevadan event (D_2). In the northern Galice, F_2 folds are strictly brittle structures which fold the S_1 cleavage, and locally refold F_1 isoclines (Harper, 1980a).

6.2 Nevadan Fault Zones

In the northern Galice, there are 5-30 meter-wide zones of intense faulting, brecciation and F_2 folding. Such fault zones were observed in exposures along Knopti Creek, Siskiyou Fork Smith River (fig. 4.7) and in the area east of Kerby, Oregon (Plate 1). The zones are generally parallel

Figure 6.5 Drag folds showing sense of displacement of
a Nevadan thrust. Exposure near Reeves Creek Road, 3
kilometers southwest of Lake Selmac. View is southwest.

Figure 6.6 Isoclinally-folded graywacke bed (outlined) in
a brittle shear zone. The bed is graded; the younging
direction is shown with arrows. The graywacke isocline is
"rootless", as it is suspended in strongly fissile shale
and thinner wacke beds.

to less deformed, uniformly dipping beds on either side. At a few localities, a "scaly" shear foliation, defined by slightly anastomosing fractures with polished surfaces, is developed in pelitic rocks. Quartz veins are present in some of the fault zones in northern California. High shear strains are evident from strongly reclined isoclinal folds and dismembered graywacke beds in the fault zones (fig. 6.6).

These fault zones are interpreted as major thrust zones (or reverse fault zones if steeply dipping), based on asymmetry of F_2 folds in the zones. The fault zones are most frequently found in strata along overturned limbs of large-scale F_1 folds (Plate 1), and possibly functioned as basal thrusts for nappe-like movement of the folds. These brittle fault zones may be similar to regional-scale north-south trending reverse faults that have repeated the crustal sequence of the Josephine ophiolite in northern California (Harper, 1980a). Large reverse faults in the Oregon Mountain area (northern part of figure 1.9) were interpreted as younger than Nevadan thrust faults (Vail, 1977). I suggest that the major fault zones observed in this study are large Nevadan thrusts, based in their inferred northwestward vergence and their close association with large-scale F_1 folds and smaller F_2 folds.

6.3 Bedding and Fold Truncations

Truncations of sets of beds and F_1 folds are conspicuous structures in rocks of the northern Galice Formation, particularly in the exposures along the east and west forks of the Illinois River (fig. 1.6). A detailed structural cross-section through a well-exposed horizontal outcrop (fig. 6.7) helps to elucidate the geometries of truncated folds and beds. Figure 6.7 is a section drawn normal to F_1 fold axes which plunge approximately 40° southwest. Most notable from this section are high-angle discontinuities between portions of F_1 folds and sets of beds. In the central part of the section, dips of beds vary over a short interval without any sign of a fold closure. This suggests truncation of some beds at depth.

A detailed map view of the southeasternmost fold in the cross-section is presented in figure 6.8. This southwest-plunging anticline is dissected by a fault defined by a covered interval with a few exposed pieces of sheared shale and blocks of graywacke. The fault separates beds of different thickness and orientation (note representative strike-and-dip symbols). Similar truncations, presumed to be faults, are associated with a large number of F_1 folds in the northern Galice. Many (perhaps most) F_1 folds occur as "monoclines" or in small groups between thicker intervals of unfolded beds. At some localities, truncations of F_1 folds

(following page)

Figure 6.7 Detailed cross-section through a 20 meter section of subvertical beds in the Galice. Exposure along West Fork Illinois River near Cave Junction, Oregon. View is to the south-southwest. Arrows show the younging directions, dashed lines are S1 and wavy dashed lines show irregular fissility in sheared shale.
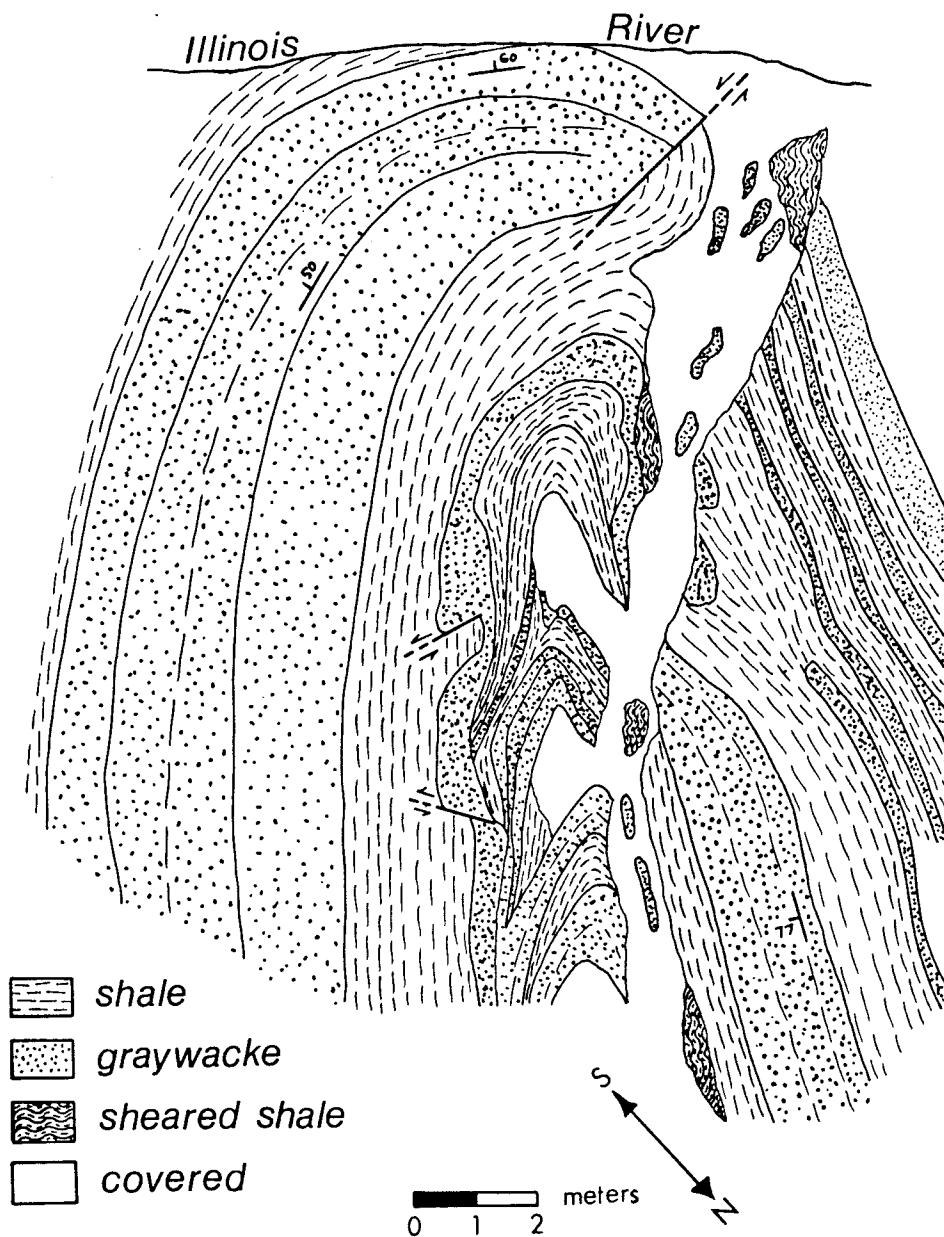
Figure 6.8 Map view of a truncated, southwest-plunging anticline exposed along West Fork Illinois River, 2 kilometers south of Pomeroy Dam. Fold is located at the left-hand edge of the cross-section in figure 6.7. See text for description.

and sets of beds are so common that they may be considered "penetrative" structures at the outcrop scale. The remaining sections of this chapter will be devoted to description of the morphologies of bedding and fold truncations and some possible models for their deveolopment.

Examples of Fold Truncations

Four line-drawings in figure 6.9 show the diversity of fold truncation geometries. Truncation surfaces occur at various angles to the limbs and axial planes of F_1 folds. Truncations are oriented parallel to the fold limbs (fig. 6.9A) or oblique to them (fig. 6.9B,C,D). Figures 6.9B and 6.10 are examples where the exposed trace of the truncating surface is parallel to the axial trace of the F_1 fold. Where younging directions could be determined (e.g. fig. 6.9A,B), beds on opposite sides of the truncating surface young in the same direction.

An unusual aspect of the truncations is that beds terminated by the truncation surface are not traceable on the opposite side of the discontinuity. Fold limbs are typically replaced by more massive beds (fig. 6.9A,B) with different orientations with respect to the truncated limbs. Fault surface features like breccia, gouge and slickenside striations are not present, although the surfaces of some graywacke beds are polished where truncations occur; for example, this is observed along the upper surface of the
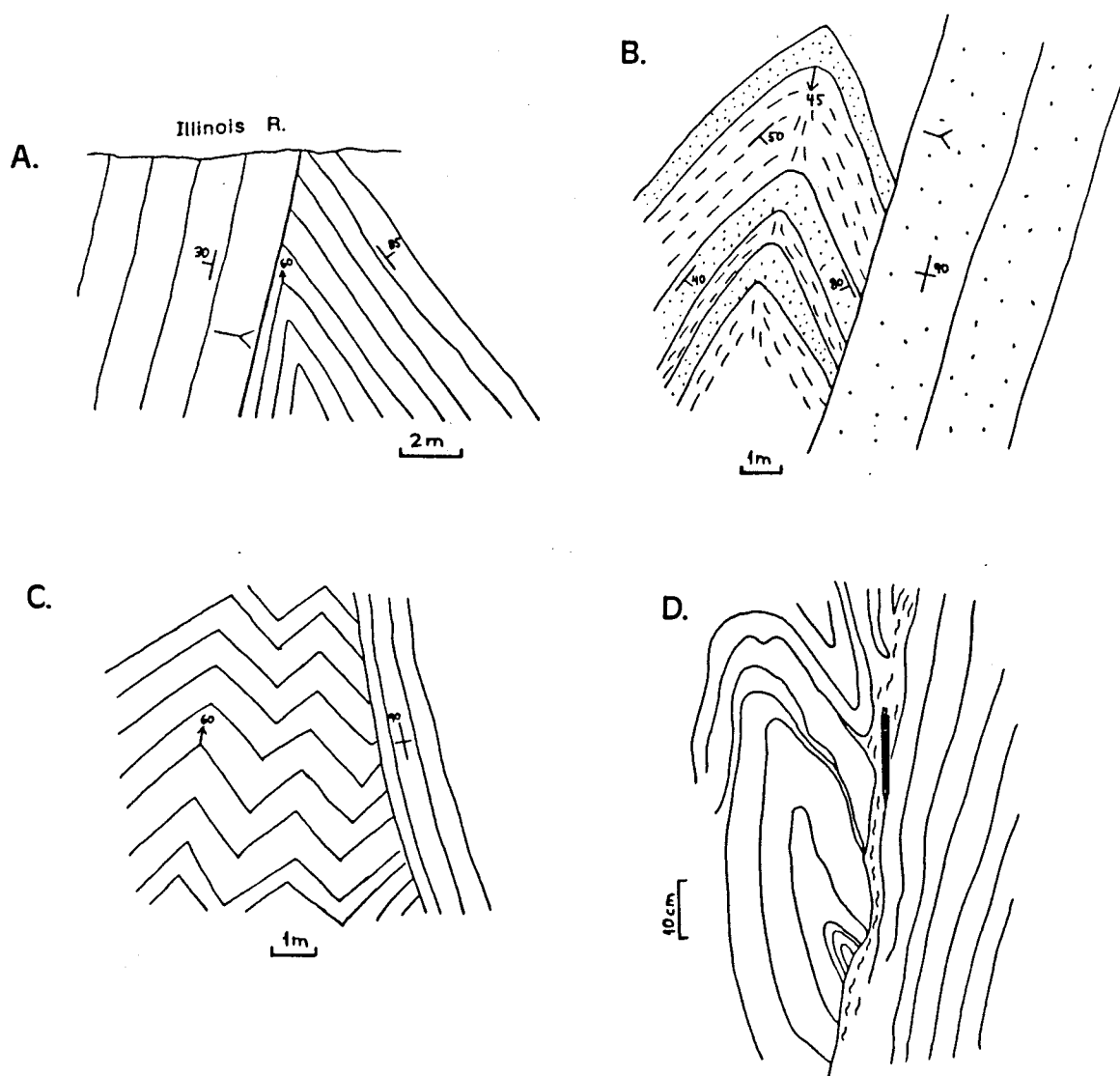
Figure 6.9 Sketches of outcrops showing geometries of F1 fold truncations. Younging directions (forked arrows), fold axes (arrows with plunges) and strike-and-dips of beds are shown where determined. S1 is weakly developed in the hinge of the fold in B. A, B and C are from horizontal exposures along West Fork Illinois River. D is from a vertical quarry exposure along Holton Creek Road in Kerby, Oregon.

Figure 6.10 Steeply-plunging syncline that is thrusted-out in its hinge zone, parallel to another set of beds. The outcrop surface dips slightly toward the viewer; the lower beds strike approximately north-south with north to the right. East Fork Illinois River near Cave Junction, Oregon.

massive wacke beds in figure 6.9B. Beds seldom curve into
parallelism with the truncation surfaces, as is the case
with drag folds in the Galice (fig. 6.5). Truncation
surfaces are sharp and well-defined (fig. 6.11). Thin beds
on the left-hand limb of the anticline in figure 6.11 were
contorted and juxtaposed against noticeably wider beds of a
different orientation.

Small folds that appear to have been thrusted-out in
their hinges parallel to slaty cleavage have been described
from the Martinsburg slate in east-central New Jersey
(Beutner, 1978), and from the southern Galice Formation
(Gray, 1985). Wilson and DeHedouville (1985) found that
many first generation folds in a sequence of low-grade
argillaceous rocks in Australia contain faults and features
resembling thrust duplexes which produce small-scale
repetitions of bedding. Slightly larger outcrop-scale
truncated folds have been observed in fold-and-thrust belts
and ancient accretionary complexes exposed on land (G.D.
Harper, W.S.F. Kidd and T. Byrne, pers. comm.).

Pseudocross-bedding

Peculiar obliquity between sets of beds, resembling
large-scale cross-bedding, occurs in the northern Galice
Formation in the absence of F_1 fold closures. Variably-
oriented sets of beds are bounded by truncation surfaces.
In an example from the "type-locality" of these structures

(following page)

Figure 6.11 Photograph and sketch of a truncated F1 fold.
Beds are contorted and pulled-apart adjacent to a well-
defined truncation surface (parallel to pencil, marker).
Several siltstone/sandstone beds are stippled in the
sketch. Horizontal outcrop along West Fork Illinois River
near Pomeroy Dam.
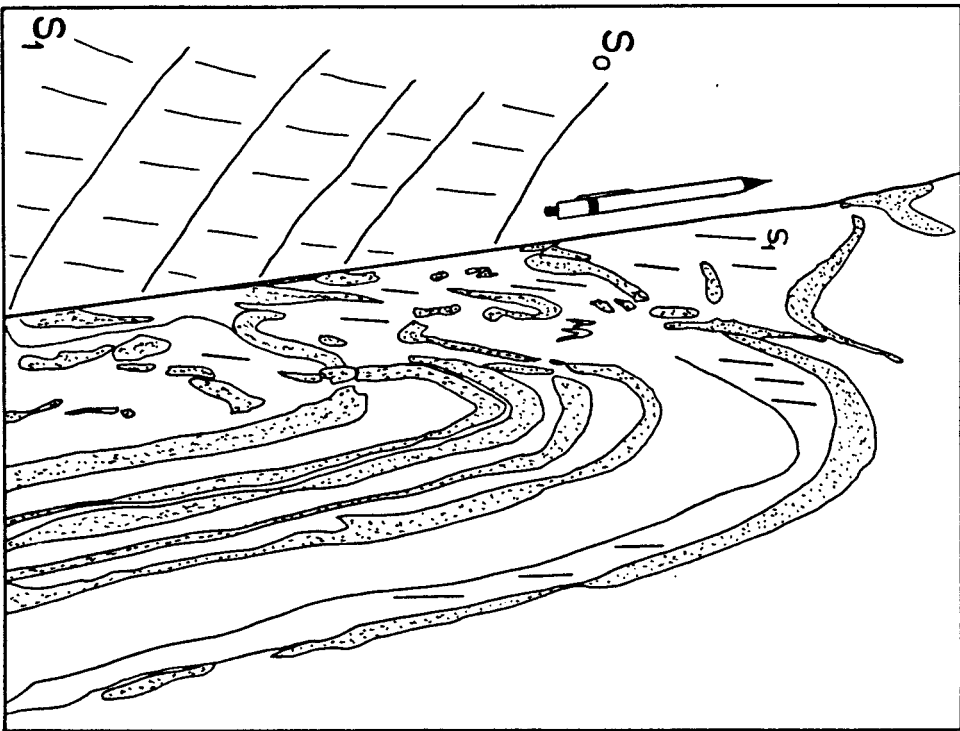
along East Fork Illinois River, truncation surfaces mark angular discordance between beds, and are represented in figure 6.12 as dark lines.

Figure 6.13 shows two examples where younging directions were determined from adjacent sets of beds separated by a truncation surface. In these examples, beds on opposite sides of the truncation young in the same direction, similar to younging observed in truncated folds. In figure 6.13B, both the horizontal beds (upper) and inclined beds (lower) are overturned; the younging direction is "downward". An important conclusion drawn from these observations is that the widespread phenomenon of "pseudocross-bedding" did not result from displacement of fold hinges (parallel to the axial plane) by faulting, because beds on both sides are observed to young in the same direction. Fault truncations parallel to one of the liombs would not result in complete elimination of the fold closure. Alternative causal mechanisms will be explored in section 6.4.

Pervasive bedding truncations are rarely described in the literature. Cross-bedding like structures are commonly observed in transposed sequences (Hobbs et al., 1976). They can be produced by attenuation of a fold limb and consequent juxtaposition with other differently-oriented limbs (Turner and Weiss, 1963). Alternatively, angular discontinuities can develop as small faults in the cores of tight folds in more brittle regimes. Fold closures may be obscured by
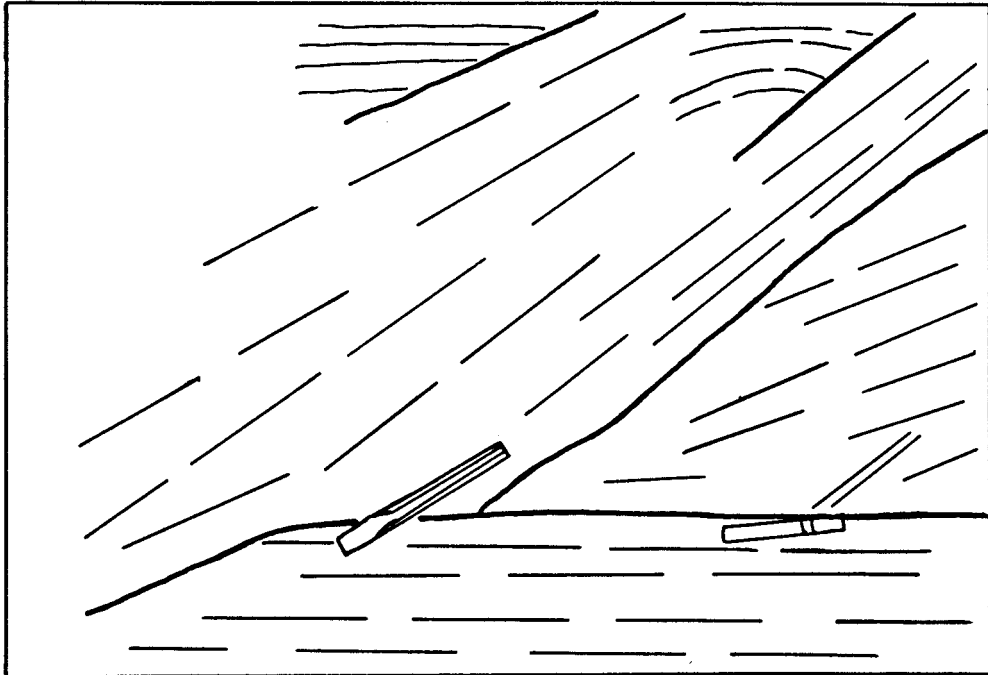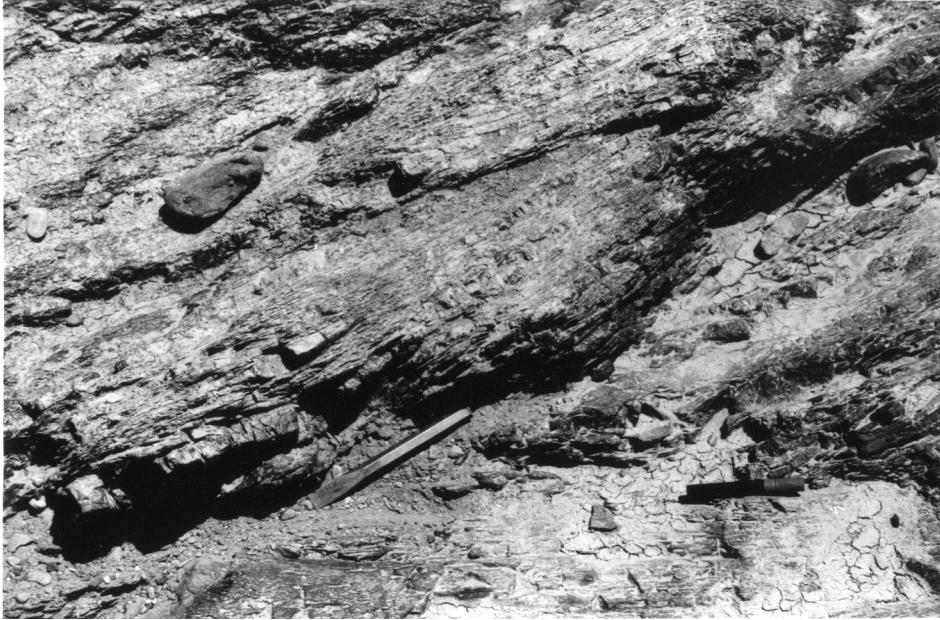
Figure 6.12 Photograph and sketch of an exposure along East Fork Illinois River near Cave Junction. Variably-oriented sets of beds form crossbedding-like structure. In the sketch, thin lines show traces of bedding and thicker lines mark the traces of truncation surfaces. Chisel and marking pen for scale.

Figure 6.13 A. (top) Angular discordance between a massive graywacke bed (right) and interbedded wackes and shales. Standard 12x18cm field book for scale. B. (bottom) Unconformity-like truncation of an inclined set of beds. Exposure 5 kilometers east of Kerby, Oregon. Coin is a US quarter. Arrows show younging of beds in both photographs.

propagation of the faults through the hinge zone (Sander, 1911).

In addition to transposition of layering, sedimentary explanations have been evoked to account for angular discordance between sets of beds. Williams and Nealon (1986) describe outcrop-scale packages of beds separated by truncation surfaces in interbedded Silurian sedimentary rocks in western Ireland which are remarkably similar to pseudocross-bedded strata in the Galice. They conclude that the bedding truncations developed from multiple tidal channel migrations, as the truncation surfaces are marked by convolute lamination and sedimentary breccia. This shallow water depositional model can clearly be ruled out in the Galice Formation. Large-scale sedimentary cross-bedding involving shale beds as well as graywackes is atypical of turbiditic flysch sequences; therefore, a deformational origin is inferred.

6.4 Models for Fold Truncations

F_1 folds in the Galice Formation commonly appear to have been thrusted-out in their hinges parallel to the axial plane. Gray (1985) noted that some F_1 folds in the southern Galice were thrust to the west along S_1 planes and are now half-anticlines and half-synclines (fig. 6.14). The resultant geometry is similar to the truncated fold in figure 6.10. Gray's (1985) observations suggest that the
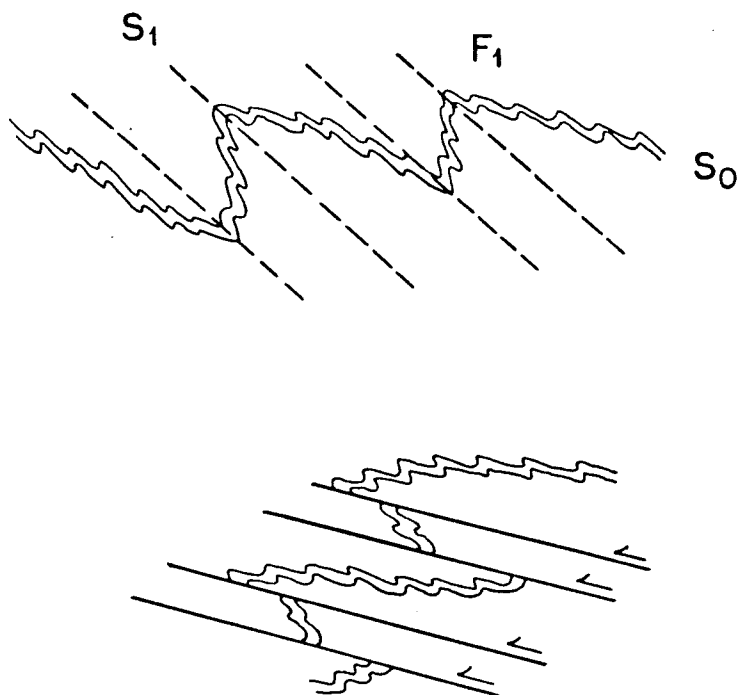
Figure 6.14 Line drawing depicting truncation of Fl fold hinges in the southern Galice parallel to Sl. (modified after Gray, 1985) See text for discussion.
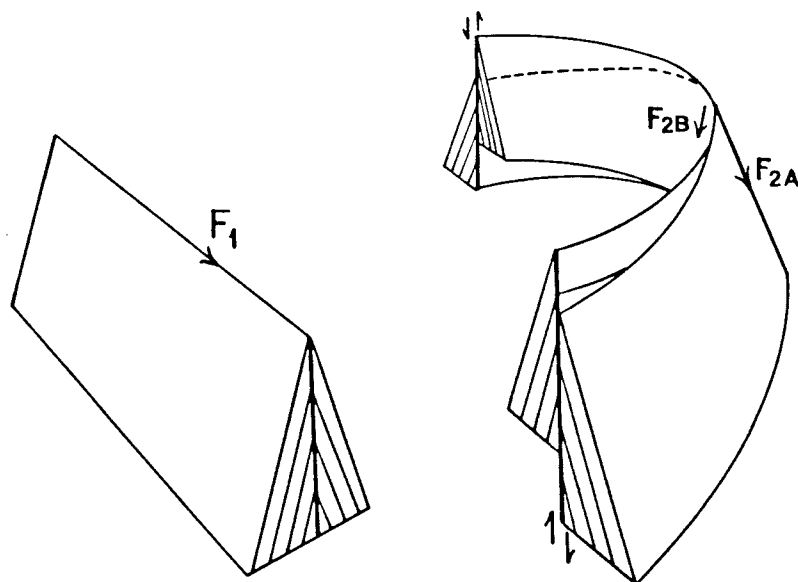
Figure 6.15 Differential displacement along an Fl axial plane resulting from refolding around an F2 axis. The Fl hinge zone is bisected, producing crossbedding-like structure (after Ramsay, 1967, fig. 10-29). See text for details.

thrusts only develop along axial planes that intersect the hinges of F_1 folds. There are examples in the northern Galice, however, where S_1-parallel thrusts cut across a fold limb and do not intersect the hinge of the fold (fig. 6.9B).

Figure 6.15 shows how displacement along an F_1 axial plane can be caused by refolding. In figure 6.4, refolding of an angular F_1 fold is accompanied by variable amounts of flexural-slip along the F_1 axial plane. Note that a geometry resembling cross-bedding forms when an angular fold is truncated and offset along its axial plane. Refolding of F_1 folds around F_2 axes, however, is rarely observed in the northern Galice. Furthermore, it is unlikely that faults would preferentially develop parallel to the weak S_1 foliation in the northernmost Galice.

Cleavage-parallel thrusting, as suggested by Gray (1985) is more evident in strongly foliated rocks in northern California, where there is little or no anisotropy parallel to bedding (i.e., monotonous slate sequences). In thin-section, offsets along some S_1 planes lack pressure solution seams, and are instead marked by strongly deformed quartz-calcite veins with inclusions of wallrock material. Pervasive slickensides on slaty cleavage planes are further evidence for cleavage-parallel shearing in the southern field area (fig. 1.9).

Bedding-Parallel Thrusting

Thrusting parallel to bedding was more important in the northern Galice during late Nevadan deformation. Figure 6.16 is a schematic line drawing demonstrating how some fold truncations may have developed by bedding-parallel thrusting. A sequence of beds is folded into tight, kink-like folds with axial traces shown as dots in figure 6.16A. Incipient fractures are dashed lines drawn parallel to bedding in the upright limbs of the folds. Displacement parallel to bedding causes truncation of the folds oblique to their axial planes. Although angular discordance between beds (bedding truncations) is produced in figure 6.16B, fold closures are not completely eliminated.

This mechanism of fold truncation appears to have occurred in the northernmost Galice for three reasons. First, F_1 folds tend to have tight, chevron or kink fold geometries (see fig. 4.2). Secondly, individual F_1 folds, or small groups of them, are typically bounded by thick, unfolded homoclinal sequences of beds. Fractures are likely to cut across the F_1 folds parallel to this strongly preferred orientation of bedding. This is especially evident along West Fork Illinois River near Pomeroy Dam, where there are mutually-parallel "packages" of folded and unfolded beds that are presumably bounded by thrusts. Note that the truncation geometry in part B of figure 6.16 is similar to that of the truncated fold in figure 6.9A.

A.

B.
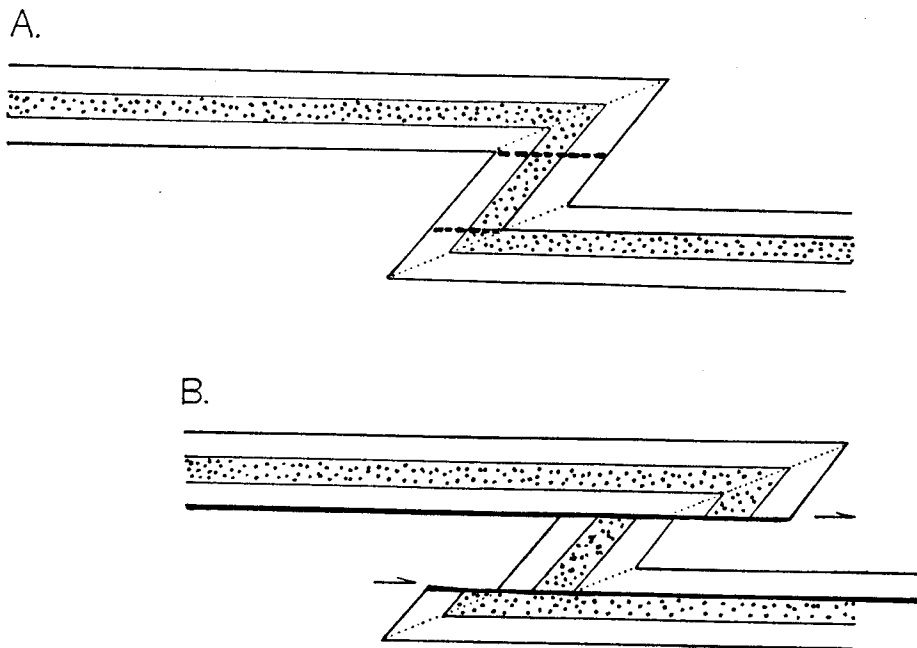
Figure 6.16 Line drawing showing the development of Fl
fold truncations in the Galice by thrusting parallel to
bedding.

slip
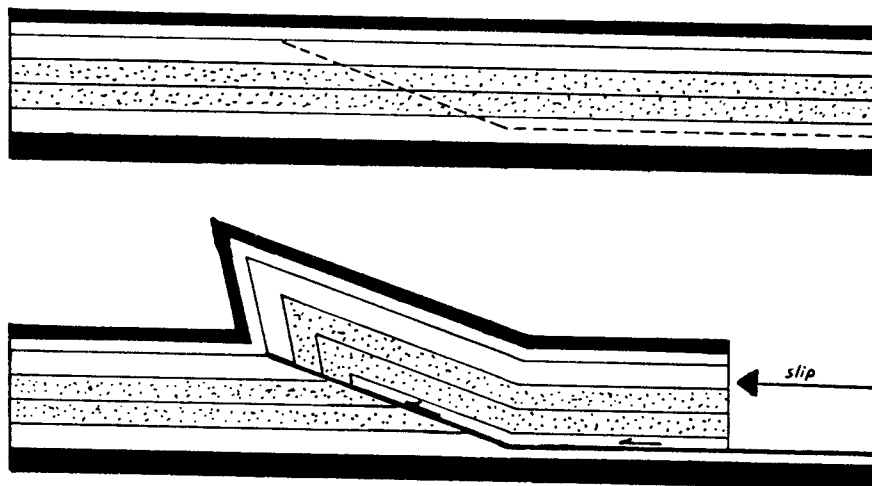
Figure 6.17 Fold truncation produced by propagation of a
thrust ramp. See text for discussion.

Thirdly, this truncation mechanism is favorable because
many tight F_1 folds in the northern field area contain
fractures and minor faults which cut through the hinge zone,
parallel to one of the fold limbs. These fractures
presumably developed in response to excessive fold
tightening and provided surfaces of weakness for subsequent
thrust displacement. Thrusting may have occurred
preferentially along these fold-related fractures.

Fault-Propagation Folding

Another mechanism that could produce truncated folds is
known as "fault-propagation folding". In figure 6.17
(bottom), strongly asymmetric folds accomodate shortening in
front of an upward-propagating thrust. Fault-propagation
folds are formed and subsequently truncated during the same
thrusting event.

This is a rather elegant analogy for the formation and
eventual truncation of angular, west-verging F_1 folds in the
northernmost Galice Formation. In fold-and-thrust belts,
fault-propagation folds are usually observed as isolated
"rootless" fragments between thrusts (Woodward et al.,
1985). This is similar to the geometries of large and
small-scale F_1 folds in the Galice observed in the area east
of Kerby, Oregon (Plate 1) and in outcrops along the
Illinois River. Indeed, there may have been an important

causal and temporal relationship between F_1 folding and Nevadan thrusting.

6.5 The Development of Pseudocross-bedding

Younging directions determined from truncated beds (e.g. fig. 6.13 A and B) indicate that the origin of pseudocross-bedding did not involve the dissection of folds in their hinge zones. Crossbedding-like structure produced by thrusting-out folds would most commonly show <u>opposite</u> directions of younging on either side of the truncation surfaces. Where younging indicators are present in the Galice, truncated sets of beds show the <u>same</u> sense of younging (fig. 6.13). Pseudocross-bedding is normally found in thinly-bedded rocks, however, in which the younging direction is in many places indeterminate.

The development of small-scale ramp-flat thrust systems may explain the younging patterns observed in truncated beds. Comparisons can be made with a model for the progressive development of a thrust duplex. Figure 6.18A shows how thrust sheets are successively imbricated by movement along layer-parallel flats connected by ramps which cut through the stratigraphy (Boyer and Elliott, 1982). The layers are flexed by "fault-bend folding" (Suppe, 1983) over closing and opening bends in the thrust. The final geometry in figure 6.18A shows several angular discordances between layering in adjacent thrust sheets. Specifically,
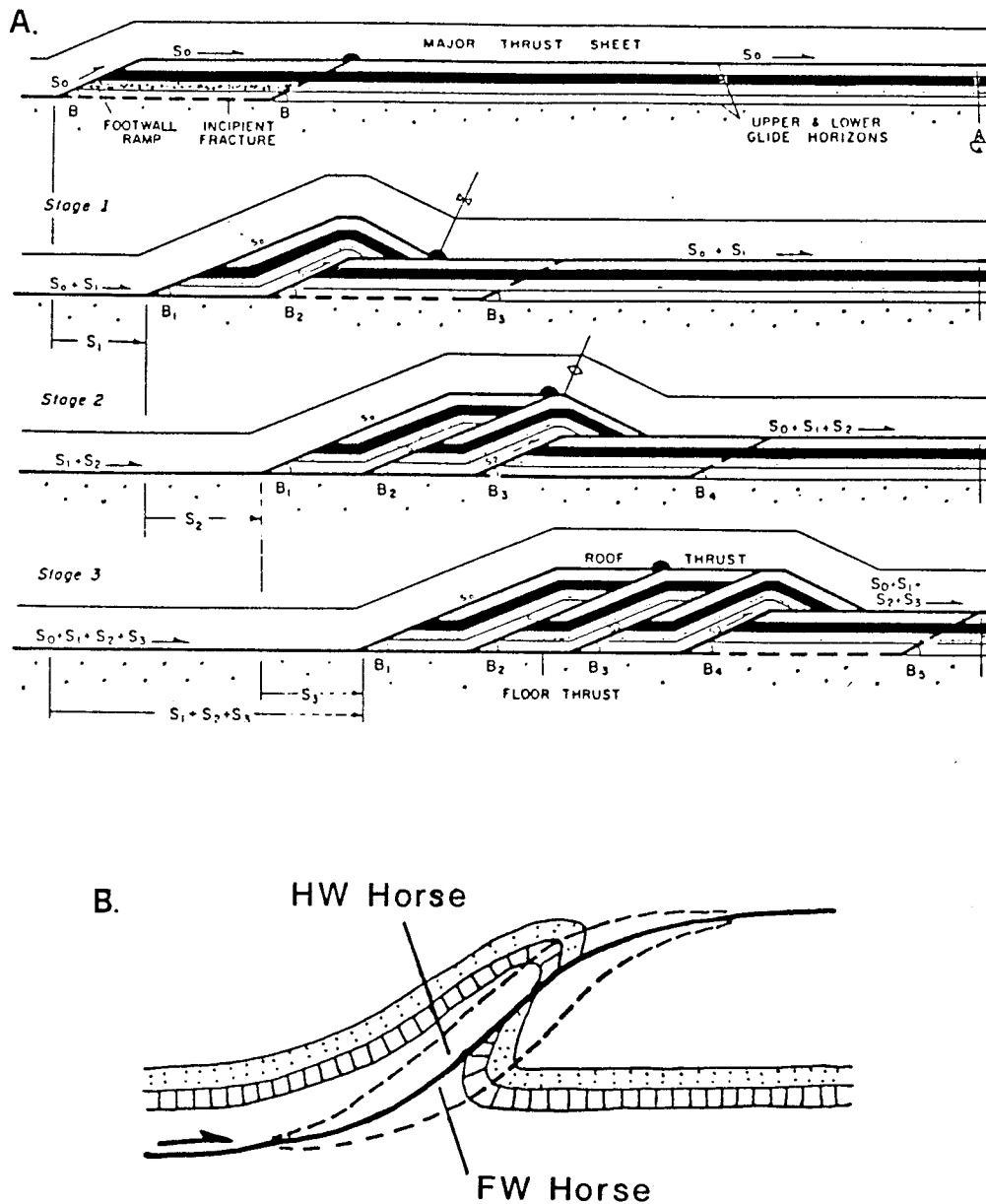
Figure 6.18 Structural analogies for pseudocross-bedding from fold-and-thrust belts. A. The progressive development of a thrust duplex by successive stacking of thrust sheets. Truncations of layering in adjacent thrust sheets form where the layers are forced to conform to the geometry of the ramp by flexural folding. (after Boyer and Elliott, 1982, fig. 19) B. Drag folds are cut by imbricate thrusts (dashed), producing thrust-bounded "horses" (after Boyer and Elliott, 1982, fig. 9).

discordance occurs along portions of the thrust where the layers have been folded to conform to the geometry of the ramp.

Compression at ramps can lead to asymmetric folding of layers in the hanging wall and footwall by drag-related flexure (fig. 6.18B). Incipient imbricate thrusts, shown as dashed lines in figure 6.18B, propagate through the fold hinges producing a pair of thrust horses. Displacement of the horses would apparently result in complex discordance between layering, as well as truncated folds. Similar imbricate thrusts, parallel to the axial planes of medium to large-scale F_1 folds were observed in the Galice Formation, approximately 8 kilometers east of Kerby, Oregon (Plate 1).

Figure 6.19 is a possible example of pseudocross-bedding formed by small-scale thrust imbrication of thinly-bedded slates. The top set of beds (upper left) is gently flexed, creating an angular discordance which increases along a well-defined planar surface. Since no fold closures were observed in this outcrop and S_1 is parallel to bedding, it is suggested that the geometry near the top of the outcrop formed at the opening bend between a thrust ramp and flat. Considering the gentle flexure of the upper set of beds, the dihedral angle of intersection between the ramp and flat (angles "B_1,B_2,..." in figure 6.18A) was probably very small. To the right of the hammer in figure 6.19 is a thrust-bounded set of beds which may be analogous to a horse, a thrust slice bounded by imbricate thrusts. Quartz
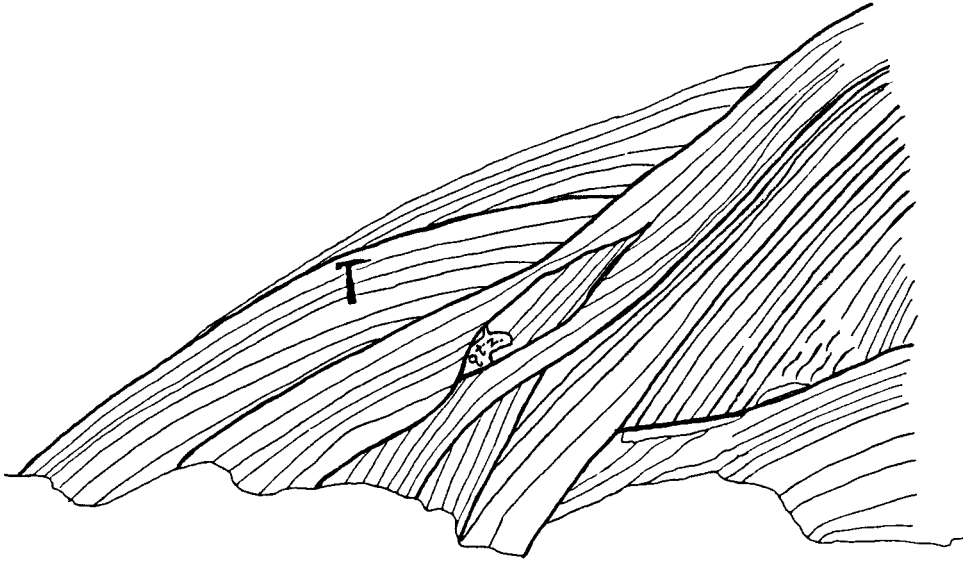
Figure 6.19 Photograph and sketch of beds from an exposure
of interbedded metasiltstone and slate along Siskiyou Fork
Smith River, 3.5 kilometers southeast of US 199. View is
to the southwest. Traces of bedding show complex angular
discordance. See text for discussion.

veins which occur parallel to bedding/S_1, and in gaps between sets of beds, may also attest to a thrusting origin of bedding truncations. Since S_1 is truncated throughout this exposure, thrusting is interpreted as post-D_1.

Similar small-scale ramp-flat geometries have recently been described from the Witwatersrand quartzites in southern Africa (Roering and Smit, 1987). Bedding-parallel thrusts in these rocks are connected by narrow, upward-cutting shear zones serving as ramps. Development of small-scale bedding-parallel detachments, thrust duplexes and thrust-related folds in stiff quartzite layers contributed to as much as 66% bulk shortening in these rocks (Roering and Smit, 1987). In a second example, outcrop-scale ramp-flat systems formed by underplating of slates and graywackes in a subduction complex exposed on Kodiak Island, Alaska (Sample and Paterson, 1988).

6.6 Summary

The latest stage of Nevadan deformation involved F_2 folding, as well as extensive thrusting, which truncated F_1 folds and produced "pseudocross-bedding" structure. F_2 folding was not accompanied by regionally penetrative cleavage development in the field areas studied for this thesis, although S_2 is a penetrative foliation south of Big Flat, California (20 kilometers south of figure 1.9). Nevertheless, F_2 folds are considered to be "Nevadan",

rather than a later event, because of their probable relationship to Nevadan thrusting and regional metamorphism (Gray, 1985; this study). Recent observations suggest that the S_1 and S_2 cleavages in the southern Galice formed during a progressive deformation that may be traced by curved quartz fibers in syntectonic veins (G.D. Harper, pers. comm.). However, in the northern Galice, F_2 folds clearly formed in conjunction with brittle shearing, under temperatures and hydrodynamic conditions that were not sufficient for penetrative cleavage development. I therefore suggest that late-stage structures in the northern Galice Formation formed during continued post-metamorphic underthrusting, possibly during uplift. The southern Galice presumably represents deeper buried (or thrusted) rocks which experienced larger penetrative strains.

Bedding- and cleavage-parallel thrusting, producing widespread bedding and fold truncations, accomodated late Nevadan (post main-phase) shortening in the northern Galice. The development of pseudocross-bedding probably involved small-scale thrust imbrication by displacement of beds along bedding-parallel detachments and cross-cutting ramps. A general conclusion from observations in this chapter is that outcrop-scale structures can be compared with regional structures involving large crustal sequences. It is unfortunate that the Galice Formation lacks suitable marker beds or lithologies which could aid in recognizing large Nevadan thrusts and quantifying displacement along them.

Chapter 7: POST-NEVADAN FOLDING AND FAULTING

7.1 F_3 Folds

Some folds in the Galice Formation are interpreted as F_3 folds. These folds are open folds or broad warps of thick sequences of beds that have wavelengths of 0.5 kilometers or more. They are interpreted as F_3 folds because they lack any associated cleavage; where observed together, smaller F_2 folds have differently oriented axes than F_3. F_3 folds range from symmetric to slightly asymmetric, and have subhorizontal fold axes. The hinge zones of F_3 folds normally coincide with the few places where the Galice is horizontal or very gently dipping.

Several F_3 folds were observed in the continuous exposures along Oregon Mountain Road (fig. 1.9). Figure 7.1 shows a limb and hinge zone of an F_3 fold with an estimated wavelength of approximately 1 kilometer. It is uncertain whether F_3 folds observed in the Galice Formation are the same generation as those folds which affect the crustal sequence of the Josephine ophiolite in northern California. Folds with axes plunging gently to the south-southeast repeat the crustal sequence and basal Galice several times (fig. 1.2), and have wavelengths on the order of tens of kilometers. These regional folds may be Nevadan, although
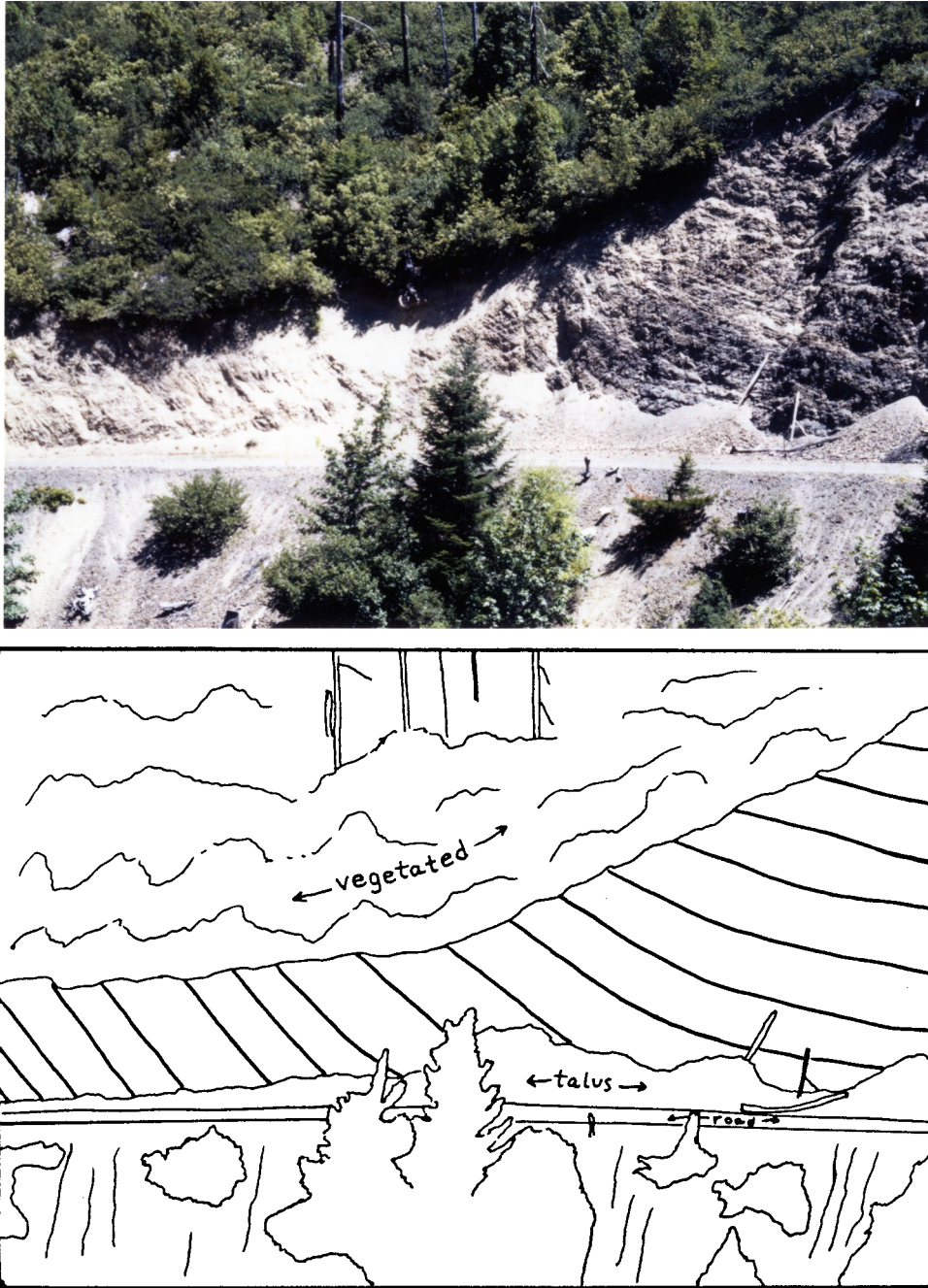
Figure 7.1 Exposure of a limb and hinge region of an F3 syncline along Oregon Mountain Road. View is to the north-northwest. Beds steepen progressively from subhorizontal (right) to dips of about 60° (left). To the right of the photo, horizontal beds in the hinge of the fold are truncated against vertical beds along a high-angle fault. Length of view is approximately 100 meters.

their north-northwest trending axes do not follow other Nevadan structural trends.

The Lower Cretaceous Horsetown Formation, exposed at Indian Hill, near O'Brien, Oregon (fig. 1.3), constrains at least some of the large-scale folding as younger than Barremian (ca. 119 Ma), the age of the youngest fossils found in this outlier (Imlay et al., 1959). These clastic sedimentary rocks were tilted (and presumably folded) about a northeast-trending fold axis. Three poles to bedding from basal conglomerates and overlying coarse sandstones are plotted in figure 7.2; this figure also shows how minimal post-Nevadan rotations (about 30°) around this axis could account for northwest-southeast dispersal of poles to S_1 in the Galice Formation. Axes of the regional-scale folds of the Josephine ophiolite (discussed above) lie at almost 90° to the inferred Indian Hill fold axis, suggesting that the two are unrelated.

Post-Nevadan folding or oroclinal bending probably produced the strong curve in the trace of the Preston Peak thrust near Cave Junction, Oregon (fig. 1.6, Plate 1). Structural trends in the Galice appear to reflect the bend in the thrust at this location (Plate 1). The thrust was significantly steepened in this area (Wells et al., 1949; Ramp, 1979; this study), in contrast to gently dipping southern portions of the thrust (Snoke, 1977; Wyld, 1985; Jachens et al., 1986).
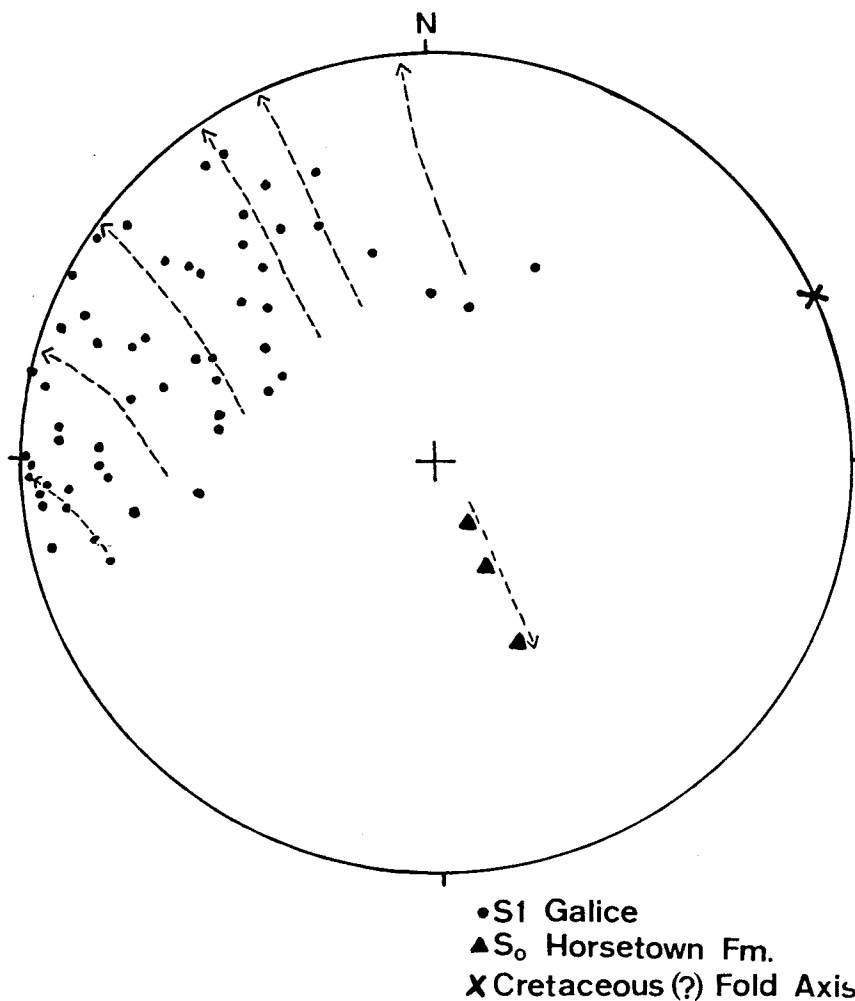
Figure 7.2 Stereographic projection of poles to S1 in the
Galice, poles to bedding in the Cretaceous Horsetown
Formation and a presumed fold axis responsible for tilting
the Cretaceous rocks. Cretaceous strata measured at
Indian Hill, near O'Brien, Oregon (fig. 1.3). Arrows show
paths of rotations around the Cretaceous fold axis, pos-
sibly accounting for dispersal of poles to S1 in the
Galice Formation.

Post-Nevadan folds and some east-west and northwest-southeast trending high-angle faults in the western Jurassic belt may have resulted from Middle(?) Cretaceous accretion of the Franciscan complex to the continental margin (Kays, 1967; Harper, 1980a). The Josephine peridotite is thrust over the Cretaceous Dothan Formation (a member of the Franciscan assemblage) in southwest Oregon along the northern extension of the Coast Range thrust. However, neither the age of this thrust, nor the precise age of the Dothan Formation have been established.

7.2 High-angle Faulting and Regional Uplift

Some late-stage steeply dipping faults in the Galice Formation and Josephine ophiolite may post-date the Cretaceous folding event described above. An example is the northeast-trending Illinois Valley normal fault system (Wells et al., 1949). One of these regional normal faults juxtaposes the Galice Formation with the Josephine peridotite along most of the exposure of the Galice in Oregon (fig. 1.2). This normal fault dips steeply to the east, and probably has a throw of at least 5 kilometers. Smaller normal faults with similar trends have been mapped in the upper plate of the Preston Peak thrust (Snoke, 1977; Ramp, 1979). Normal faults displace Nevadan thrusts, reverse faults and large-scale folds in the Galice and Rogue

Formations (Kays, 1967; Vail, 1977) and may be as young as Oligocene (Wyld, 1985).

Gray (1985) mapped northeast-trending strike-slip faults which truncate F_1 and F_2 folds in the southern Galice Formation. He also mapped a series of right-lateral strike-slip faults in the upper plate of the Preston Peak thrust, some of which offset the thrust. Gray (1985) suggested that F_3 and F_4 folds which deform earlier Nevadan structures formed by oroclinal flexure along these faults.

Right-lateral strike-slip faults in the Galice Formation and upper plate of the Preston Peak thrust may radiate from the Condrey Mountain dome (Gray, 1985; Jachens et al., 1986). The Condrey Mountain dome provides a window through the low-angle Orleans thrust, exposing the Condrey Mountain schist, a possible eastward-transported equivalent of the Galice Formation (see fig. 1.1). Tilting of plutons in the western Paleozoic and Triassic belt was probably linked to doming of the Condrey Mountain schist during early to mid-Tertiary uplift of the Klamaths (Barnes et al., 1986). Displacement along major normal and strike-slip faults may have been related to Cenozoic regional uplift. Miocene bench gravels at the top of the "Klamath peneplain" in northern California attest to approximately 1 kilometer of post-Miocene uplift (Cater and Wells, 1953; Harper, 1980a).

Chapter 8: SUMMARY

8.1 Conclusions and Interpretations

Important conclusions drawn from this study of the Galice Formation include the following:

(1) As discussed in chapter 3, the Galice was not extensively deformed prior to lithification. Bedding-parallel extensional structures and "type 1" melange are strictly local features which may be related to either sedimentary or tectonic processes. Sliding along layer-parallel decollements and local ramps, however, may have occurred at an early stage of underthrusting, similar to the structural respose of modern turbidites being thrust beneath the Barbados Ridge (Westbrook and Smith, 1983). There is little evidence that the Galice was disrupted in a soft-sediment state during tectonic emplacement by underthrusting.

(2) From bedding orientation data (fig. 4.4), it is apparent that the Galice was tightly folded on a regional scale during the main-phase Nevadan deformation. However, the low percentage of overturned beds determined from abundant younging indicators in the northern field area (15%) suggests that large-scale F_1 folds are sparce and interspersed in thick sequences of upright, unfolded strata.

Outcrop-scale F_1 folds are apparently sparse in rocks south of the Oregon-California border. Potential factors obscuring F_1 folds in the southern field area are transposition of bedding into parallelism with S_1 and cleavage-parallel thrusting.

(3) S_1 is dominantly parallel to bedding in the Galice Formation. To a large extent, this phenomenon must be a result of extensive isoclinal folding; however, this becomes difficult to reconcile with the scarcity of F_1 fold closures (Harper, 1980a; Wyld, 1985; this study) observed in the southern field area (fig. 1.9). In this study, the hinges of large-scale F_1 folds were difficult to locate with bedding-cleavage relationships alone, as S_1 is rarely at a high angle to bedding. Small-scale transposition of bedding into parallelism with S_1 is common, but did transposition in the Galice occur on a regional scale? The scarcity of large-scale F_1 hinge zones suggests that they were probably eliminated by post-F_1 thrusting (fig. 6.14).

(4) F_1 folds and Nevadan thrusts clearly show vergence to the west and northwest, normal to the strike of the Orleans fault. In the area near Cave Junction, Oregon, F_1 folds are either overturned to the northwest (fig. 4.2), or have northwest-dipping limbs that are shorter, and dip steeper than southeast-dipping limbs. In the southern study area, F_1 folds generally verge to the west-northwest (figs. 4.3, 4.7); slightly different vergence to the south possibly reflects the broadly arcuate geometry (convex toward the

Pacific) of the western Klamaths (see fig. 1.1). The dominantly eastward dips of upright beds, overturned beds (figs 4.4, 4.5) and the S_1 cleavage (fig. 4.6A) reflect large-scale overturned F_1 folds with northwest vergence.

The orientations of outcrop-scale thrust faults and the regional Orleans thrust also suggest northwest vergence (figs. 4.22, 6.5). Gravity data indicate that low-density material extends uninterrupted for at least 110 kilometers beneath the Orleans fault (Jachens et al., 1986). Therefore, a major westward component of displacement along this fault is probable. Moreover, large-scale east-dipping reverse faults which repeat the Josephine ophiolite and Galice Formation (Harper, 1980a) are west-vergent, late Nevadan structures (see section 6.2). In conclusion, east-directed Nevadan folding and thrusting suggested in the northern Sierra Nevadan (Day et al., 1985) and the western Klamaths (Roure, 1984) is incompatible with structural observations in this thesis and previous studies (Snoke, 1977; Harper, 1980a; Gray, 1985), as well as interpretations of the sense of displacement along the Orleans thrust (Gray, 1983; Jachens et al., 1986).

(5) There is a strong north-south gradient in Nevadan penetrative strain which is coincident with a change in regional metamorphic grade. Syntectonic fibers in slate from the northern field area record an average of 33% shortening normal to S_1, wheras slates from the southern field area were shortened an average of 68% (fig. 5.12).

33% is a <u>maximum</u> estimate of cleavage-related shortening in the northernmost Galice, considering that S_1 is typically weakly-developed or absent, and pencil structure, formed after only 9-26% shortening (Reks and Gray, 1981), is commonly associated with gentle F_1 folds. Note that shortening values estimated from most F_1 folds in this area are much higher (see section 5.4). Plane strain with considerable volume-loss during S_1 development may account for low extension values measured from fibers in <u>northern</u> Galice slates. 68% tectonic shortening normal to S_1 in the southern field area is similar to shortening values determined from the dimensions of reduction spots (Wood, 1974), chlorite stacks (Beutner, 1978), and lengths of syntectonic fibers in other slate belts (Beutner and Diegel, 1985).

(6) Syntectonic fibers in pressure shadows of pyrite framboids record a coaxial extension history, consistent with pure flattening during formation of S_1. Non-coaxial strains, known to occur along rotated limbs of overturned folds (Wickham and Anthony, 1978; Beutner and Diegel, 1985) or in rocks deformed by syn-kinematic thrusting (Beutner et al., 1983; Sample and Fisher, 1986) are <u>not</u> recorded by fibers in slates examined in this study.

A coaxial strain history during cleavage development suggests one of three conclusions about the timing of cleavage formation and fiber growth. First, S_1 may have formed by pure flattening of upright F_1 folds which were

subsequently inclined during post-kinematic regional simple shear. A second possibility is that fiber growth was restricted to a late stage of flattening and did not record non-coaxial strains related to limb rotation (e.g., Beutner and Diegel, 1985). Thirdly, earliest-formed non-coaxial fiber increments may have been dissolved when the distal portions of pressure shadows were removed from the sheltering effect of the pyrite framboid. This third possibility is not preferred, as shorter pressure shadows also contain coaxial (straight) fibers.

(7) Most Nevadan thrusts in the Galice are younger than the main-phase Nevadan structures (F_1 and S_1). Coaxial syntectonic fibers in Galice slates adjacent to Nevadan thrusts and the Preston Peak (Orleans) thrust suggest that Nevadan thrusting was post-S_1. Moreover, F_1 folds are ubiquitously thrusted-out and S_1 is truncated by small thrusts in the area near Cave Junction and to the south in northern California (Gray, 1985; this study). Pseudocross-bedding and cleavage-parallel slickensides are also interpreted as post-main phase thrust-related structures.

Brittle-Ductile Transition

A general interpretation from the observations made in this thesis is that the northernmost Galice (area of Plate 1) was deformed at a higher structural level than rocks to the south. The Galice near Cave Junction, Oregon, shows

weak S_1 development and no visible signs of metamorphism, probably suggesting metamorphic temperatures of less than $200^{\circ}C$. South of Gasquet, California (fig. 1.2), metamorphic temperatures were in the range of $250-300^{\circ}C$ (G.D. Harper, pers. comm.) and S_1 is a strong slaty cleavage or pyllitic foliation in metapelites and a schistosity in metagraywackes.

In the northern field area, brittle shortening mechanisms (chevron folding, thrusting) were important throughout the Nevadan deformation. Since there are no apparent north-south differences in the tightness of F_1 folds or the extent of thrusting, I suggest that total Nevadan shortening (F_1, F_2 and thrusting combined) was relatively constant over the north-south extent to the Galice.

The north-south gradient in metamorphism and penetrative strain may reflect continued underthrusting during differential regional uplift or tilting. Other factors that could have influenced this gradient are north-south variations in thickness of the sediments and the geometry and timing of closure of the Josephine basin.

Alternatively, underthrusting of the Josephine/Galice plate beneath the continental margin along the Orleans thrust may have had a small southward component of strike-slip, so that deeper structural levels are now exposed to the south. Southeastward underthrusting, slightly oblique

to the continental margin, may account for northwest
vergence observed from both field areas in this study.

Structural History

Figure 8.1 is a diagrammatic summary of the structural
history of the Galice Formation. Structures in the northern
and southern field area of this study are sketched in their
inferred sequence of development. Brittle-ductile contrasts
between structures in the north and south are most notable.
F_1 folds probably initiated by buckling and flexural-slip in
rocks in the northernmost Galice. While these fold
mechanisms probabaly operated to the south, penetrative
shortening related to S_1 development may have occurred early
in the F_1 fold history. Tight F_1 folds formed largely by
flexural-slip and kink folding in the northern Galice,
wheras fold tightening was dominated by ductile processes to
the south. Fracturing occurred in tight, angular F_1 folds
near Cave Junction, Oregon, presumably when flexural-slip
was no longer operable. In contrast, isoclinal folding and
transposition are evidence of flattening of F_1 folds in the
southern Galice.

The post-main phase period was dominated by development
of brittle thrust-related structures. The geometries
resulting from bedding- and cleavage-parallel truncation of
F_1 folds are sketched in figure 8.1. Imbrication of beds
forming pseudocross-bedding structure was also important

(following page)

Figure 8.1 Series of sketches showing the structural evo-
lution of the Galice Formation in the northern and southern
field areas of this study. Three stages in the structural
history are recognized: a main-phase deformation, Nevadan
thrusting and post-Nevadan deformation. Post-Nevadan
faults (normal and strike-slip) were omitted. Pseudocross-
bedding and F3 folds occur in both field areas; thus, they
are placed in the center of the diagram.
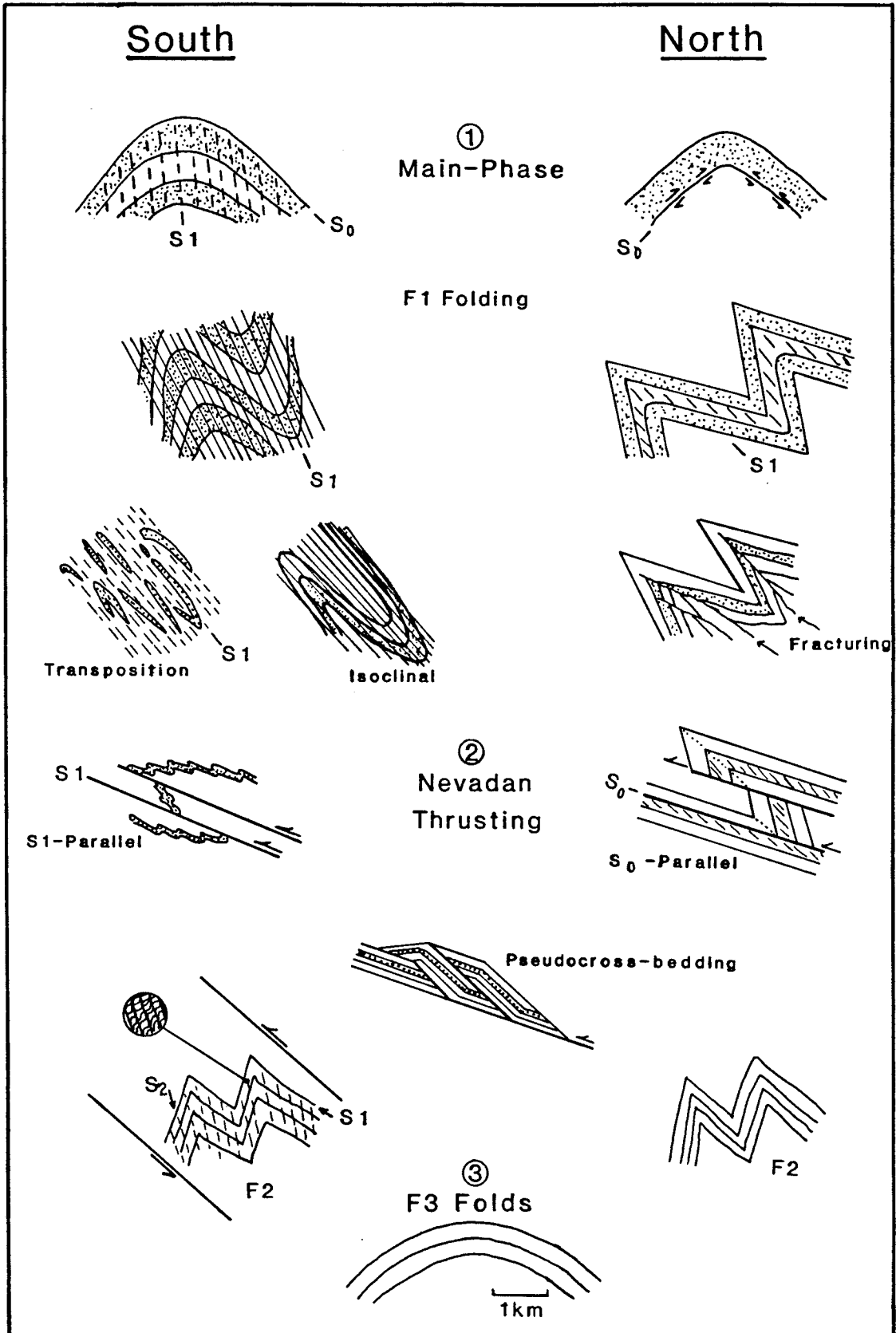
during late Nevadan thrusting. Angular discordance between sets of beds is common in both field areas. Therefore, pseudocross-bedding may have contributed significantly to late-stage Nevadan shortening in the Galice.

F_2 folds are interpreted as post-main phase structures which may be related to Nevadan thrusting. The timing of F_2 development with respect to thrust-related structures such as truncated F_1 folds is uncertain. However, since no truncated F_2 folds were observed, they are younger than, or coeval with the formation of bedding and fold truncations.

Broad, kilometer-scale F_3 folds are the youngest structures shown in figure 8.1; they are interpreted as Cretaceous or younger structures. These folds have horizontal, northwest-trending axes which are markedly different from the northeast Nevadan trends. Furthermore, the folds gently warp Lower Cretaceous sedimentary rocks. Their styles are atypical of folds in sediments deformed by underthrusting (e.g., Byrne, 1984; Sample and Paterson, 1988).

8.2 Further Research

Several structural problems in the Galice may be addressed in future studies. Careful analysis of the problems listed below may lead to a better understanding of the deformational kinematics in the Galice, and related implications for Nevadan orogenesis.

(1) $\underline{L_1}/\underline{F_1}$ Relationships. Determination of any consistencies or variations in the attitude of L_1 could improve present understanding of the kinematics of the main-phase Nevadan deformation. It is unclear why L_1 is oriented parallel to F_1 fold axes (Harper, 1980a) and at a high angle to the inferred west-northwest Nevadan transport direction. A future investigation might focus on why F_1 fold axes in the northern Galice appear parallel to the $\underline{X}$ direction (maximum extension direction) of the finite strain ellipsoid.

(2) Slickenside analysis. Measurement of abundant slickensides on cleavage planes and along Nevadan thrusts could provide additional constraints on the late Nevadan thrusting direction.

(3) Fiber analysis. Galice slates are excellent rocks for analysis of syntectonic fibers, as most samples contain rigid spherical pyrite framboids. Perhaps the greatest potential lies in fibers in pelitic rocks from the southern Galice, where S_2 is a strong regionally-penetrative pressure-solution cleavage in slates. In these rocks, it may be possible to trace fibers related to S_1 extensions through some reorientation into parallelism with the S_2 cleavage. Such contiuous fibers would verify that the two fabrics formed during a single progressive deformation.

From the present study of the northern Galice, it is apparent that no such S_1-S_2 continuity exists; in rocks containing S_2, S_1-related fibers in pressure shadows are

simply crenulated along with the S_1 fabric, and no fiber growth was observed parallel to S_2. In contrast, metamorphic conditions sufficient for cleavage development and fiber growth presumably persisted during F_2 folding in the southern Galice (Gray, 1985). Syntectonic fibers in the southern Galice may uniquely reflect non-coaxial strains associated with thrusts or shear zones which were active during regional metamorphism.

REFERENCES

Alterman, I.B., 1973, Rotation and dewatering during slaty cleavage formation: Some new evidence and interpretations: _Geology_, v.1, p. 33-36.

Barnes, C.G., Rice, J.M., and Gribble, R.F., 1986, Tilted plutons in the Klamath Mountains of California and Oregon: _Journal of Geophysical Research_, v.9, p. 419-427.

Bateman, P.C. and Clark, L.D., 1974, Stratigraphic and structural setting of the Sierra Nevada batholith: _Pacific Geology_, v.8, p.78-89.

Berner, R.A., 1970, Sedimentary pyrite formation: _American Journal of Science_, v.268, p.1-23.

Beutner, E.C., 1978, Slaty cleavage and related strain in Martinsburg slate, Delaware Water Gap, New Jersey: _American Journal of Science_, v.278, p.1-23.

Beutner, E.C., 1980, Slaty cleavage unrelated to tectonic dewatering: The Siamo and Michigamme slates revisited: _Geological Society of America Bulletin_, v.91, p.171-178.

Beutner, E.C., and Charles, E.G., 1985, Large volume loss during cleavage formation, Hamburg sequence, Pennsylvania: _Geology_, v.13, p. 803-805.

Beutner, E.C. and Diegel, F.A., 1985, Determination of fold kinematics from syntectonic fibers in pressure shadows, Martinsburg slate, New Jersey: _American Journal of Science_, v.285, p. 16-50.

Beutner, E.C., Jancin, M.D. and Simon, R.W., 1977, Dewatering origin of cleavage in light of deformed calcite veins and clastic dikes in Martinsburg slate, Delaware Water Gap, New Jersey: _Geology_, v.5, p. 118-122.

Beutner, E.C., Fisher, D.M. and Kirkpatrick, J.L., 1983, Kinematics of deformation at a thrust fault ramp from syntectonic fibers in pressure shadows: _unpubl. manuscript_, Franklin and Marshall College, Lancaster, Pa., 40p.

Biju-Duval, B., Le Quelle, P., Mascle, A., Renard, V. and Valery, P., 1982, Multibeam bathymetric survey and high-resolution seismic investigations of the Barbados Ridge complex: A key to the knowledge and interpretation of an accretionary wedge: Tectonophysics, v.86, p. 275-304.

Blackwelder, E., 1914, A summary of the orogenic epochs in the geologic history of North America: Journal of Geology, v.22, p. 633-654.

Bogen, N.L., 1984, Stratigraphy and sedimentary petrology of the Upper Jurassic Mariposa Formation, western Sierra Nevada, California, in Crough and Bachman (eds.), Tectonics and Sedimentation along the California Margin: Soc. of Economic Paleontologists and Mineralogists, p. 119-134.

Bogen, N.L., Kent, D.V. and Schweickert, R.A., 1985, Paleomagnetic constraints on the structural development of the Melones and Sonora faults, central Sierran foothills, California: Journal of Geophysical Research, v.90, p. 4627-4638.

Borradaille, G.J., 1977, On cleavage and strain: Results of a study in West Germany using tectonically deformed sand dykes: Journal of the Geological Society of London, v.133, p. 146-164.

Bosellini, A. and Winterer, E., 1975, Pelagic limestones and radiolarites of the Tethyan Mesozoic: a genetic model: Geology, v.3, p. 279-282.

Boulter, C.A., 1974, Tectonic deformation of soft-sedimentary clastic dikes from the Precambrian rocks of Tasmania, Australia, with particular reference to their relation with cleavages: Geological Society of America Bulletin, v.85, p. 1413-1420.

Boulter, C.A., 1983, Compaction-sensitive accretionary lapilli: a means for recognizing soft-sedimentary deformation: Journal of the Geological Society of London, v.140, p. 789-794.

Boyer, S.E. and Elliott, D., 1982, Thrust systems: American Association of Petroleum Geologists Bulletin, v.66, p. 1196-1230.

Bryant, B. and Reed, J., 1969, Significance of lineation and minor folds near major thrust faults in the southern Appalachians and the British and Norwegian Caledonides: Geological Magazine, v.106, p. 412-429.

Byrne, Y., 1984, Early deformation in melange terranes of the Ghost Rocks Formation, Kodiak Island, Alaska, in L. Raymond (ed.), Melanges: Their Origin and Significance: Geological Society of America Special Paper, p. 21-52.

Cannat, M. and Boudier, F., 1985, Structural study of intra-oceanic thrusting in the Klamath Mountains, northern California: Implications on accretion geometry: Tectonics, v.4, p. 435-452.

Cater, F.W. and Wells, F.G., 1953, Geology and mineral resources of the Gasquet quadrangle, California-Oregon: U.S. Geological Survey Bulletin, v.995-C, p.79-133.

Chappel, W.M., 1978, Mechanisms of thin-skinned fold-and-thrust belts: Geological Society of America Bulletin, v.88, p. 1189-1198.

Choukroune, P., 1971, Contibution a l'etude des mechanismes de la deformation avec schistosite grace aux cristallisations syncinematiques dans les zones abritees: Bulletin of the Geological Society of France, v.13, p. 257-271.

Cowan, D.S., 1982, Deformation of partly dewatered and consolidated Franciscan sediments near Piedras Blancas Point, California, in J. Leggett (ed.), Trench and Forearc Sedimentation and Tectonics: Geological Society of London, p. 439-457.

Cowan, D.S., 1985, Structural styles in Mesozoic and Cenozoic melanges in the western Cordillera of North America: Geological Society of America Bulletin, v.96, p. 451-462.

Cowan, D.S. and Silling, R.M., 1978, A dynamic, scaled model of accretion at trenches and its implications for tectonic evolution of subduction complexes: Journal of Geophysical Research, v.83, p. 5398-5396.

Craig, J., Fitches, W.R. and Maltman, A.J., 1982, Chlorite-mica stacks in low-strain rocks from central Wales: Geological Magazine, v.119, p. 243-256.

Davis, D., Suppe, J. and Dahlen, E., 1983, Mechanics of fold-and-thrust belts and accretionary wedges: Journal of Geophysical Research, v.88, p. 1153-1172.

Day, H.W., Moores, E.M. and Tuminas, W.D., 1985, Strudture and tectonics of the northern Sierra Nevada: Geological Society of America Bulletin, v.96, p. 436-450.

Dick, A.J.B., 1976, The origin and emplacement of the Josephine peridotite of southwestern Oregon, [Ph.D]: New Haven, Conn., Yale University, 409p.

Diller, J.S., 1907, The Mesozoic sediments of southwestern Oregon: American Journal of Science, v.23, p. 401-421.

Diller, J.S. and Kay, G.F., 1924, Description of the Riddle Quadrangle, in: Geologic Atlas of the United States: U.S. Geological Survey, libr. ed. no. 218.

Dionne, J.C. and Shilts, W.W., 1974, A Pleistocene clastic dyke, upper Chandiere Valley, Quebec: Canadian Journal of Earth Science, v.11, p. 1594-1605.

Donovan, R.N. and Foster, R.J., 1972, Subaqueous shrinkage cracks from the Caithness Flagstone series of northeast Scotland: Journal od Sedimentary Petrology, v.42, p. 309-317.

Durney, D.W. and Ramsay, J.G., 1973, Incremental strains measured by syntectonic crystal growths, in deJong and Scholten (ed.), Gravity and Tectonics: New York, Wiley, p. 67-96.

Elliott, D., 1972, deformation paths in structural geology: Geological Society of America Bulletin, v.83, p. 2621-2638.

Ellis, M.A., 1986, The determination of progressive deformation histories from antitaxial syntectonic crystal fibers: Journal of Structural Geology, v.8, p. 701-709.

Fahan, M.R. and Wright, J.E., 1983, Plutonism, volcanism, folding, regional metamorphism and thrust faulting: Contemporaneous aspects of a major Middle Jurassic orogenic event within the Klamath Mountains, northern California: GSA Abstracts with Programs, v.15, p. 272.

Fisher, D. and Byrne, T., 1987, Structural evolution of underthrusted sediments, Kodiak Islands, Alaska: Tectonics, v.6, p. 775-793.

Flinn, D., 1962, On folding during three-dimensional progressive deformation: Geological Society of London Quarterly Journal, v.118, p. 385-433.

Garcia, M.O., 1979, Petrology of the Rogue and Galice Formations, Klamath Mountains, Oregon: Identification of a Jurassic island arc sequence: Journal of Geology, v.86, p. 29-41.

Garcia, M.O., 1982, Petrology of the Rogue River island arc complex, southwest Oregon: American Journal of Science, v.282, p. 783-807.

Geiser, P.A., 1974, Cleavage in some sedimentary rocks of the central Valley and Ridge province, Maryland: Geological Society of America Bulletin, v.85, p. 1399-1412.

Geiser, P.A., 1975, Slaty cleavage and the dewatering hypothesis- An examination of some critical evidence: Geology, v.3, p. 717-720.

Ghosh, S.K., 1968, Experiments of buckling of multilayers which permit interlayer gliding: Tectonophysics, v.6, p. 165-174.

Gorman, C.M., 1985, Geology, geochemistry and geochronology of the Rattlesnake Creek Terrane, west-central Klamath Mountains, California [M.S.]: Salt Lake City, Utah, University of Utah, 111p.

Gray, D.R., 1977, A morphologic classification of crenulation cleavage: Journal of Geology, v.85, p. 229-235.

Gray, D.R., 1978, Cleavages in deformed psammitic rocks from southeastern Austalia; their nature and origin: Geological Society of America Bulletin, v.89, p. 577-590.

Gray, D.R. and Durney, D.W., 1979, Investigations of the Mechanical Significance of Crenulation Cleavage: Tectonophysics, v.58, p. 35-79.

Gray, G.G., 1983, A kinematic analysis of thrust faulting, west-central Klamath Mountains, California [abstract]: GSA Abstracts with Programs, v.15, p. 585.

Gray, G.G., 1985, Structural, geochronologic and depositional history of the western Klamath Mountains, California and Oregon: Implications for the Early to Middle Mesozoic tectonic evolution of the western North American Cordillera [Ph.D.]: Austin, Texas, University of Texas-Austin, 161p.

Gregg, W.J., 1979, The redistibution of pre-cleavage clastic dikes by folding at New Paltz, New York: Journal of Geology, v.87, p. 99-104.

Groshong, R.H., 1976, Strain and pressure solution in Martinsburg slate, Delaware Water Gap, New Jersey: American Journal of Science, v.276, p. 1131-1146.

Hamilton, W., 1969, Mesozoic California and the underflow of Pacific mantle: Geological Society of America Bulletin, v.80, p. 2409-2430.

Hamilton, W., 1969, Tectonics of the Indonesian region: USGS Professional Paper, no. 1078, 304p.

Harding, D., 1986, Tectonite structures of the Josephine peridotite, Oregon: A record of plastic flow in the mantle during formation of the Josephine ophiolite [Ph.D.]: Ithaca, New York, Cornell University.

Harland, W.B., Cox, A.V., Llewellyn, P.G., Pickton, C.A.G., Smith, A.G. and Walters, R., 1982, A geologic time scale: New York, Cambridge Univ. Press, 128p.

Harper, G.D., 1980a, Structure and petrology of the Josephine ophiolite and overlying metasedimentary rocks, northwestern California [Ph.D.]: Berkely, California, University of California, 260p.

Harper, G.D., 1980b, The Josephine ophiolite- remains of a Late Jurassic marginal basin in northwestern California: Geology, v.8, p. 333-337.

Harper, G.D., 1982, Inferred high primary volatile contents in lavas erupted in an ancient back-arc-basin, California: Journal of Geology, v.90, p. 187-194.

Harper, G.D., 1983, A depositional contact between the Galice Formation and a Late Jurassic ophiolite in northwestern California and southwestern Oregon: Oregon Geology, v.45, p. 3-9.

Harper, G.D., 1984, The Josephine ophiolite, northwestern California: Geological Society of America Bulletin, v.95, p. 1009-1026.

Harper, G.D. and Wright, J.E., 1984, Middle to Late Jurassic tectonic evolution of the Klamath Mountains, California-Oregon: Tectonics, v.3, p. 759-772.

Harper, G.D., Saleeby, J.B. and Norman, E.A., 1985, Geometry and tectonic setting of sea-floor spreading for the Josephine ophiolite, and implications for Jurassic accretionary events along the California margin, in D. Howell (ed.), Terrane Analysis of the Pacific Basin: American Association of Petroleum Geologists, p. 239-257.

Harper, G.D., Saleeby, J.B., Cashman, S. and Norman, E., 1986, Isotopic age of the Nevadan orogeny in the western Klamath Mountains, California-Oregon: GSA Abstracts with Programs, v.10, p. 99.

Helwig, J., 1970, Slump folds and early structures, northeastern Newfoundland, Appalachians: Journal of Geology, v.78, p. 172-187.

Hershey, O.H., 1911, Del Norte County [California] Geology: Mineral and Science Press, v.102, p. 468.

Hobbs, B.E., Means, W.D. and Williams, P.F., 1976, An Outline of Structural Geology: New York, Wiley, 519p.

Holeywell, R. and Tullis, T., 1975, Mineral reorientation and slaty cleavage in the Martinsburg Formation, Lehigh Gap, Pennsylvania: Geological Society of America Bulletin, v.86, p. 1296-1304.

Hotz, P.E., 1971a, Plutonic rocks of the Klamath Mountains, California and Oregon: USGS Professional Paper, no. 684-B, 19p.

Hotz, P.E., 1971b, Geologic map of the Klamath Mountains province, California and Oregon, in Geology of Lode Gold Districts in the Klamath Mountains, California and Oregon: U.S. Geological Survey Bulletin, no.1290, scale 1:500,000.

Hsu, K.J., 1968, Principles of melanges and their bearing on the Franciscan-Knoxville paradox: Geological Society of America Bulletin, v.79, p. 1063-1074.

Hubbert, M.K. and Rubey, W.W., 1959, Role of fluid pressure in mechanics of overthrust faulting: Geological Society of America Bulletin, v.70, p. 115-206.

Imlay, R.W., 1980, Jurassic paleobiology of the conterminous United States in its continental setting: USGS Professional Paper no. 1062, 125p.

Imlay, R.W., Dole, H.M., Wells, F.G. and Peck, D., 1959, Relations of certain upper Jurassic and lower Cretaceous formations in southwestern Oregon: American Association of Petroleum Geologists Bulletin, v.43, p. 2770-2785.

Ingersoll, R.V. and Schweickert, R.A., 1986, A plate-tectonic model for Late Jurassic ophiolite genesis, Nevadan orogeny, and forearc initiation, northern California: Tectonics, v.5, p. 901-912.

Irwin, W.P., 1960, Geologic reconnaissance of the northern Coast Ranges and Klamath Mountains, California, with a summary of the mineral resources: Bulletin of the California Division of Mines, v.179, 80p.

Irwin, W.P., 1964, Late Mesozoic orogenies in the ultramafic belts of northwestern California and southwestern Oregon: USGS Professional Paper, no. 501-C, p. C1-C9.

Irwin W.P., 1966, Geology of the Klamath Mountains province, in Bailey, E.H. (ed), Geology of Northern California: California Division of Mines, v.190, p. 19-38.

Irwin, W.P., 1972, Terranes of the western Paleozoic and Triassic belt in the southern Klamath Mountains, California: USGS Professional Paper, no. 800-C, p. C103-C111.

Irwin, W.P., 1977, Ophiolitic terranes of California, Oregon and Nevada: Bulletin of the Oregon Dept. of Geology and Mineral Industries, v.95, p. 75-92.

Irwin, W.P., 1981, Tectonic accretion of the Klamath Mountains, in W.G. Ernst (ed.), The Geotectonic Development of California: Englewood Cliffs, New Jersey, Prentice-Hall, p. 29-49.

Irwin, W.P., 1985, Cryptic tectonic domains of the Klamath Mountains, California and Oregon: preprint for R.H. Jahns Memorial Volume, Elsevier Publ. Co., 24p.

Jachens, R.C., Barnes, C.G. and Donato, M.M., 1986, Subsurface configuration of the Orleans fault: Implications for deformation in the western Klamath Mountains, California: Geological Society of America Bulletin, v.97, p. 388-395.

Karig, D.E. and Sharman, G.F., 1975, Subduction and accretion in trenches: Geological Society of America Bulletin, v.86, p. 377-389.

Kays, M.A., 1976, Tectonic framework of mineralization, Upper Jurassic rocks, in, The Almeda Mine, Josephine County, Oregon: Oregon Department of Geology and Mineral Industries, Short Paper 24, p. 43-53.

Klein, C.W., 1977, Thrust plates of the north-central Klamath Mountains near Happy Camp, California: California Division of Mines Special Report, no. 129, p.23-26.

Lanphere, M.A., Irwin, W.P. and Hotz, P.E., 1968, Isotopic age of the Nevadan orogeny and older plutonic and metamorphic events in the Klamath Mountains, California: Geological Society of America Bulletin, v.79, p. 1027-1052.

Lanphere , M.A., Blake, M.C. and Irwin, W.P., 1978, Early
    Cretaceous metamorphic age of the South Fork Mountain
    Schist in the northern Coast Ranges of California:
    American Journal of Science, v.278, p. 798-815.

Lash, G.G. and Drake, A.A., 1984, The Richmond and Greenwich
    slices of the Hamburg Klippe in eastern Pennsylvania--
    Stratigraphy, structure and plate tectonic implications:
    USGS Professional Paper 1312, 39p.

Maltman, A,J., 1981, Primary bedding-parallel fabrics in
    structural geology: Journal of the Geological Society of
    London, v.138, p. 475-483.

Maxwell, J.C., 1962, Origin of slaty and fracture cleavage
    in the Delaware Water Gap area, New Jersey and
    Pennsylvania, in Petrologic Studies (Buddington Volume):
    New York, Geol. Soc. Am., p.281-311.

Morris, A.P., 1981, Competing deformation mechanisms and
    slaty cleavage in deformed quartzose meta-sediments:
    Journal of the Geological Society of London, v.138, p.
    455-462.

Nevin, S.M., 1949, Principles of Structural Geology: New
    York, Wiley, 320p.

Newell, N.D., 1972, The Permian Reef Complex of the
    Gaudalupe Mountains Region, Texas and New Mexico: New
    York, Hafner, 226p.

Page, N.J., Moring, B., Gray, F., Cannon, J., and Blair,
    W.N., 1981, Reconnaissance Geological Map of the Selma
    Quadrangle, Josephine County, Oregon: USGS Miscellaneous
    Field Studies Map, MF-1349, scale 1:62,500.

Park-Jones, R., 1988, Sedimentology, structure and
    geochemistry of the Galice Formation: Sediment fill of a
    back-arc basin and island arc in the western Klamath
    Mountains [M.S.]: Albany, New York, SUNY at Albany.

Pinto-Auso, M. and Harper, G.D., 1985, Sedimentation,
    metallogenesis and tectonic origin of the basal Galice
    Formation overlying the Josephine ophiolite, northwestern
    California: Jounal of Geology, v.93, p. 713-725.

Potter, P.E. and Pettijohn, F.J., 1963, Paleocurrents and
    Basin Analysis: Berlin, Springer Verlag, 296p.

Powell, C.M., 1969, Intrusive sandstone dykes in the Siamo
    Slate near Negaunee, Michigan: Geological Society of
    America Bulletin, v.80, p. 2585-2594.

Ramp, L., 1979, Geolologic Map of Josephine County, Oregon, in Oregon Department of Geology and Mineral Industries Bulletin no. 100, scale 1:126,720.

Ramp, L., 1986, Geologic Map of the Northwest Quarter of the Cave Juction Quadrangle, Josephine County, Oregon: Oregon Department of Geology and Mineral Industries, GMS-38, scale 1:24,000.

Ramp, L. and Peterson, N.V., 1979, Geology and mineral resources of Josephine County, Oregon: Oregon Department of Geology and Mineral Industries Bulletin, no. 100, 45p.

Ramsay, J.G., 1967, Folding and Fracturing of Rocks: New York, McGraw Hill, 562p.

Ramsay, J.G. and Huber, M.I., 1983, The Techniques of Modern Structural Geology, Volume 1: Strain Analysis: London, England, Academic Press, 307p.

Reks, I.J. and Gray, D.R., 1982, Pencil structure and strain in weakly deformed mudstone and siltstone: Journal of Structural Geology, v.4, p. 161-176.

Rettger, R.E., 1935, Experiments of soft rock deformation: American Association of Petroleum Geologists Bulletin, v.19, p. 271-292.

Roering, C. and Smit, C., 1987, Bedding-parallel shear, thrusting and quartz vein formation in Witwatersrand quartzites: Journal of Structural Geology, v.9, p. 419-427.

Roure, 1984, Une coupe geologique de Golconda au Pacifique (Oregon, nord-ouest du Nevada, nord de la Californie): Evolution Mesozoique et Cenozoique de la marge ouest Americaine [thesis]: Paris, France, Univ. de Pierre et Marie Curie, 250p.

Roy, A.B., 1978, Evolution of slaty cleavage in relation to diagenesis and metamorphism: a study from the Hunsruckschiefer: Geological Society of America Bulletin, v.89, p. 1775-1785.

Saleeby, J.B., 1981, Ocean floor accretion and volcano-plutonic arc evolution of the Mesozoic Sierra Nevada, California, in W.G. Ernst (ed.), The Geotectonic Development of California: Englewood Cliffs, New Jersey, Pretice Hall, p. 132-181.

Saleeby, J.B., 1984, Pb/U zircon ages from the Rogue River area, western Jurassic belt, Klamath Mountains, Oregon [abstract]: GSA Abstracts with Programs, v.16, p. 331.

Saleeby, J.B. and Moores, E., 1979, Zircon ages on northern Sierra Nevada ophiolite remnants and some possibe regional correlations [abstract]: GSA Abstracts with Programs, v.11, p. 125.

Saleeby, J.B., Harper, G.D., Snoke, A.W. and Sharp, W.D., 1982, Time relations and structural-stratigraphic patterns in ophiolite accretion, west-central Klamath Mountains, California: Journal of Geophysical Research, v.87, p. 3831-3848.

Saleeby, J.B., Blake, M.C. and Coleman, R.G., 1986, Pb/U zircon ages on thrust plates of the west central Klamath Mountains and Coast Ranges, northern California and southern Oregon [abstract]: EOS Transactions, Americal Geophysical Union, v.64, p. 45.

Sample, J. and Fisher, D., 1986, Duplex accretion and underplating in an ancient accretionary complex, Kodiak Island, Alaska: Geology, v.44, p. 160-163.

Sample, J. and Paterson, S., 1988, The development of slate and graywacke belts during underplating in "hot" accretionary wedges [abstract]: GSA Abstracts with Programs, v.20, p. 227.

Sander, B., 1911, Uber Zusammenhange Zwichen Teilbewegung und Gefuge in Gesteinen: Tschermaks Miner. Petr. Mitt., v.30, p. 381-384.

Sanderson, D.J., 1979, The transition from upright to recumbent folding in the Variscan fold belt of southwest England: a model based on the kinematics of simple shear: Journal of Structural Geology, v.1, p. 171-180.

Schultz, K. and Levi, S., 1983, Paleomagnetism of Middle Jurassic plutons of the north-central Klamath Mountains [abstract]: GSA Abstracts with Programs, v.15, p. 427.

Schweickert, R.A. and Cowan, D.S., 1975, Early Mesozoic tectonic evolution of the western Sierra Nevada, California: Geological Society of America Bulletin, v.86, p. 1329-1336.

Schweickert, R.A., Bogen, N.L., Girty, G.H., Hanson, R.E. and Merguerian, C., 1984, Timing and structural expression of the Nevadan orogeny, Sierra Nevada, California: Geological Society of America Bulletin, v. 95, p. 967-979.

Shackleton, R.M., 1958, Downward-facing structures of the Highland Border: Quarterly Journal of the Geological Society of London, v.113, p. 361-392.

Silver, E.A. and Beutner, E.C., 1980, Melanges: Geology, v.8, p. 32-34.

Silver, E.A. and Moore, J.C., 1979, The Molluca Sea collision zone, Indonesia: in The Geology and Tectonics of Eastern Indonesia, proceedings of the CCOP-IOC SEATAR Working Group meeting, special publication, Geological Research and Development Centre, p. 327-340.

Smith, K.G., 1952, Structure plan of clastic dikes: AGU Transactions, v.33, p. 889-892.

Smith, A.J. and Rast, N., 1954, Sedimentary dikes in the Dalradian of Scotland: Geological Magazine, v.95, p. 234-240.

Snoke, A.W., 1977, A thrust plate of ophiolitic rocks in the Preston Peak area, Klamath Mountains, California: Geological Society of America Bulletin, v.88, p. 1641-1659.

Suppe, J., 1983, Geometry and kinematics of fault-bend folding: American Journal of Science, v.283, p. 684-721.

Turner, F.J. and Weiss, L.E., 1963, Stuctural Analysis of Metamorphic Tectonites: New York, McGraw Hill, 545p.

Vail, S.G., 1977, Geology and geochemistry of the Oregon Mountain area, southwestern Oregon and northern California [Ph.D]: Corvallis, Oregon, Oregon State University, 159p.

Varga, R., 1985, Mesoscopic structural fabric of early Paleozoic rocks in the northern Sierra Nevada, California, and implications for Late Jurassic plate kinematics: Journal of Structural Geology, v.7, p. 667-682.

Vollmer, F.W. and Bosworth, W., 1984, Formation of melange in a foreland basin overthrust setting: Example from the Taconic Orogen: GSA Special Paper, no.198, p. 58-70.

Weber, K., 1981, Kinematic and metamorphic aspects of cleavage formation in very low-grade metamorphic slates: Tectonophysics, v.78, p. 291-306.

Wells, F.G., Hotz, P.E., and Cater, F.W., 1949, Preliminary description of the geology of the Kerby quadrangle, Oregon: Bulletin of the Oregon Department of Gelogy and Mineral Industries, no.40, 23p.

Wells, F.G. and Walker, G.W., 1953, Geology of the Galice quadrangle, Oregon: USGS Quadrangle Map GQ-25, scale 1:62,500.

Westbrook, G.K., Smith, M.J., Peacock, J.H. and Poulter, M.J., 1982, Extensive underthrusting of deformed sediment beneath the accretionary conplex of the Lesser antilles subduction zone: Nature, v.300, p. 625-628.

Westbrook, G.K. and Smith, M.J., 1983, Long decollements and mud volcanoes: evidence from Barbados Ridge complex for the role of high pore-fluid pressure in the development of an accretionary complex: Geology, v.11, p. 279-283.

White, S.H. and Knipe, R.J., 1978, Microstructure and cleavage development in selected slates: Contibutions to Mineralogy and Petrology, v.66, p. 165-174.

White, S.H. and Wilson, C.J.L., 1978, Microstructure of some quartz pressure fringes: N. Jb. Miner. Abh., v.134, p. 33-51.

Wickham, J.S., 1973, An estimate of strain increments in a naturally deformed carbonate rock: American Journal of Science, v.273, p. 23-47.

Wickham, J.S. and Anthony, M., 1977, Strain paths and folding of carbonate rocks near Blue Ridge, central Appalachians: Geological Society of America Bulletin, v.88, p. 920-924.

Williams, P.F., 1972a, Development of metamorphic layering and cleavage in low grade metamorphic rocks at Bermagui, Australia: American Journal of Science, v.272, p. 1-47.

Williams, P.F., 1972b, Pressure shadow structures in foliated rocks from Bermagui, New South Wales: Journal of the Geological Society of Australia, v.18, p. 371-377.

Williams, P.F., Collins, H.R. and Wiltshire, R.G., 1969, Cleavage and penecontemporaneous deformation structures in sedimentary rocks: Journal of Geology, v.77, p. 415-425.

Williams, D.M. and Nealon, T., 1986, The significance of large-scale sedimentary structures in the Silurian succession of western Ireland: Geological Magazine, v.124, p. 361-366.

Wilson, C.J.L. and De Hedouville, P., 1985, Early cleavage development in the Late Ordovician of northeast Victoria, Australia: Journal of Structural Geology, v.7, p. 401-408.

Woodcock, N.A., 1976, Structural style in slump sheets: Ludlow series, Powys, Wales: Journal of the Geological Society of London, v. 132, p. 399-415.

Wyld, S.A., 1985, Geology of the western Jurassic belt, South Fork Trinity area, Klamath Mountains, California [M.S.]: Berkeley, California, University of California-Berkeley, 168p.

Wyld, S.A. and Wright, J.E., 1988, The Devils Elbow ophiolite remnant and overlying Galice Formation: New constraints on the Middle to Late Jurassic evolution of the Klamath Mountains, California: Geological Society of America Bulletin, v.100, p. 29-44.